

On the potential of parallel powertrains to reduce the cost of energy from offshore wind turbines

Godwin Akpan Jimmy

A thesis submitted for the degree of Doctor of Philosophy

Institute of Energy and Environment

Department of Electronic and Electrical Engineering

University of Strathclyde

Glasgow, UK

2019

This thesis is the result of the author's original research. It has been composed by the author and has not been previously submitted for examination which has led to the award of a degree. The copyright of this thesis belongs to the author under the terms of the United Kingdom Copyright Acts as qualified by the University of Strathclyde Regulation 3.50. Due acknowledgement must always be made of the use of any material contained in, or derived from, this thesis.

Godwin Akpan Jimmy

February 2019

Abstract

Offshore wind turbine operating conditions are challenging with access for maintenance being limited by weather to a greater degree than for onshore turbines, resulting in prolonged downtime and reduced availability. This makes operational costs (helicopter, crew transfer or heavy lift vessels) more expensive, leads to loss of energy production and tends to increase the cost of energy of offshore wind farms. It is therefore important to investigate potential strategies that could improve availability, energy production and at the same time reduce operation and maintenance (O&M) cost and cost of energy in the long run.

One possible option for availability improvement and cost of energy reduction is through the powertrain design. Most of the existing wind turbine types could be distinguished through their powertrain configurations. Conventional wind turbine powertrain exhibits single-input-single-output topology (one gearbox coupled to a generator with a power converter) while some exist with no gearbox (gearless drive). Although some of the geared and gearless powertrains have some good availability, yet they are still susceptible to prolonged downtime and consequently significant energy loss. This has alarmed the need to introduce the concept of parallelism into the design of offshore wind turbine powertrain.

This research, therefore, focusses on a configuration with single-input-multiple-output (parallel powertrain) subsystems as a strategy for improvements in availability, energy production and cost of energy reduction. The novelty of this work comes from the availability improvement of small parallel subsystem with reduced failure rate, extra energy production at failure states, reduction in (O&M) cost due to high repair rate and the resulting cost of energy reduction of parallel powertrain.

The highest-level research question amongst all of the research questions answered in this work is:

“Can parallel powertrains reduce the cost of energy of offshore wind turbines?”

In attempting to address this key question and other secondary research questions, in Chapter 3 the author carries out survey and analysis of failure and repair rate data from published sources to determine how they vary with powertrain configuration, power ratings, and sizes. In Chapter 4, a baseline powertrain availability and that of different

parallel powertrains are evaluated using Markov state space model (MSSM). In Chapter 5, the annual energy production (*AEP*) of parallel powertrain is analysed using Raleigh probability distribution and the rated power in order to quantify any extra benefit at below rated wind speed. The ideal *AEP* is analysed at rated power, rated wind speed and at no-failure state. Also, the losses and efficiency of parallel powertrain at failure states are evaluated. Chapter 6 estimates the O&M costs of parallel powertrains using offshore accessibility tool. Chapter 7 calculates the cost of energy of parallel powertrain using *AEP* and O&M cost results from previous chapters in combination to initial capital cost (*ICC*). Finally, a general conclusion is made in Chapter 8.

The novel results from each chapter provide some new insight into the potential of the parallel powertrain. The thesis concludes that an increase in the number of parallel systems, N , does not automatically lead to a higher availability for a wind turbine powertrain; however, when failure and repair rates scale with module power ratings then there is an improvement. It is possible to have extra *AEP* at below rated wind speed and at the various failure states of parallel powertrain. Potential reduction in the cost of energy is also observed with the parallel powertrain at below rated wind speed and failure states.

The results shown in this thesis will be useful for offshore wind farm developers, operators and wind turbine manufacturers. It can be useful to developers when deciding and selecting the type of powertrain. Operators can gain insight into the driving factors of O&M costs. Manufacturers can consider which type of wind turbine powertrain to develop and manufacture to satisfy one of their key customer requirements, a lower cost of energy.

Acknowledgments

My greatest thanks and honour go to the God Almighty through His beloved son Jesus Christ for the grace, wisdom, understanding and knowledge he gave to me so I could successfully complete this Thesis.

I would like to begin by gratefully acknowledging the Niger Delta development commission (NDDC), University of Strathclyde and Mrs Emem Jimmy for their contribution in funding this work. I would also like to thank the Wind Energy Systems CDT management team (Professor Bill Leithead, Professor David Infield and Dr Alasdair McDonald) and administrative staff (Drew Smith and Sheila Campbell) for the immense support they offered in the course of my study.

Special thanks must go to my first supervisor Dr Alasdair McDonald for his guidance, advice and sacrificing his time to read my work and giving me very useful feedbacks during the period of my research. I am extremely blessed and thankful to God for leading me to such an amazing and outstanding supervisor and mentor for the period of my PhD.

Through Alasdair, I had the opportunity to work with Dr James Carroll, whose past work assisted with my research. I would like to thank Dr Iain Dinwoodie and the TIC Low Carbon Power and Energy Systems group for access to their AM02 model and guidance.

I am also very grateful to my friends and colleagues in my research team led by Dr Alasdair McDonald for the encouragement and support they gave to me. I would like to thank my friends within and outside the Electronic and Electrical Engineering department for their support also. Finally, and most importantly I would like to thank my wife Emem for her financial and moral support, my daughter Hephzibah whose birth gave me so much joy while I was writing up and preparing for my viva. Special thanks to my sisters (Patience, Glory, Aniekan and Blessing), my brother Daniel, and my parents Helen and Akpan for all their love and support.

CONTENTS

ABSTRACT	II
ACKNOWLEDGMENTS	IV
CONTENTS	V
LIST OF FIGURES	X
LIST OF TABLES	XVI
NOMENCLATURE AND ABBREVIATIONS	XVIII
CHAPTER 1 INTRODUCTION	1
1.1 RESEARCH QUESTION	3
1.2 APPROACH TAKEN/METHODOLOGY	5
1.3 STRUCTURE.....	6
1.4 MOTIVATION AND NOVELTY OF RESEARCH	6
1.5 RESEARCH OUTPUTS.....	10
CHAPTER 2 LITERATURE REVIEW	11
2.1 INTRODUCTION TO WIND TURBINE	11
2.2 DESCRIPTION OF THE WIND TURBINE POWERTRAIN	12
2.3 GEARBOX	13
2.3.1 Classification of Gearbox	14
2.3.2 Arrangement of gears	14
2.3.3 Comparison of Gear arrangement	18
2.3.4 Losses in gearbox	19
2.3.5 Problems and downtime of gearbox	21
2.4 GENERATORS	22
2.4.1 Squirrel cage induction machines-generator	22
2.4.2 Wound rotor induction generator	23
2.4.3 Doubly fed induction generators.....	24
2.4.4 Electrically Excited Synchronous Generator.....	24
2.4.5 Permanent Magnet Synchronous Generator	25
2.5 POWER CONVERTERS.....	26
2.5.1 Description of power electronics.....	26
2.5.2 Power converter in renewable energy.....	26
2.5.3 Types of power converter	27
2.5.4 Early years of power electronics converters in wind turbine systems.....	30
2.5.5 Power quality demand.....	31

2.5.6 Wind turbine power converters.....	32
2.6 COMPARISON OF DIFFERENT WIND TURBINE POWERTRAINS	36
2.7 RELIABILITY	39
2.7.1 Reliability and Availability parameters.....	39
2.7.2 Bathtub curve.....	40
2.7.3 Reliability of wind turbines	41
2.7.4 Reliability of powertrains.....	43
2.7.5 Condition monitoring system.....	44
2.8 REDUNDANCY IN WIND TURBINE POWERTRAINS.....	45
2.8.1 Introduction to fault tolerance.....	45
2.8.2 Fault tolerance in generators.....	46
2.9 WIND TURBINE PARALLEL POWERTRAINS	50
CHAPTER 3 RELIABILITY SURVEY OF FAILURE AND REPAIR RATE OF POWERTRAIN EQUIPMENT FOR PARALLEL POWERTRAIN	55
3.1 INTRODUCTION.....	55
3.2 POWERTRAIN FAILURE RATE DATA	55
3.2.1 Failure rate of electrical machines from other industries.....	55
3.2.2 Onshore and offshore failure rate of wind turbine powertrain from wind turbine manufacturer	57
3.2.3 Failure data for German and Danish wind turbines.....	59
3.2.4 Failure data for Swedish wind turbines.....	62
3.3 DERIVING USEFUL RELATIONSHIPS BETWEEN RATINGS AND POWERTRAIN FAILURE AND REPAIR RATES	63
3.4 RELIABILITY BLOCK DIAGRAMS	67
3.5 FAILURE MODE AND EFFECT ANALYSIS	69
3.6 CHAPTER CONCLUSION	72
CHAPTER 4 MARKOV STATE SPACE MODELS FOR AVAILABILITY	73
4.1 INTRODUCTION.....	73
4.2 METHODOLOGY	74
4.2.1 Markov state space modelling.....	74
4.2.2 Simple Markov model for N=1	76
4.2.3 Simple Markov model for N=2	78
4.2.4 Simple Markov model for N	80
4.2.5 Developed case with more realistic repair transition paths.....	81
4.2.6 Case with failure and repair rates changing with N	82
4.2.7 Case with varying parallel powertrain subsystem power rating	83
4.3 RESULTS.....	85

4.3.1 Results for a generic powertrain	85
4.4 DISCUSSION	89
4.4.1 Implications of the equivalent availability model.....	89
4.4.2 Application of the equivalent availability models	91
4.4.3 Assumptions and limitations of the equivalent availability models	93
4.5 CHAPTER SUMMARY AND CONCLUSION	93
CHAPTER 5 MODELLING OF ANNUAL ENERGY PRODUCTION AT DIFFERENT FAILURE STATES	95
5.1 INTRODUCTION.....	95
5.1.1 Conventional and parallel wind turbine powertrains	98
5.2 METHODOLOGY	101
5.2.1 Failure state probabilities model	102
5.2.2 New power curves for F failures	102
5.2.3 Energy production calculation with different power curves for different failure states	103
5.2.4 Annual energy production	104
5.2.5 Effect of failure and repair rate on the annual energy production	106
5.3 RESULTS AND SENSITIVITY ANALYSES	106
5.3.1 Annual Energy Production.....	106
5.3.2 Annual energy production for different parallel powertrain configurations	107
5.3.3 Sensitivity analysis - Impact of constant failure rate and varying repair rates on AEP	109
5.3.4 Effect of different failure and repair rates using different powertrain topologies..	110
5.4 DISCUSSIONS ON AEP MODEL	111
5.4.1 Influence of N on AEP.....	111
5.4.2 Annual energy production for different parallel powertrain configurations	112
5.4.3 Effect of failure and repair rate of different powertrain on AEP.....	112
5.4.4 Neglecting additional powertrain losses in failure states.....	113
5.5 LOSSES AND EFFICIENCY OF PARALLEL POWERTRAIN IN FAILURE STATES.....	113
5.5.1 Methodology.....	114
5.6 RESULTS BASED ON LOSSES	121
5.7 CONCLUSIONS	125
CHAPTER 6 OPERATION AND MAINTENANCE COST OF OFFSHORE WIND TURBINES WITH PARALLEL	126
POWERTRAIN	126
6.1 INTRODUCTION.....	126
6.2 METHODOLOGY	127

6.2.1	<i>The use of an offshore wind farm accessibility model to find O&M costs and their relationship to the number of parallel powertrain modules.....</i>	<i>128</i>
6.2.2	<i>Analysis of different operation and maintenance and vessel strategies for parallel wind turbine powertrain.....</i>	<i>130</i>
6.2.3	<i>Variation of O&M cost with N.....</i>	<i>133</i>
6.3	RESULTS.....	134
6.3.1	<i>Results of Annual operation and maintenance costs and their relationship to the number of parallel powertrain modules</i>	<i>134</i>
6.3.2	<i>Comparison of different operation and maintenance and vessel strategies for parallel wind turbine powertrain</i>	<i>136</i>
6.3.3	<i>Result of waiting strategy-different batch threshold</i>	<i>137</i>
6.3.4	<i>Using CTV for major replacement of parallel subsystem.....</i>	<i>138</i>
6.3.5	<i>Assumptions on data used in the O&M accessibility model.....</i>	<i>139</i>
6.4	SUMMARY AND CONCLUSIONS.....	140
CHAPTER 7	COST OF ENERGY ASSESSMENT OF PARALLEL POWERTRAIN	141
7.1	INTRODUCTION.....	141
7.2	METHODOLOGY: NET BENEFIT BASED ON AVAILABILITY IMPROVEMENT	142
7.2.1	<i>Initial capital cost of a different configuration of parallelism.....</i>	<i>145</i>
7.3	RESULTS AND SENSITIVITY ANALYSES OF NET BENEFIT	146
7.3.1	<i>Results for different powertrain topologies.....</i>	<i>147</i>
7.3.2	<i>Results for different parallel powertrain configurations.....</i>	<i>149</i>
7.3.3	<i>Sensitivity to different failure and repair rates from different turbine types and sizes ..</i>	<i>150</i>
7.3.4	<i>Sensitivity to different sites and wind speed distribution</i>	<i>151</i>
7.4	COST OF ENERGY ASSESSMENT OF PARALLEL POWERTRAIN	152
7.4.1	<i>Cost of Energy definition.....</i>	<i>152</i>
7.4.2	<i>Cost of energy analysis for parallel powertrain</i>	<i>152</i>
7.4.3	<i>Results for cost of energy for different methods.....</i>	<i>153</i>
7.4.4	<i>Cost of Energy comparison for different parallel powertrain configuration</i>	<i>155</i>
7.5	SUMMARY AND CONCLUSION	155
CHAPTER 8	CONCLUSION AND FUTURE WORK.....	157
8.1	RESEARCH QUESTIONS AND OVERVIEW OF CONCLUSION	157
8.2	SUMMARY OF CONCLUSIONS	158
8.2.1	<i>Key points from Chapter 3</i>	<i>158</i>
8.2.2	<i>Key points from Chapter 4</i>	<i>158</i>
8.2.3	<i>Key points from Chapter 5</i>	<i>159</i>
8.2.4	<i>Key points from Chapter 6</i>	<i>160</i>

8.2.5 Key points from Chapter 7	161
8.3 ASSUMPTIONS, LIMITATIONS, AND UNCERTAINTIES	162
8.4 SENSITIVITY ANALYSES	162
8.5 CONTRIBUTION TO KNOWLEDGE	163
8.5.1 Chapter 3 contribution	163
8.5.2 Chapter 4 contribution	163
8.5.3 Chapter 5 contribution	164
8.5.4 Chapter 6 contribution	164
8.5.5 Chapter 7 contribution	164
8.6 FUTURE WORK	165
8.6.1 Reducing Uncertainty	165
8.6.2 Use of more sophisticated approach to predict failure rate of small parallel modules ..	165
8.6.3 Use of more sophisticated operation and maintenance tool for parallel powertrain	166
8.6.4 Switching operation at failure states of parallel module.....	166
8.6.5 Extension of parallel powertrain systems to gearbox design.....	166
8.7 REFERENCES.....	167

List of Figures

Figure 1.1 Drivetrain choices for larger wind turbines [3][4][5].....	3
Figure 1.2 Steps to complete this Thesis	5
Figure 2.1: Wind turbine showing the various components and powertrain [13].....	12
Figure 2.2: Simple gears.....	13
Figure 2.3: Simplified Arrangement of planetary gearing system [15][16]	15
Figure 2.4: Helical gearbox (3-stage) [17].....	16
Figure 2.5: Planetary gearbox with one ring (3-stage) [17].....	16
Figure 2.6: Planetary gearbox with two rings (3-stage) [17].....	17
Figure 2.7: Extended planetary gearbox (4-stage) [17].....	17
Figure 2.8: Multistage gearbox (4-stage) [17]	18
Figure 2.9: Doubly-fed induction Generator [37].....	24
Figure 2.10: Different classes of semiconductors [39].....	27
Figure 2.11: Classification of AC↔DC power converters [39]	28
Figure 2.12: Three phase 2-level VSC and Three phase 2 level CSC [39]	29
Figure 2.13: Types of Multilevel converters [39]	29
Figure 2.14: Wind turbine growth and trend of power electronic converter [40].....	30
Figure 2.15: Demand of power quality [40]	31
Figure 2.16: Partial rated converter [40].....	32
Figure 2.17: Full rated converter [40]	32
Figure 2.18: Two level back-to-back voltage source converter [39]	33

Figure 2.19: Three- level neutral- point diode clamped back-to-back converter [40]	34
Figure 2.20: Three- level H-bridge back-to-back converter [40]	34
Figure 2.21: Five- level H-bridge back- to- back converter [40]	35
Figure 2.22: Three- level neutral-point clamped and five –level H-bridge converter [40]	35
Figure 2.23: Generators type based on grid connection [32]	37
Figure 2.24: Bathtub Curve showing phases of life cycle of a component [27]	41
Figure 2.25: Reliability characteristics of wind turbine of sub-assemblies [31][60]	44
Figure 2.26: Six phase synchronous generator system [77]	48
Figure 2.27: A 1.5MW single output and multiple output powertrain [15]	51
Figure 2.28: Schematic of multiple output powertrain [86]	52
Figure 3.1: Failure rate data from turbine in Denmark and Germany [97]	59
Figure 3.2: Growth of wind turbine sizes in the Danish and German population [97]	59
Figure 3.3: Failure rate based on Swedish wind turbines [101]	62
Figure 3.4: Failure rate versus rating of powertrain	65
Figure 3.5: Mean time to repair versus rating of powertrain showing the linear regression type for the powertrain	66
Figure 3.6: Reliability block diagram for (a) series and (b) parallel arrangement of system components	68
Figure 3.7: Breakdown of wind turbine powertrain sub assembly and components	69
Figure 4.1: Wind turbine powertrains: (a) Single-input-single-output system, $N = 1$ (b) Powertrain system with both generator and power converter in parallel, $N = 2$ (c)	

Powertrain system with only generator in parallel, $N = 2$ (d) Powertrain system with only power converter in parallel, $N = 2$	75
Figure 4.2: State space model of a single component, $N = 1$ system	77
Figure 4.3: State space model of two parallel components, $N = 2$ system: (a) Simplified model with four states (b) Simplified model with reduced states (c) Simplified model with alternative repair path.	78
Figure 4.4: Effect of α and N on the equivalent availability of a 3MW parallel wind turbine powertrain (generator and power converter) based on generic powertrain failure ($m_\lambda = 0.357$) and repair data ($m_{MTTR} = 0.0048$)	86
Figure 4.5: Effect of α and N on the equivalent availability of a 3MW parallel wind turbine powertrain (generator only) based on generic powertrain failure ($m_\lambda = 0.2635$) and repair data ($m_{MTTR} = 0.006$)	86
Figure 4.6: Effect of α and N on the equivalent availability of a 3MW parallel wind turbine powertrain based on generic powertrain (converter only) failure ($m_\lambda = 0.0933$) and repair data ($m_{MTTR} = 0.0012$)	87
Figure 4.7: Effect of α and N on the equivalent availability of a 3MW parallel wind turbine powertrain (generator and power converter) based on generic powertrain failure ($m_\lambda = 0.357$), repair data ($m_{MTTR} = 0.0048$) and including rest of turbine availability $A_{RoT(inc.gb)}$	88
Figure 4.8: Effect of α and N on the equivalent availability of a 3MW parallel wind turbine powertrain (generator only) based on generic powertrain ($m_\lambda = 0.2635$) and repair data ($m_{MTTR} = 0.006$) and including rest of turbine availability $A_{RoT(inc.gb,pc)}$...	88
Figure 4.9: Effect of α and N on the equivalent availability of a 3MW parallel wind turbine powertrain (power converter only) based on generic powertrain failure ($m_\lambda = 0.0933$) and repair data ($m_{MTTR} = 0.0012$) and including rest of turbine availability $A_{RoT(inc.gb,gen)}$	89

Figure 5.1: Wind turbine power curve for a wind turbine with a conventional (single gearbox, single generator and single power converter) powertrain	95
Figure 5.2: Power curves for a wind turbine with a conventional powertrain (<i>Power curve, 0 failures</i>) and a parallel powertrain ($N=4, \alpha=1$) in various failure states.	96
Figure 5.3: (a) Flowchart showing the procedure to derive the annual energy production based on equivalent availability in Chapter 4 (b) Flowchart showing the procedures to derive the annual energy production based on the multi-state energy method in this chapter.....	101
Figure 5.4: Results of <i>AEP</i> using probability state failure and equivalent availability at rated wind speed of 11m/s and at $\alpha=1/N-1$. (<i>AEP</i> =14.8 GWhr for no-parallelism i.e. $N=1$).....	107
Figure 5.5: Comparison of <i>AEP</i> for parallel powertrain configurations: parallelism in generator and power converter, parallelism in generator only, parallelism in power converter only.....	108
Figure 5.6: Sensitivity analysis to show the impact of repair rate on the <i>AEP</i> while the failure rate is kept constant for number of parallel subsystems for a 3MW wind turbine	109
Figure 5.7: Sensitivity analysis to show the impact of failure rate on the <i>AEP</i> while the repair rate is kept constant for parallel subsystems for a 3MW wind turbine	110
Figure 5.8: Sensitivity analysis: Comparison of <i>AEP</i> for different powertrain number of parallel subsystems (generator and power converter combined) for a 3MW wind turbine.....	111
Figure 5.9: Flowchart showing the procedure to derive the resultant annual energy production of parallel powertrain at failure states using the probability of wind speed and the probability of each failure state.....	115

Figure 5.10: Torque of each healthy parallel powertrain modules against wind speed showing different new rated wind speeds and maximum torques. This case is for $N = 10$, $\alpha = 1/(N-1)$ and shows the first four failure states ($F=0-3$)	121
Figure 5.11: New current of wind turbine with parallel powertrain modules when $F=0-3$ at various failure states	122
Figure 5.12: New copper of wind turbine with parallel powertrain modules when $F=0-3$ at various failure states	122
Figure 5.13: Marginal energy loss at failure states per parallel module	123
Figure 5.14: Relative efficiency at various failure states	123
Figure 5.15: Results of <i>AEP</i> when losses at failure states are considered at rated wind speed of 11m/s and at $\alpha=1/N-1$. (<i>AEP</i> =13.94 GWh for no-parallelism i.e. $N=1$)....	124
Figure 6.1: Model structural overview and interdependencies [123].....	129
Figure 6.2: Expected number of visits for repairs with increasing number of parallel subsystems	133
Figure 6.3: Comparison of operation and maintenance cost for wind turbine with different parallel subsystem. (<i>AOM</i> =253.6±0.8 k£/turbine/year for no-parallelism i.e. $N=1$).....	134
Figure 6.4: Comparison of operation and maintenance cost for wind turbine with different parallel subsystem using different maintenance and vessel strategy. JV used for all major replacement of wind turbine components.....	136
Figure 6.5: Comparison of operation and maintenance cost using different batch threshold for the waiting strategy and the same vessel strategy – FoFUC.....	137
Figure 6.6: Comparison of operation and maintenance cost using CTV instead of JV for major replacement of parallel subsystems.....	138
Figure 7.1: Maximum net benefit comparison of different powertrain types and number of parallel components for a 3MW wind turbine	148

Figure 7.2: Net benefit comparison of parallel powertrain configurations: parallelism in generator and power converter, parallelism in generator only and parallelism in power converter only.....	149
Figure 7.3: Comparison of maximum net benefit based on different powertrain failure and repair rates drawn from different wind turbine populations.....	150
Figure 7.4: Sensitivity analysis of maximum net benefit to sites using generic powertrain failure and repair rates.....	151
Figure 7.5: Comparison of cost of energy for wind turbine with different parallel subsystem. ($CoE=101.6$ £/MWh for no-parallelism i.e. $N=1$).....	153
Figure 7.6: New cost of energy considering losses at failure states.....	154
Figure 7.7: Comparison of cost of energy for different parallel subsystem	155

List of Tables

Table 1.1 Expected potential impact of technical innovations on the Cost of Energy of a typical offshore wind farm [1].	2
Table 2.1: Comparison of Gearbox arrangements showing both planetary (P) and helical (H) gears [18].....	19
Table 2.2: Requirements of wind turbine power converter	31
Table 2.3: Failure rate of powertrain components [60]	44
Table 3.1: Reliability data from other industry based on power ratings of motors [94]	56
Table 3.2: Failure rate for generators and power converter.....	57
Table 3.3: Reliability characteristics for different subassemblies in the WMEP programme [31].....	61
Table 3.4: Typical comparison between reliability field data of a 0.3MW and a 1MW wind turbine main assembly failure rates [99][100].....	61
Table 3.5: Failure rate of wind turbine powertrain components based on power rating [57][95][100][102]	64
Table 3.6: Downtime and repair time of wind turbine powertrain components based on powertrain rating [95][100][102][103-104].....	64
Table 3.7: Other trendlines and the R^2	66
Table 3.8: Failure modes of powertrain modules identified through FMEA [27].....	70
Table 3.9: Sub-system Failure Rate estimation (failures/year) for conventional turbine	70
Table 4.1: Input data for the availability model of different parallel powertrain configurations: (a) Generator and power converter in parallel (b) Parallel generator only (c) Parallel power converter only	85

Table 5.1: Wind turbine parameters used in <i>AEP</i> model.....	106
Table 7.1: Wind turbine and site details for sensitivity analysis [135][95].....	144
Table 7.2: Data for sensitivity analysis for different 3MW powertrain types [104]	144
Table 7.3: Input data for net benefit of different parallel powertrain configurations: (a) Generator and a power converter in parallel (b) Parallel generator only (c) Parallel power converter only 57][95][100][102].....	145
Table 7.4: Input cost data for cost of energy assessment [52][124].....	146

Nomenclature and Abbreviations

Roman Letters

<i>Symbol</i>	<i>Description</i>
c	Scale parameter
erf	error function
F	Failure states
N	Number of parallel modules
t	Time
v	wind speed

Greek Letters

<i>Symbol</i>	<i>Description</i>
α	OVERRATING OF POWERTRAIN
β	Available capacity of powertrain at failure states
γ	Notation for the change in gradient of availability against α
λ	Failure rate
λ_{opt}	Optimal speed ratio
ρ	Density of air
μ	Repair rate
Ω	Rotor speed of wind turbine
ω	Angular velocity

Abbreviations

<i>Acronym</i>	<i>Description</i>
2PH	Two Stage Planetary Helical
2L-BTB	Two Level Back To Back
3PPH	Three Stage Planetary Helical
AC	Alternating Current
AEP	Annual Energy Production
AOM	Annual Operation and Maintenance
BoP	Balance of Plant

CAPEX	Capital Expenditure
CHB	Cascade H-Bridge
CMS	Condition Monitoring Systems
CoE	Cost of Energy
Cp	Power Coefficient
CSC	Current Source Converter
CTV	Crew Transfer Vessel
DC	Direct Current
DD	Direct Drive
DFIG3G	Doubly Fed Induction Generators with Three Stages
DFIG	Doubly Fed Induction Generator
EESG	Excited Synchronous Generator
EWEA	European Wind Energy Association
FCR	Fixed Charge Rate
FLC	Flying Capacitor Converter
FMAC	Fixed Monthly Annual Charter
FMEA	Failure Modes and Effect Analysis
FoFUC	Fix On Fail Until Complete
GTO	Gate Turn –Off
HLV	Heavy Lift Vessel
ICC	Initial Capital Cost
IEGTs	Injected Enhanced Gate Transistors
IEEE	Institute of Electrical and Electronics Engineering
IG	Induction Generator
IGBT	Insulated Gate Bipolar Transistor
IGCTs	Insulated Gate Commutated Thyristors
IWES	Institute for Wind Energy System
JV	Jack up vessel
kWh	Kilowatt-Hour
LCOE	Levelised Cost Of Energy
LDT	Logistic Delay Time
LWK	Landwirtschaftskammer

MMF	Magneto Motive Force
MS	Medium Speed
MSSM	Markov State Space Model
MTBF	Mean Time Between Failures
MTTF	Mean Time To Failure
MTTR	Mean Time To Repair
MW	Mega-Watt
MWh	Megawatt-Hour
NPC	Neutral Point Clamped
NREL	National Renewable Energy Laboratory
O&M	Operations and Maintenance
OPEX	Operational Expenditure
PLC	Purchase Lifetime Charter
PMG1G	Permanent Magnet Generator with Single Stage Gearbox
PMG	Permanent Magnet Generator
PMSG	Permanent Magnet Synchronous Generator
PRC	Partially Rated Converter
PWM	Pulse Width Modulation
SCADA	Supervisory Control and Data Acquisition
SCIG	Squirrel Cage Induction Generator
SG	Synchronous Generator
SGCTs	Symmetrical Gate Commutated Thyristors
SiC	Silicon Carbide
SISO	Single-Input-Single-Output
SRM	Switched Reluctance Machines
TBF	Time Between Failures
THD	Tower Head Diameter
UPS	Uninterrupted Power Supply
VAWT	Vertical Axis Wind Turbines
VSC	Voltage Source Converter
WMEP	Scientific Measurement and Evaluation Program
WRIG	Wound Rotor Induction Generator

WSD

Wind Stats Deutschland

WSDK

Windstats Survey in Denmark

Chapter 1 Introduction

Globally there is an increase in the use of renewable energy in power systems because of a growing concern over environmental issues. Amongst the mix of renewable energy sources, wind energy systems have enjoyed high growth. Onshore wind energy can be cost competitive with conventional power plants; however, for offshore wind turbines, there is still need to reduce the levelised cost of energy. Wind farm developers are seeking to harness the bountiful wind resources in offshore areas. This environment poses certain undeniable challenges that seem to hamper the swift response to powertrain (gearbox, generator, and power converter) repairs and maintenance in the event of fault. Such conditions may culminate prolonged downtime leading to relatively low availability. Consequently, high (*CoE*) is expected for the offshore wind power generation due to long distance from shore, access difficulties, resource requirements, elongated downtime and low availability. The present state of concern in the wind industry is to reduce cost, increase annual energy production and availability.

There is a serious move by the Government, researchers, industry and wind developers to migrate wind power generation from the currently dominant onshore sites to the offshore environment where there are plethora of wind resources. However, the challenges of low availability, reduced energy production and resultant cost of energy have motivated the quest for new emerging technology. Different wind turbine technology innovations have been researched and the effect of each on capital cost, operating costs, energy production and the risk involved have also been evaluated. It is very important to view adequately any proposed technology from an economic standpoint to ascertain its potential benefits. Recently, BVG on behalf of Crown Estate carried out an investigation on the viability of some technical innovations and their potential impact on the levelised cost of energy. Table 1.1 reveals interesting findings and rankings of some innovations.

Table 1.1 Expected potential impact of technical innovations on the Cost of Energy of a typical offshore wind farm [1].

Innovation	Relative impact of innovations on LCOE
Increase in turbine power rating	-8.5%
Optimization of rotor diameter, aerodynamics, design, and manufacture	-3.7%
Introduction of the next generation drivetrains	-3.0%
Improvements in jacket foundation design and manufacturing	-2.8%
Improvements in aerodynamic control	-1.9%
Improvements in support structure installation	-1.9%
Greater level of array optimization and front-end engineering design (FEED)	-1.2%
About 30 other innovations	-5.6%

From that study, an increase in the rating of the turbine is seen to have the potential of decreasing the *CoE* by about eight percent, which comes from the increase in the size of the turbine to 6MW upward. Such larger turbine with optimum sized rotor may have higher energy production. Besides larger turbine ratings, one important innovation accounting for three percent *CoE* decrease comes from the introduction of next generation powertrains such as direct drive, and medium speed generators aimed at OPEX cost reduction because of the expected impact on reliability. Recent studies show that further drop in *CoE* is possible as a result of technology innovations [2]. For larger wind turbines, certain choices of powertrain technology have been made by developers and manufacturers as shown in Figure 1.1 below.

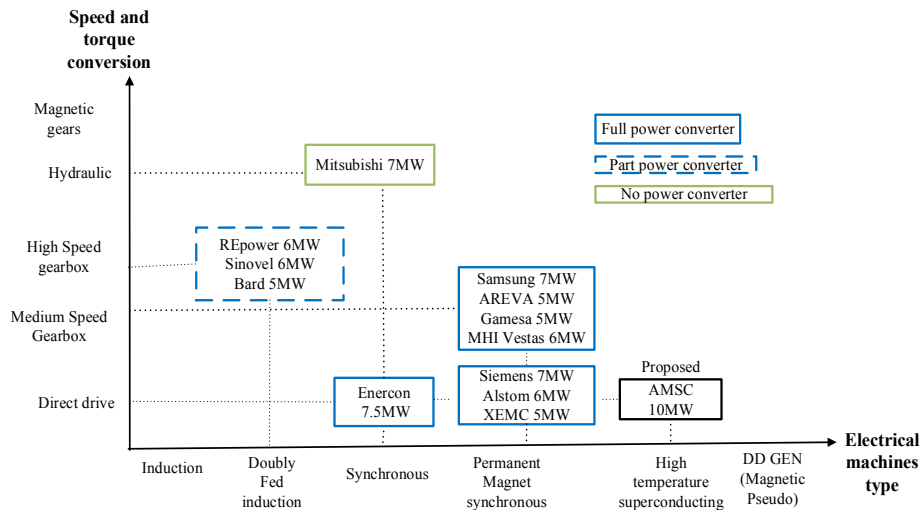


Figure 1.1 Drivetrain choices for larger wind turbines [3][4][5]

This research proposes an option of parallel powertrain topologies, a scenario where, for example, a single large generator common to the conventional or baseline system is replaced with smaller numbers of parallel generators in the powertrain to keep the wind turbine operational during failure of any of its subassemblies/components, though at a reduced power level. Powertrain with replicated subassemblies or components could bolster a turbine’s effective availability, keeping the wind turbine operational during some faults scenario, increasing *AEP* and reducing the cost of energy for the offshore wind turbines.

1.1 Research question

In view of the problem statement that “relatively high *CoE* is expected for offshore wind projects, in part because failures in wind turbine powertrains lead to significant downtime and O&M costs”, this thesis seeks to answer the following research question:

“Can parallel powertrains reduce the cost of energy of offshore wind turbines?”

To answer this primary research question, a number of other smaller secondary research questions must first be answered.

- How do failure and repair rates of powertrain equipment vary with size and power?
- Is any improvement in availability possible using parallel powertrain?

- What degree of parallelism is most beneficial in terms of availability?
- Can parallel powertrains generate ‘extra’ energy at failure states and consequently increase annual energy production? If so, by how much?
- What happens to the torque, T of the system at failure states of parallel powertrain? Does efficiency suffer with parallel powertrain?
- Do parallel powertrains affect the O&M cost due to the additional number of repair visits?
- What strategy is best to introduce parallelism in terms of availability improvement and Cost of Energy reduction?
 - Parallel generator and power converter combined
 - Parallel generator only
 - Parallel power converter only
- What degree of parallelism is most effective in terms of availability improvement, net benefit and cost of energy reduction?

These secondary research questions are answered throughout each chapter of this thesis. The beginning of each chapter will set out the secondary research question to be answered in that chapter. The conclusion of each chapter will answer the secondary research questions and contribute towards answering the primary research question stated above.

1.2 Approach taken/methodology

To answer the primary research question outlined in Section 1.2, the following steps must be taken:

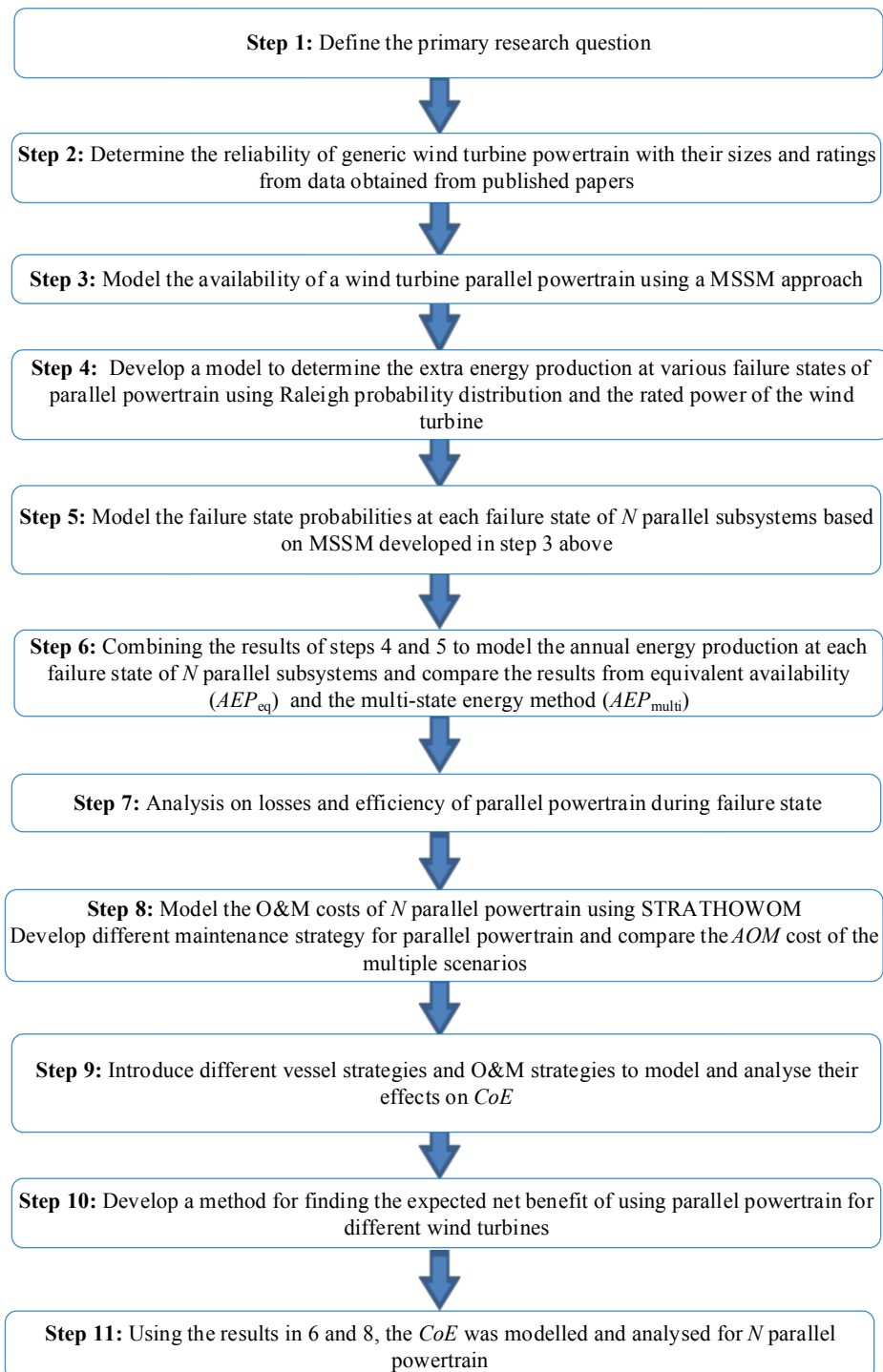


Figure 1.2 Steps to complete this Thesis

1.3 Structure

Every chapter consists of a short introduction/background section to the work carried out in that chapter, an overview of the methodology used to obtain the results shown in that chapter and finally a results section. The end of each chapter will have a conclusion sub-section. The references for each chapter are also provided at the end of that chapter. There will be an overall conclusion at the end of the thesis.

1.4 Motivation and Novelty of Research

The offshore wind site is associated with: (i) access challenge to the wind site (ii) potential for prolonged downtime, in part due to the powertrain (iii) expected high cost of energy for the offshore site. Halting the operation of the offshore wind turbine due to fault for a considerable time will definitely reduce the *AEP* and increase the *CoE*. Circumventing such scenario of complete zero energy or power production due to powertrain failures suggest the need for a powertrain design that will remain operational during failure of any components. With parallel powertrain configuration, availability improvement, extra energy production at failure states, ease of repair of smaller parallel units are possible. This research is novel because relatively few analyses have been carried out (or at least published on) in the following areas:

- Analysis of parallel powertrain components as a means of providing partial redundancy and availability improvements in wind turbine systems
- Potential of parallel powertrain to produce extra energy at failure states and consequently increase annual energy production of wind turbine
- Modelling of operation and maintenance costs for the parallel power train based on variations of failure rates resulting from scaling down of the ratings of the wind turbine powertrain

There are novel sections within each of the steps, 2-11, outlined in Figure 1.2. The novelty of each step/chapter is discussed in the following paragraphs.

- Step 2/Chapter 3:

The novelty in step 2 was in the reliability analysis carried out on a population of onshore and offshore wind turbine powertrains with particular attention to their sizes and ratings. This was done to establish how failure rate and repair rate may change as N increases and the size of the equipment in each parallel powertrain becomes smaller. Such analysis has scarcely been done and allowed for the novel comparison of wind turbine parallel powertrain with conventional singular subsystems. The result based on data from wind turbine industry and other industries show that failure rate and repair rates of electrical machines and powertrain components vary with their size. Details of this systematic approach used are explained in Chapter 3 and the findings from this work contributed to one of the IEEE journal publications (*“Parallel wind turbine powertrains and their design for high availability”*).

Step 3/Chapter 4:

The novelty in Step 3 was in the development of availability model for a wind turbine parallel powertrain using a MSSM. This was done to show the availability improvement of parallel powertrains. Relatively few analyses have been reported on the subject of parallel powertrain components as a means of providing partial redundancy and availability improvements in wind turbine systems. The results show that equivalent availability can be increased when using a parallel powertrain. Details of this systematic approach are explained in Chapter 4 and the findings from this work contributed to one of the IEEE journal publications (*“Parallel wind turbine powertrains and their design for high availability”*).

Step 4/Chapter 5:

The novelty in Step 5 lies in the development of a model to determine the extra energy production at various failure states of parallel powertrain using Raleigh probability distribution and the rated power of the wind turbine. This was vital to consider power not only at the rated power but to take into account the rest of the power curve. To address this, equations are developed that allow a baseline power curve to be modified so that a new rated power $P_{r,new}$ and rated wind speed $v_{r,new}$ can be used when there are failures in the parallel powertrain.

Details of this systematic approach are explained in Chapter 5 and the findings from this work contributed to one of the IEEE journal publications (“*Energy yield and operations and maintenance costs of parallel wind turbine powertrains*”).

Step 5/Chapter 5:

The novelty in step 5 comes from the modelling of the probability of failure at each state or failure mode such that the probability of one failure, two failures etc. could be analysed. The method adopted in this thesis was based on MSSM, to analyse the probability of failure at various transition states and was done for each parallel module/subsystem, N .

Details of this systematic approach are explained in Chapter 5 and the findings from this work contributed to one of the IEEE journal publications (“*Parallel wind turbine powertrains and their design for high availability*”).

Step 6/Chapter 5:

The novelty in step 6 comes from stepping forward from the idealized AEP in step 5 above to modelling of the AEP . The energy production was addressed using two methods (i) equivalent availability method ($AEP_{eq.}$) from step 3 and (ii) the multi-state energy method ($AEP_{multi.}$) using the idealized AEP in step 4 and the failure state probabilities developed in step 5. Details of this systematic approach is explained in Chapter 5 and the findings from this work contributed to one of the IEEE journal publications (“*Energy yield and operations and maintenance costs of parallel wind turbine powertrains*”).

Step 7/Chapter 5:

The novelty in this step was in the analysis of copper losses at failure states. This was then used to find the annual energy production comparing it with the AEP_{multi} earlier analysed in Chapter 5 where the losses were neglected. This is important to investigate the effect of parallel powertrain subsystem failures on the torque, I^2R losses and efficiency. Details of this systematic approach are explained in Chapter 5.

Step 8/Chapter 6:

The novelty in step 8 comes from the analysis of the effect on O&M cost of having more subsystems in a parallel powertrain. To do this, this research employs an offshore wind farm accessibility model and investigates the O&M costs as the number of parallel powertrain components varies. Details of this systematic approach are explained in Chapter 6 and the findings from this work contributed to one of the IEEE journal publications (“*Energy yield and operations and maintenance costs of parallel wind turbine powertrains*”).

Step 9/Chapter 6:

The novelty in this step is in the introduction of different vessel strategies and O&M strategies to model and analyse their effect on cost. Details of this systematic approach are explained in Chapter 6.

Step 10/Chapter 7:

The novelty in step 10 was in the development of net benefit model for a wind turbine parallel powertrain using the equivalent availability from step 3 and other variables, which include parallel powertrain cost, revenue due to parallel powertrain, availability of rest of turbine and other wind site parameters. This was vital to investigate the ‘net benefit’ expected from parallel powertrains because of their improved powertrain availability and was performed for a site with four different types of powertrain configurations. The results show that using larger N generally gives a higher net benefit, with the effect levelling out at different N for different powertrain types. Details of this systematic approach are explained in Chapter 4 and the findings from this work contributed to one of the IEEE journal publications (“*Parallel wind turbine powertrains and their design for high availability*”).

Step 11/Chapter 7:

The novelty in step 11 comes from the modelling of CoE for N parallel powertrain. To do this, the results of the steps above (AEP , AOM etc.) are used as input to the CoE model. This step was relevant in determining the cost of energy potential of the parallel powertrain compared to the baseline conventional powertrain. From the cost of energy modelling results, it can be seen that the cost of energy is lower for a parallel

powertrain than for an equivalent non-parallel powertrain (the best parallel powertrain has a 7% lower cost of energy). Details of this systematic approach are explained in Chapter 7 and the findings from this work contributed to one of the IEEE journal publications (“*Energy yield and operations and maintenance costs of parallel wind turbine powertrains*”).

1.5 Research outputs

Peer Reviewed Journals published:

[1] **G. Jimmy**, A. McDonald, J. Carroll “*Energy yield and operations and maintenance costs of parallel wind turbine powertrains,*” IEEE Transactions on Sustainable Energy (early access), 01 March 2019.

[2] A. McDonald and **G. Jimmy**, “*Parallel wind turbine powertrains and their design for high availability,*” IEEE Transactions on Sustainable Energy, vol. 8, no. 2, pp. 880-890, April 2017.

Peer Reviewed Conferences:

[3] Mueller M., Lopez R., McDonald A., **Jimmy, G.A.**, “*Reliability Analysis of Wave Energy Converters*”, IEEE International Conference on Renewable Energy Research and Applications (ICRERA), Birmingham, UK, 20-23 Nov. 2016

[4] **Jimmy, G.A.** and McDonald A., “*A study of Conceptual Parallel Powertrains for Offshore Wind Turbines Focusing on Availability*”, Power Engineering Conference (UPEC), Stoke on Trent, UK, 1-4 Sept. 2015

Chapter 2 Literature review

2.1 Introduction to wind turbine

Wind energy as a pollution free and clean renewable energy source has been in use for many years ago for milling grains, pumping water and other mechanical power application. It grew beyond mechanical power production to generation of electricity for powering houses, turning out as an easy solution for remote areas far from grid [6]. Initially, the device for mechanical energy production from the wind was called a windmill, but today as the technology evolved into generation of electricity from wind energy, the nomenclature of wind turbines, wind energy conversion systems, wind generators are now used. The first attempt to generate electricity from the wind has been attributed to the effort of Professor James Blyth in 1887 at Glasgow who built the energy conversion device (wind turbine). At the time, the electricity generated from the small scale wind turbine could only be used for battery charging and lighting of a single dwelling.

Globally, the demand for carbon emission reduction has grown drastically, necessitating search for a viable source of renewable energy for electricity generation. With the various pollution-free sources of energy, wind energy appears to be the most appreciated choice in terms of potential for improved technology and increased rate of installed capacity. In the year 2010, over 35GW of wind power was added to the total capacity which at the end of that fiscal year was well over 194GW and 539GW as at 2017 [7][8]. These figures represent a steady annual growth rate of about 15% with the likelihood of increment as innovation emerges while harnessing offshore site wind resources. With the current accelerated growth in the wind industry, it is anticipated that by 2030, in Europe, an installed capacity (i.e. maximum output expected under ideal conditions) of 150GW of wind power will be reached, covering 14% of EU electricity demand [9]. In view of the progress made annually, the EWEA target for installed capacity is observed to be changing, reflecting the high prospect and development in the industry [10].

In the UK, the growth of wind energy was reported to have risen above other sources of electricity production by about 37% on a particular day in March 2017 [11]. In the

first quarter of 2018, 63% of renewable energy production came from wind energy and this represents more than 19% of the UK's average electricity generation (amount of electricity produced over a specified period of time) of 90.1TWh [12].

2.2 Description of the wind turbine powertrain

The growth in wind power installed capacity and operating experience has resulted in different wind turbine powertrain configuration being designed and built. The term *powertrain* refers to the arrangement of gearbox, generator and the power converter together or any two or one of the components. In some sources, it is called the drivetrain [13][14]. In this thesis, the term powertrain is used more frequently.

Whatever the nomenclature, the powertrain acts as the energy conversion system within the turbine, changing the kinetic energy of the low rotational speed of the wind into high rotational speed (in the gearbox) and then converting this mechanical energy into electrical energy in the generator. The main aim of the powertrain is to obtain electrical power or generate electricity from the variable rotor speed and torque of the wind turbine. Figure 2.1 below shows some of the various parts of the wind turbine.

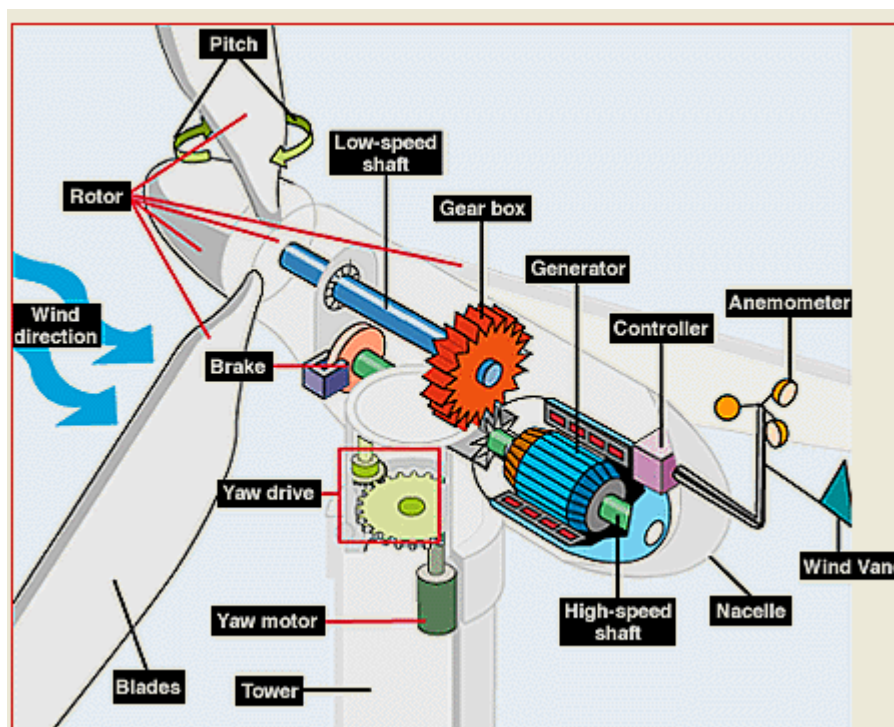


Figure 2.1: Wind turbine showing the various components and powertrain [13]

As a major part of the wind turbine, finding the best-optimised powertrain for continuous operation of the wind turbine is a major focus for academics and industry [14]. A significant percentage of the wind turbine downtime or unavailability is attributed to the state of the wind turbine powertrain components. Reliability, high availability, and efficiency may be described or evaluated as indicators of a good powertrain. Historically, wind turbine developers and manufacturers have considered the need to pay significant attention to the powertrain design during the developmental stage to achieve these performance indicators.

2.3 Gearbox

Most – but not all – turbines use a gearbox. The wind turbine gearbox acts as a torque-speed converter, changing the low speed of the wind turbine rotor to the high speed often required by the generators. Its purpose is to increase the low rotational speed of the wind turbine rotor to the desired rotational high speed required by the rotor of the wind turbine generator. Conversely, the torque is stepped down by the same ratio K .

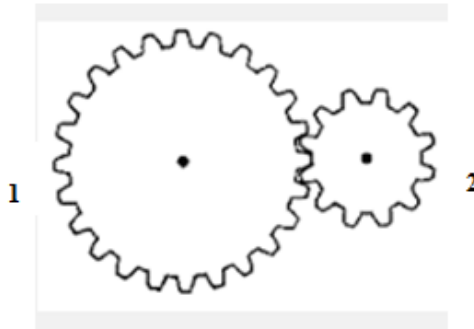


Figure 2.2: Simple gears

The gear ratio K is the ratio of speed N or radius R of the driven gear to the speed or radius of the driving gear. Normally if gear 1 is the driven and 2 is the driving, then the output of 2 is faster than the input of 1 as shown in Figure 2.2.

$$K = \frac{R_1}{R_2} = \frac{N_1}{N_2} \quad (2.1)$$

High-level gearbox equation for wind turbine powertrain is given as

$$\Omega_{\text{HSS}} = K\Omega_{\text{LSS}} \quad (2.2)$$

$$T_{\text{HSS}} = \frac{T_{\text{LSS}}}{K} - T_{\text{loss}} \quad (2.3)$$

where Ω_{LSS} and Ω_{HSS} are the rotational speed from the low-speed shaft and the high-speed shaft while T_{LSS} and T_{HSS} are the torque from the low speed shaft and high speed shaft respectively. From equations 2.1, 2.2 and 2.3, it can be seen that the speed ratio is exact while the torque ratio is not exact but have some losses T_{loss} .

2.3.1 Classification of Gearbox

Gearboxes can be classified based on the different stages in the gearbox system as single stage and multiple stage [15]. There are different types of gears inside the gearbox:

- Spur gear
- Helical gear

The spur gears have their teeth parallel to the axis of rotation. Their speed conversion ratio K is limited to relatively low numbers in order to maintain the noise level. Helical gears have teeth with a helix angle. The axial forces produced in helical gears tend to pull the gears apart, which have resulted to the use of contact bearing to keep these forces at a minimal level. They have better power, speed ratio and peripheral speed than the spur gears. Although industrial gearing systems use spur gears, wind turbine applications prefer the helical system to reduce noise level, vibration magnitude and improved load carrying capability with a resultant compactness in the overall gearbox structure.

2.3.2 Arrangement of gears

The gears in the gearboxes are arranged into parallel shaft and epicyclic gears. In parallel shaft gears, the shafts are all stationary in space. The gear wheels in this arrangement could be made of spur, helical or herringbone gears. In epicyclic gear trains, the gears are mounted so that the centre of one gear revolves around the centre of another. A carrier connects the centres of two or more gears and rotates to carry

some of the gears (the planet gears) around the other gear (sun gear) as shown in Figure 2.3. An outer ring (or annulus) which has inward facing teeth gear meshes with the planet gear or gear. An epicyclic gear train with a fixed ring and rotating planetary carrier and sun gear is called a planetary gear train. For the wind turbine gearbox, the planetary load carrier is connected to the low-speed shaft/rotor hub while the sun gear is attached to the higher speed shaft.

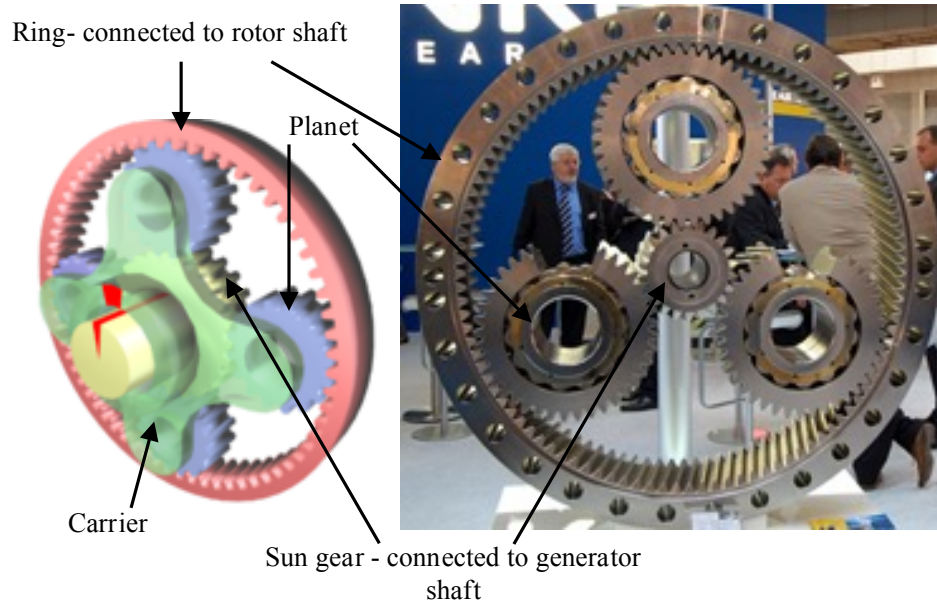


Figure 2.3: Simplified Arrangement of planetary gearing system [15][16]

The gear ratio of a planetary gear stage can be found using:

$$K = \frac{N_a}{N_s} + 1 \quad (2.4)$$

where the number of teeth on the sun gear is N_s and the number of teeth on the ring is N_a . For the gearbox to function, the equation below must be satisfied [2.12]

$$N_a = N_s + 2N_p \quad (2.5)$$

where the number of teeth on the planet gear is N_p

Planetary gears are typically classified as simple and compound planetary gears. The simple planetary has one sun, one outer ring, one carrier and one planet set. A multistage system has two or more planets sets and allows a higher overall step-up ratio.

One of the benefits of the compound planetary system is the possibility of getting a larger transmission ratio with equal or smaller volume [16]. Gearboxes could have compound planetary with multistage of the same type of gears in order to increase the speed ratio. Some of the wind turbine gearboxes usually have three stages which are made of one planetary and two parallel stages or two planetary and one parallel stage. Each stage is typically limited to a gear ratio of $K \leq 5$. To have larger overall gear ratio, several stages are used. Wind turbines generally require more than one stage. Figures 2.4-2.8 show different types and stages of planetary gearbox [17].

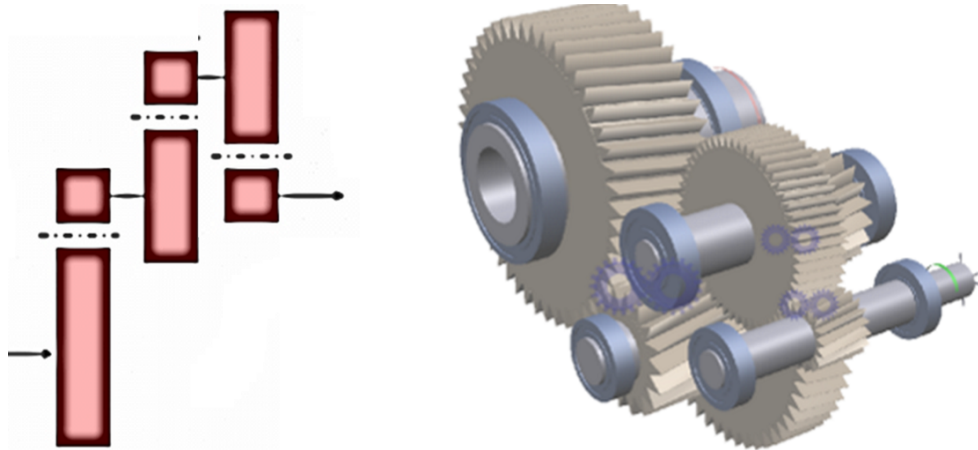


Figure 2.4: Helical gearbox (3-stage) [17]

In Figure 2.4, the gearbox is mounted with helical gears. This type of gearbox can be found in a standard industrial application with power output reaching 750kW.

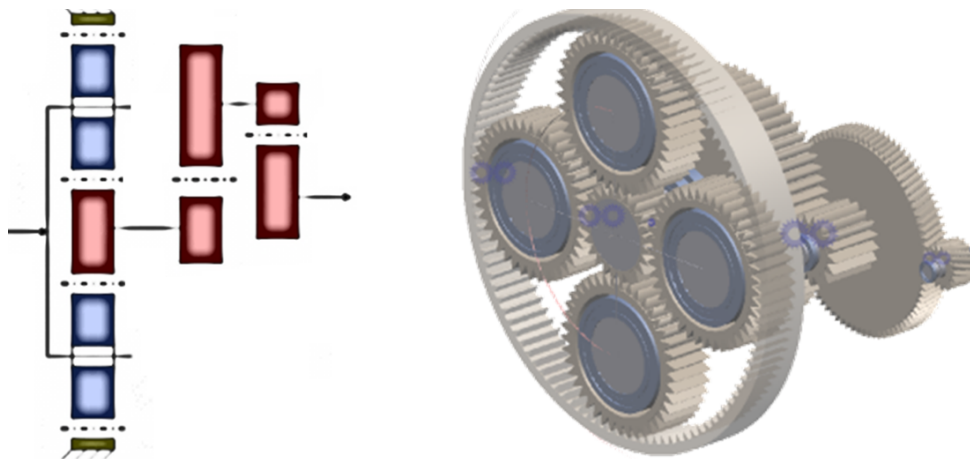


Figure 2.5: Planetary gearbox with one ring (3-stage) [17]

The first helical gear shown in Figure 2.4 could be replaced with a planetary gear stage giving rise to the gearbox shown in Figure 2.5. This type of gearbox has higher power output and may be suitable for turbines with 750kW to 2000kW.

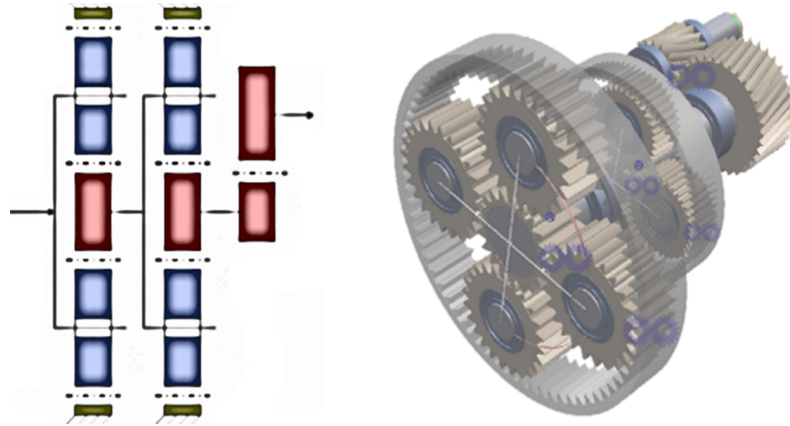


Figure 2.6: Planetary gearbox with two rings (3-stage) [17]

From Figure 2.6, two planetary gear stages are used in the gearbox design, which may be useful for turbines with 2500kW to 5000kW.

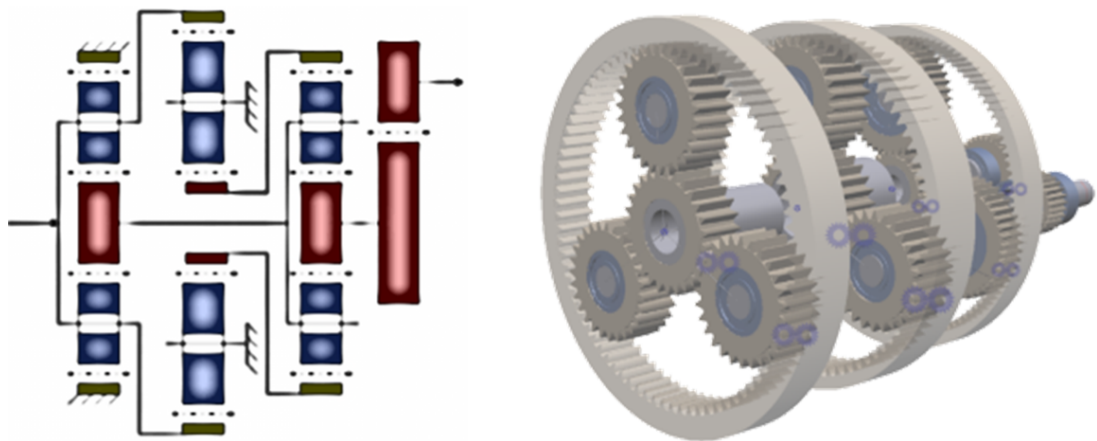


Figure 2.7: Extended planetary gearbox (4-stage) [17]

The gearbox design in Figure 2.7 has two planetary stages with a power split, one differential and one spur gear stage. The benefit in this design is the ease in servicing the parallel design and the weight reduction capability.

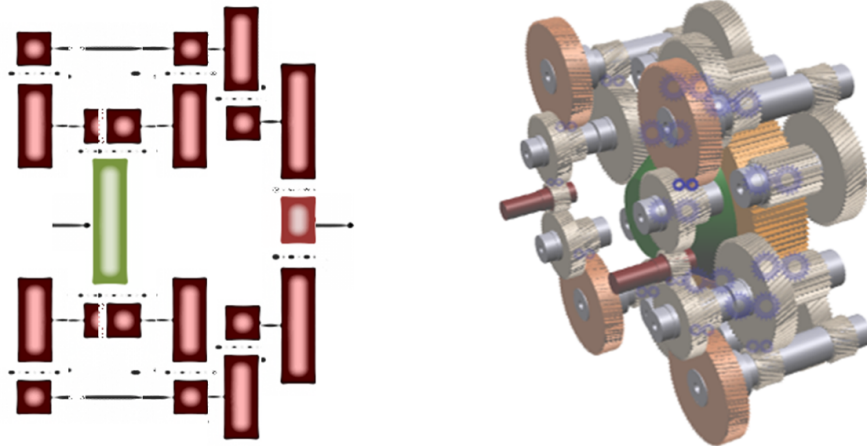


Figure 2.8: Multistage gearbox (4-stage) [17]

Considering the offshore wind turbine requirements, the design in Figure 2.8 with multi-power-split could be useful. This design is based on helical gear stages and could have up to two generators on the high-speed side for variable power output. Interestingly, this gearbox has high power density, lightweight design and potential application for the parallel powertrain design.

Some benefits have been added to the planetary gears system [16]:

- High power density
- Reduction in volume, multiple combinations, torsional reactions and coaxial shifting
- Increased high torque density
- Even distribution of load between planets

However, inaccessibility, design complexity, constant lubrication requirements and high bearing loads are amongst the downsides of the system.

2.3.3 Comparison of Gear arrangement

Most of the wind turbine gearbox designs have one or two planetary stages with one or two helical stages at the high-speed end. The best choice gearbox is one that has a balance of low weight and cost, and high compactness, reliability and efficiency. Some authors have made decision based on overall size, weight and cost of each arrangement. In wind turbine designs, the size and the weight of the gearing system will affect the tower designs as they contribute to the THD of the nacelle. In terms of size and the weight, the planetary gear arrangement seems to be a preferred option.

Table 2.1: Comparison of Gearbox arrangements showing both planetary (P) and helical (H) gears [18]

Gearbox ratio	Gearbox type	Stage 1	Stage 2	Stage 3	Number of planets	Relative volume	Relative weight	Relative cost
10:ratios	2PH	P	H	NA	5	1.43	1.25	1.12
20:ratios	2PH	P	H	NA	5		1.52	1.21
40:ratios	3PHH	P	H	H	5	2.1	1.52	1.45
60:ratios	3PPH	P	P	H	5,4	1.11	1.28	1.25
80:ratios	3PPH	P	P	H	5,4	1.06	1.32	1.26
100:ratios	3PPH	P	P	H	5,4	1	1.28	1.2
120:ratios	3PPH	P	P	H	5,4	1	1	1

Table 2.1 shows different gearbox arrangements with their relative volume and cost advantage, based on the optimal design in each band of gearbox ratio [18]. The 3PPH appear to have the lowest cost. It appears that the increase in the number of stages does not necessarily result in increase in the weight and cost. As the ratio exceeds 40:1, the two planetary stages and one helical stage seem better than the one planetary stage and two helical stages [18].

2.3.4 Losses in gearbox

Losses in the gearbox occur because of the friction existing between moveable contact parts like the gear teeth, rolling elements and the bearing raceways. Some other losses include losses due to meshing of gear teeth, losses resulting from gears dipping into oil, bearing losses and losses coming from the seals of gearbox. The friction between gear teeth will normally result in power loss, reduced efficiency and at the same time influence the operating temperatures of lubricant. Frictional losses have been reported to be responsible for gearbox degradation, wear, tear, failure and the eventual reduction in the reliability and expectancy of the gearboxes. Although the efficiency of wind turbine gearbox has been evaluated as 95% with heat loss of 150kW for 3MW capacity, it is likely to have higher losses as the rating increases beyond 6MW [19]. According to [20], planetary gearing system accounts for 1% power loss, while helical gear may have up to 2% loss per stage. It has been suggested that a viscous loss of 1% is quite reasonable and that the losses are proportional to the speed as shown in the equations below [15][21][22][23],

$$P_{\text{gearbox loss}}(n) = x P_{\text{rated}} \frac{n}{n_{\text{rated}}} \quad (2.6)$$

where x is the losses in percentage, n is the actual rotational speed (r/min), n_{rated} is the rated rotational speed (r/min)

$$P_V = P_{VZO} + P_{VZP} + P_{VLO} + P_{VLP} + P_{VD} + P_{VX} \quad (2.7)$$

where P_{VZO} is the no-load gear loss (kW), P_{VZP} is the load-dependent gear loss (kW), P_{VLO} is the no-load bearing loss (kW), P_{VLP} load-dependent bearing loss (kW), P_{VD} is seal loss (kW) and P_{VX} is the auxiliary loss (kW). The load-dependent gear loss P_{VZP} in the mesh during power transmission could follow the basic coulomb law [24]:

$$P_{VZP} = F_R \cdot v_{\text{rel}} \quad (2.8)$$

where F_R the friction is force in KN and v_{rel} is the relative velocity in m/s

Gear and bearing losses have been described as the major contributor to the overall power loss in the gearbox and can be divided into no-load losses and load-dependent losses [24][25]. No-load losses can occur without power transmission. They are related to the viscosity and density of lubricant and to the immersion depth of the components. Consequently, the no-load gear losses will depend on these two important properties. The no-load bearing losses depend on the bearing type, size, arrangement, lubricant viscosity and supply.

Load-dependent losses will normally occur in the contact of power transmitting components and depend on transmitted load, coefficient of friction and sliding velocity in the areas of contact. The load-dependent bearing loss is a function of the bearing size and type, load and sliding condition and on the type of lubricating oil.

The efficiency of the gearbox which is the ratio of power output P_o , to power input P_i is often reduced by the losses and is given as:

$$\eta = \frac{P_o}{P_i} \quad (2.9)$$

The difference between the power input and the power output is the total power loss P_V ,

$$P_V = P_i - P_o \quad (2.10)$$

2.3.5 Problems and downtime of gearbox

Operational experiences so far in the wind turbine industries have identified the gearboxes at the megawatt rated power level as the weakest-link-in-the-chain component. Wind gust and turbulence are seen to most frequently causing the misalignment of the wind turbine powertrain resulting in the incessant failure of the gear components [26]. The failures in the gearbox of wind turbine have a resultant effect in increasing the overall operating cost, increasing the downtime and reducing the reliability. The gearbox system which converts the rotor blade rotational speed from 5-22 rpm to the generator required rotational speed of 1000-1600rpm is estimated to have a failure frequency of five years (approximately 0.24 annual failure frequency), requiring replacement [60]. The problematic maintenance issue associated with the gearboxes of the wind turbine has precipitated numerous research and pragmatic suggestions for innovative designs that circumvent the use of gearbox such as direct drive system.

Inability to account and identify the critical design load, unpredictability of the transfer loads between gearbox and the mounting fixtures and the unreliability of the individual components of the gearbox system of wind turbine has been identified as the common causes of the gearbox failures [28]. The early years of wind turbine development were submerged with failures due to gearbox design errors thereby initiating a collaboration with wind turbine industry, gearbox manufacturers, bearing consultants and designers, lubrication engineers which resulted in international designs standard of gearboxes [28][29]. It was reported by [26] that in 2006, German Allianz received damage claims of 1000 wind turbines leading to maintenance plan requirements of gearbox replacement at 4-5 years interval. This herculean and costly task is reported to have created a 10% upsurge in installation and construction cost of wind turbines [30]. Gearboxes normally do not fail very often but they can have a prolonged downtime when failure occurs as predicted in [31].

2.4 Generators

Globally, generation of electrical energy from the wind is increasing rapidly. One challenge with the wind turbine is that of converting a variable low-speed wind impinging on the rotor into a fast and steady alternating current (AC) output for the grid network. The electrical generators play a very dominant role in this energy conversion process. In [32], four major generators used in the wind turbine were identified as Induction Generators (IG), doubly fed induction Generators (DFIG), Electrically excited synchronous Generators (EESG) and permanent magnet generators (PMSG).

2.4.1 Squirrel cage induction machines-generator

Induction machines either as motor or generators have a wide range of application in the industry today. For domestic use, they are found in for example fans and pump applications. They have a near-constant speed operation and the rotor does not require direct excitation as in the case of synchronous machines. When delivering a torque, they operate at speed less than the synchronous speed – if a motor – hence the name asynchronous machine.

When connected to an AC grid, voltage is induced into the rotor winding. A large current flow around the bars and a magnetic field is generated inside the rotor causing the machine to rotate. The rotor magnetic field follows the rotating stator magnetic field, lagging slightly behind it for a motor. The difference in rotational speed between the stators rotating magnetic field (stator synchronous speed, N_s) and the rotor speed (N_r) is referred to as the slip, s . This slip must exist for torque to be developed in the rotor shaft.

$$s = \frac{N_s - N_r}{N_s} \quad (2.11)$$

Attaching a heavier load to the machine means that there is a need for a stronger rotor magnetic field. This increase in field strength needs a stronger rotor MMF. As rotor MMF is proportional to the rotor current, it needs a rotor voltage, and the only way that this can be achieved is by having a larger rate of change of flux linkage, i.e. a

slower rotor speed. The same principle applies for squirrel cage induction generator, although the rotor speed must always be above the rated synchronous speed.

Squirrel cage induction machines can be used for variable speed operation with full rated converters in wind turbines and are cheaper to manufacture when compared to the wound rotor type [33][34]. The Middelgrunden offshore wind turbines in Denmark are equipped with the squirrel cage induction generators with annual energy production of 89GWh per year [35].

2.4.2 Wound rotor induction generator

The arrangement of the structure in terms of the stator is same as in the case of the squirrel cage. The core rotor is a solid laminated steel core with slots on the outer surface to carry the rotor windings which is a distributed polyphase winding similar to that of stator and of same number of poles. The phases are star connected with ends attached to slip rings making contact with carbon brushes.

In terms of cost, squirrel cage machine is cheap, robust and almost maintenance free due to the absence of moving contacts and has good application in adverse weather condition like areas prone to explosive and contamination. The key setback in this machine is the low starting torque and the large starting current.

The wound rotor generator when compared to the squirrel cage can achieve high starting torque and low starting current by the introduction of external resistance via the slip rings. Deployment of resistance gives the added advantage of having minor speed control. It is however more expensive than the cage type and prone to failures due to damaged brush gears and slip rings.

In a wound rotor machine, resistances are placed in series with the rotor windings during starting to decrease the starting current, locked rotor current while increasing the starting torque and locked rotor torque. When used in wind turbine, the variation of the rotor resistance allows the slip and thus the power output in the system to be controlled leading to maximum power point tracking [36]. Varying wind speed of the wind turbine allows maximum power to be extracted from the wind. This involves adjusting the generator terminal frequency and hence the turbine shaft speed.

2.4.3 Doubly fed induction generators

These induction generators have windings on the stationary (stator) and the rotating part (rotor) with both windings transferring electrical power with the electrical system. The stator is attached to the grid while the rotor winding is fed from/to the grid via a frequency converter as shown in Figure 2.9. It has multiphase wound rotor and slip ring with brushes for connection to the rotor windings. An alternative to the slip ring assembly is the use of brushless doubly fed induction generators, although these machines are still in development [37].

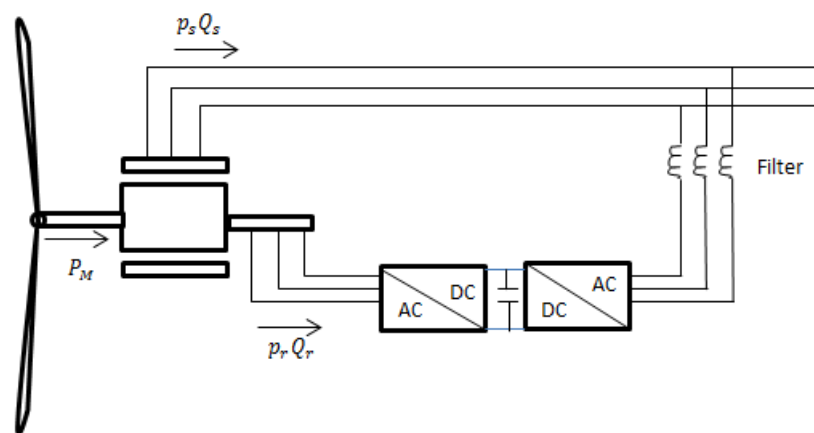


Figure 2.9: Doubly-fed induction Generator [37]

The rotor windings are connected to the grid via slip rings and a back to back voltage source converter which controls both the rotor and the grid currents making it possible to adjust active and reactive power ($P_r Q_r$) fed to the grid. Active and reactive power ($P_s Q_s$) can be controlled independently. Also, the current and voltage control allows synchronisation of the machine with the grid while the turbine wind speed varies. Cost is reduced since it can operate with the frequency converter rated at 30% of the total power.

2.4.4 Electrically Excited Synchronous Generator

Synchronous generators are normally of two types depending on the excitation method of the rotor. The rotor poles are excited either by permanent magnet – and thus called a PMSG – or by a dc current source – thus described as Electrically excited synchronous generator.

In the latter machine, the field windings are wound on the rotor and the armature is on the stator. The stator core is made of laminated and insulated steel. The core is slotted and the armature windings are placed in the slots. The rotor field is either made of the non-salient pole type or salient pole type. The non-salient pole types are known as cylindrical rotor, and it is common for these machines to be high speed with only two or four poles. Salient pole rotors are made of laminated poles with the winding under the pole head.

When voltage V_1 is applied to the armature winding around the core, a rotating magneto motive force (MMF) of constant magnitude F_s will be produce. The MMF will act upon the reluctance in its path resulting in magnetic flux ϕ_s . The speed of the revolving magnetic field n_s has a relationship with the supply frequency f and the number of the poles p as shown in the equation 2.12 [38]:

$$n_s = \frac{120f}{p} \quad (2.12)$$

When used in wind turbine, the generator stator is interconnected to the grid through a full-scale frequency converter as shown in Figure 2.17.

2.4.5 Permanent Magnet Synchronous Generator

The permanent magnet generator is the opposite of the EESG in terms of the excitation source; in this case, the field is excited by a permanent magnet instead of a coil. Synchronous generators have their rotor and magnetic field rotating at the same speed. The rotor magnetic field is generated through permanent magnet assembly that is mounted onto rotor yoke, attached to the shaft. As the rotor rotates, an emf and hence current is induced in the stationary armature. Normally the rotating assembly called the rotor, which contains the magnets, is positioned at the centre of the generator and the stationary armature (stator) which has three sets of coils representing three phases are electrically connected to a load.

The permanent magnet generator eliminates losses from the rotor coil excitation and does not require the use of slip rings and brushes. The cost of permanent magnets is a major economic issue coupled with uncontrollable air gap flux which makes it difficult to regulate the voltage of the machine. The strong magnetic field strength creates an

unsafe situation during installation, assembly, repairs and servicing [38]. The permanent magnet generator has a wide range of application in the wind energy turbine having greater potential for the offshore wind farm when compared to the Field excited machines.

2.5 Power converters

2.5.1 Description of power electronics

Power electronic technology is used to convert electrical energy or power from one form to another in order to match the application characteristics. It involves the application of solid state devices for the control, processing conversion of electrical power. In modern power electronics systems, the conversion is performed using semiconductor switching devices such as diodes, thyristors and transistors. Power electronics has found numerous applications in both consumers' electronics devices such as television sets, personal computers, battery charges and in industrial equipment like variable speed drives for induction motor control. The power conversion process is achieved based on the nature of the input and output power: DC to AC (inverter), AC to DC (rectifier), DC-to-DC (converter), and AC-to-AC (converter). Some applications require combinations of these input and output power conversion units as a whole system described as power converter [39].

2.5.2 Power converter in renewable energy

Most renewable energy systems such as the photovoltaic cells PV and wind energy normally have a set of optimal operational conditions (frequency, voltage) which represent good energy capture/conversion efficiency but the power quality may not match the grid requirements or consumer specification. The power converter is then used to provide the needed connection between the generation units and the grid/consumer system to achieve high efficiency, good power quality and meet the grid code including frequency, voltage, harmonics, flicker, active and reactive power and ride-through capabilities [39]. Consequently, they are becoming increasingly useful in the development of modern wind energy systems.

2.5.3 Types of power converter

The rapid development of power electronic technology has emerged with the development of semiconductor devices, circuit topologies, modulation and control methods been constantly improved to meet the required efficiency performance and cost driven objective in the wind energy industries. The semiconductor, as the main component in the power electronic circuit acts as a switching device. Three classes are shown in Figure 2.10.

The two key parameters in the semiconductor device are the rated current and the breakdown voltage, which are constantly increasing. New developments in the semiconductors device are been researched for improved materials like SiC with the capability of increasing the power density of the converters [39].

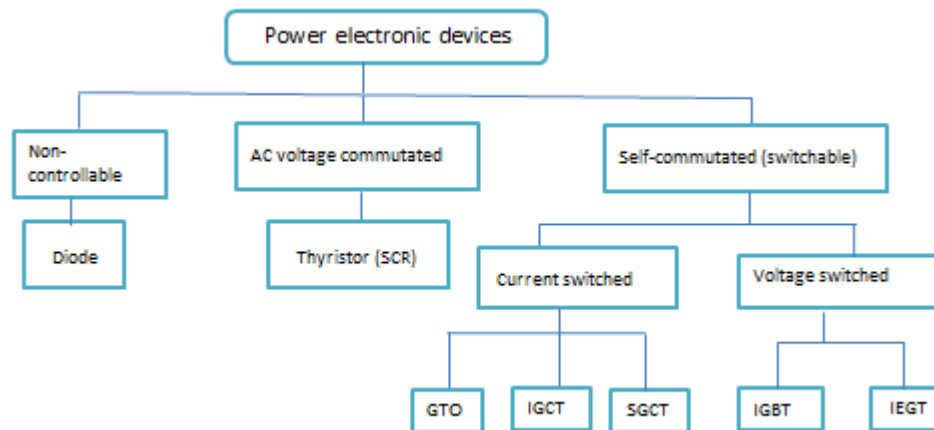


Figure 2.10: Different classes of semiconductors [39]

The self-commutated semiconductor devices may be further divided into current-switched and voltage-switched devices depending on the required gate characteristics. Turning a current switched device on or off requires a gate current while turning a voltage switch devices on or off depends on gate voltage. Current switching devices mainly include IGCTs (Insulated Gate Commutated Thyristors), SGCTs (Symmetrical Gate Commutated Thyristors) and GTOs (Gate Turn-Off Thyristors) while the voltage switched devices include IGBTs (Insulated Gate Bipolar Transistors) and IEGTs (Injected Enhanced Gate Transistors). Most commonly used switching devices are the IGBTs and IGCTs. Although the IGCT has a high maximum current rating, its maximum switching frequency is low. The high switching speed of the IGBT has the

capability of improving the harmonics performance at the expense of high switching losses. IGBTs have wider applications in power electronic converters and are available for higher voltage ratings (up to 4500V) and current ratings (3000A).

Power electronic converters are constructed with semiconductor devices, driving, protection and control circuits to perform the conversion and control of voltage /current magnitude and frequency. The converters may be classified as shown in Figure 2.11 below depending on the particular type of devices used.

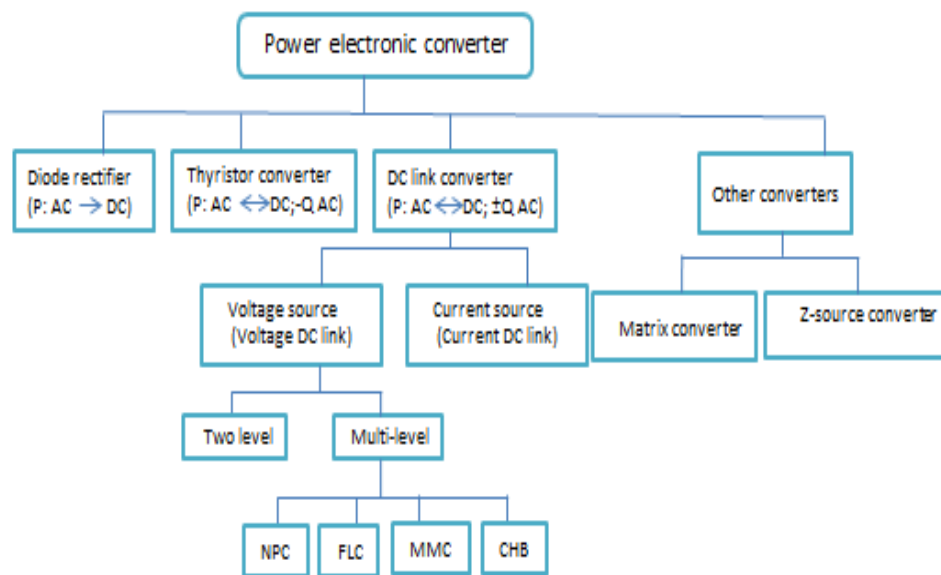


Figure 2.11: Classification of AC↔DC power converters [39]

A diode rectifier can only convert AC into DC power. The grid-commutated converters with high power capacity thyristors are mainly used for very high voltage and power applications such as conventional HVDC systems and synchronous motor drives. A thyristor can transfer active power in both directions (AC→DC or DC→AC), but consumes inductive reactive power and is not able to control the reactive power. The self-commutated converters can transfer active power in both directions i.e. AC→DC or DC → AC and can control the AC side of the reactive power in both directions (inductive and capacitive). The most common types in use are the DC link converters, which divides into VSC and CSC depending on the type of DC link as shown in Figure

2.12. Most of the power electronic converters used in wind power turbines are the VSC.

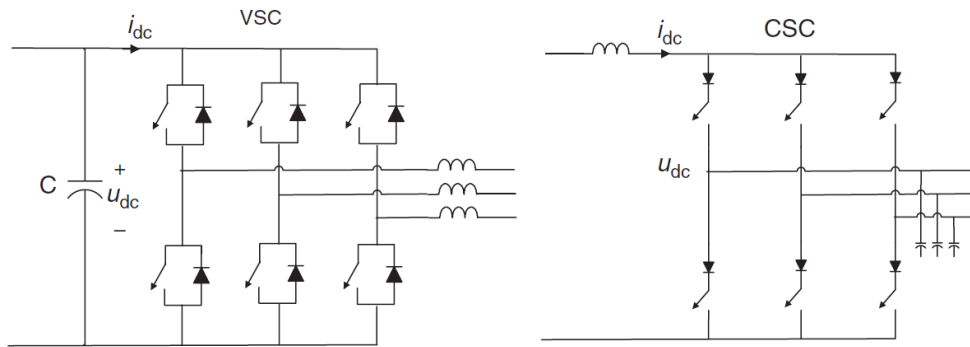


Figure 2.12: Three phase 2-level VSC and Three phase 2 level CSC [39]

Based on high power and lower harmonics operation, power converters may be designed for multi-level configurations. Multi-level converters include Neutral Point Clamped (NPC), Flying Capacitor Converter (FLC), and Multi-level and Cascade H-Bridge (CHB) converter [39] as shown in Figure 2.13. Multi-level converters have the capability of varying their output between several voltage levels thereby improving the voltage waveforms, reducing filtering requirements, common mode voltage and electromagnetic interference impact. Three-level NPC are readily implemented with IGBT and IGCT, making it applicable in large wind turbine generators.

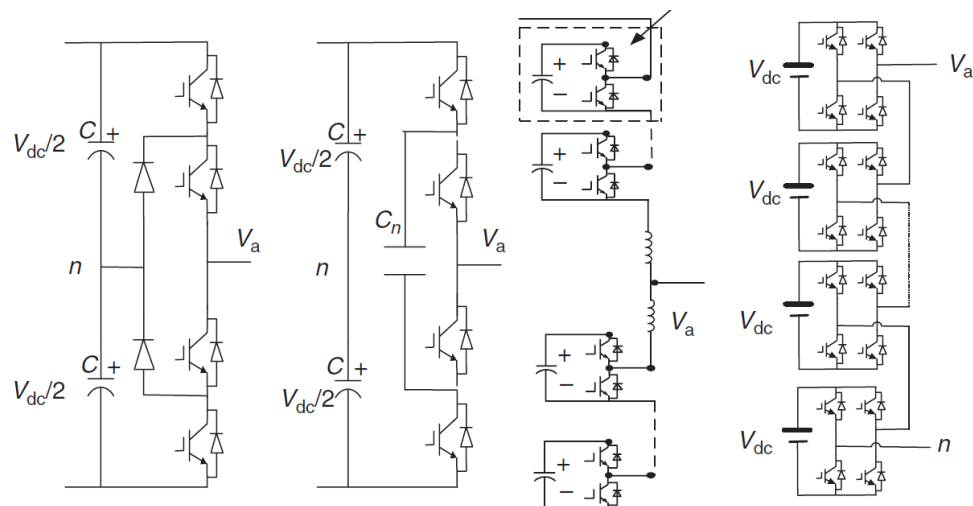


Figure 2.13: Types of Multilevel converters [39]

2.5.4 Early years of power electronics converters in wind turbine systems

During the nascent stage of the wind turbine, impact on the transmission grid and the power system distribution network was imperceptible even with the direct grid connection strategy. Then the generators were directly connected to the grid with no interface of power electronic components. Though capacitor banks were installed in the powertrain, they were for power factor correction at the point of coupling. The variable characteristics of the wind often create pulsating power output from the generator and transferred it to the grid in the absence of power converters. Power quality was compromised limiting the dynamic active power and reactive power control due to total or partial absent of power electronics control capabilities that are now dominant in modern wind turbine control systems. Power electronics utilisation in the wind industry has now grown from the initial thyristor-based soft starter used in 1980s to the rotor resistance control with a diode bridge which was used in the 1990s, as depicted in Figure 2.14. Today, as the wind turbine sizes increases, changing grid requirements, improved output power quality in terms of regulated frequencies and voltages have precipitated the need to install power converters as a link between the powertrain and the grid [40]. With the power electronics, the mere characteristics of the wind turbine being a source of electrical energy has changed to active power source for the grid [40].

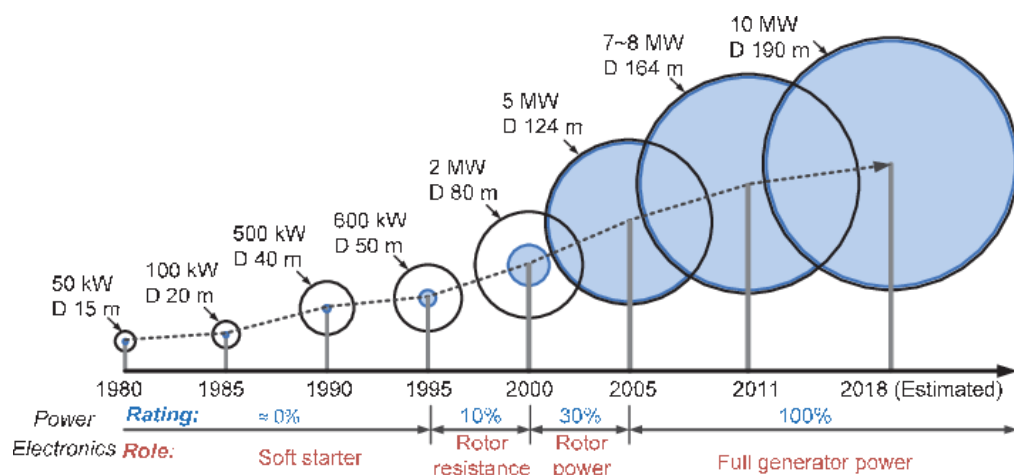


Figure 2.14: Wind turbine growth and trend of power electronic converter [40]

2.5.5 Power quality demand

In 2003, German electricity distribution company E.on Netz GmbH placed some new code requirements on the wind turbine operators, demanding or aiming at built-in capacity for active grid support in event of major grid fault [2.38]. Inadvertently, certain demands were placed on the various wind turbine converters to improve the power quality as shown in Figure 2.15 and Table 2.3.

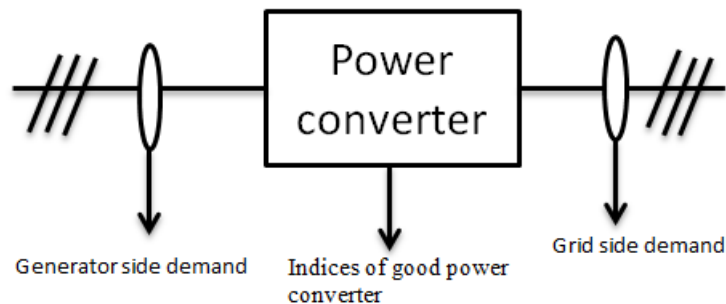


Figure 2.15: Demand of power quality [40]

Table 2.2: Requirements of wind turbine power converter

Power quality demand from wind turbine Converter		
<p>Generator side</p> <ul style="list-style-type: none"> ▪ Control of stator current to adjust torque and rotational speed ▪ Handling of the generator variable frequency and voltage amplitude 	<p>Grid side</p> <ul style="list-style-type: none"> ▪ Compliance with grid codes irrespective of wind speed variation ▪ Control over inductive & capacitive reactive power, Q ▪ Perform timely response to active power P ▪ Stabilise the frequency and voltage amplitude at specified value ▪ Maintain low level of total harmonic distortion of the current 	<p>Indices of good Power converter</p> <ul style="list-style-type: none"> ▪ Cost effective ▪ Easy to maintain - quick replacement ▪ High reliability ▪ High power density ▪ ity potential-redundancy for continuous operation ▪ Active power storage capability

The demand on every power converter used in wind turbines is of two fold, basically on the generator and the grid sides as shown in Figure 2.15. To achieve the expected power quality, the converter will have to control the current flowing in the generator stator thereby adjusting the torque and the rotating speed. Moreover, the variable frequency and the voltage amplitude of the generator output require control by the

converter. The result of generator side control produces active power balancing during normal operation and in the event of grid fault. On the grid side, control of the reactive (inductive/capacitive) power is required and fast response performed on the active power. The varying voltage and frequency is stabilised at a fixed value while the total harmonic distortion of the current is kept as low as possible.

2.5.6 Wind turbine power converters

Early years wind turbine development favoured the design of the fixed speed wind turbines, using induction generators IG without power converters. The stator of generator windings was directly connected to the grid. Partial rated frequency converters (rated at 30% of the generator) are commonly used with DFIG, to give variable speed-controlled wind rotor on the rotor circuit. As shown in Figure 2.16, the stator is connected directly to the grid while the rotor of the generator is coupled to the partial scale power converter to control the frequency and speed of the rotor. Here the frequency converter offers smooth grid connection over a limited range of the speed. This concept uses slip rings and lacks capability of offering any or full grid fault protection and control.

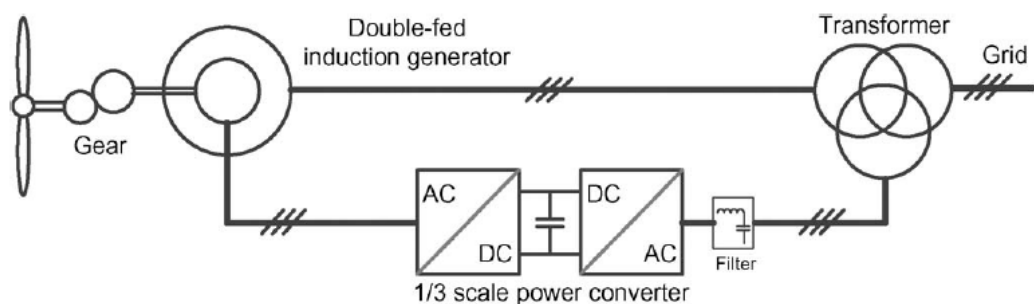


Figure 2.16: Partial rated converter [40]

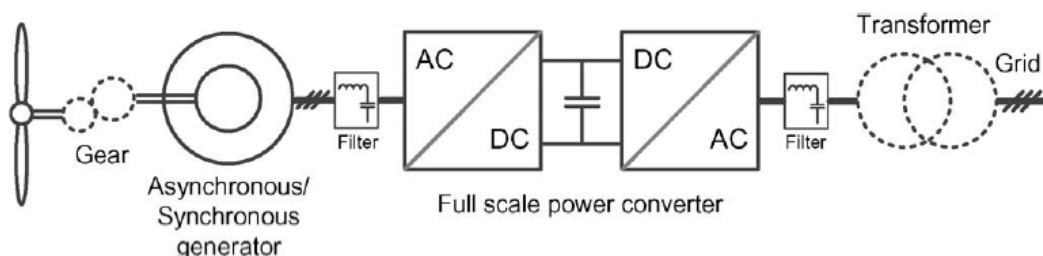


Figure 2.17: Full rated converter [40]

Using FRC in the variable speed wind turbine allows the converter to perform reactive power control and smooth grid connection for the entire speed range. The stator of the generator is connected to the grid via full rated converters as shown in Figure 2.17. Most recent offshore wind turbine manufacturers have preferred option for full rated power converter with SCIG, PMSG, WRIG and direct drive generator DDG [40][41]. At the moment, most of the commercially available wind turbines have half rated back-to-back power converters while some are integrated with full scale power converter [42]. As wind turbine sizes increase, the challenge for power control becomes obvious, hence solutions to tackle the various power level has been suggested. The diode bridge seems best for the lower level power (less than 1MW) while the two level VSC and the multilevel converters may suit the high power applications [40][43].

The pulse width modulation (PWM) VSC with two level output voltage (2L-PWM-VSC) has gained much popularity amongst three phase converters in the wind turbine industry. It consists of two bidirectional PWM VSC connected back to back in such a way that one is on the generator side and the other on the grid side. Both converters share a common DC link. The integration of the two level back-to-back 2L-BTB shown in Figure 2.18 allows a simple structure and few components usage creating better reliability performance. The use of PWM VCS allows the control of both active and reactive power at its AC terminals, while the BTB optimises the generator operation and satisfies the grid integration demands. It has application in the DFIG design with many manufacturers using the FRC with the SCIG [41][42][44]. One key setback of the configuration is the increase in switching losses and lower efficiency as the power and voltage range of the wind turbine assume the MW and MV level.

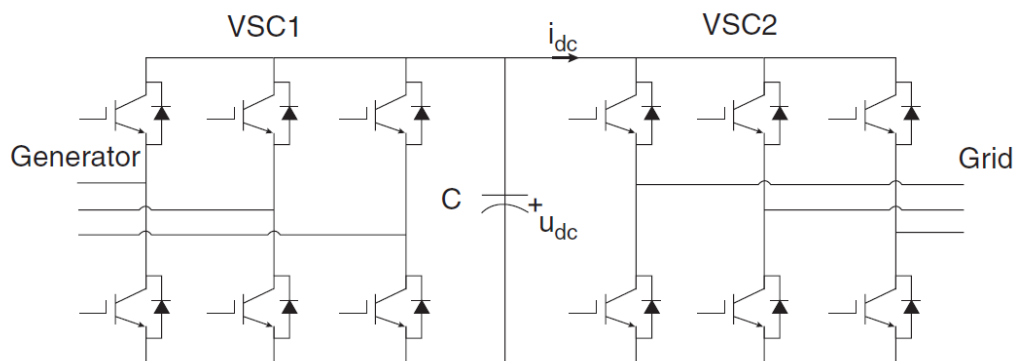


Figure 2.18: Two level back-to-back voltage source converter [39]

For power and voltage at the mega level, the multilevel converters shown in Figures 2.19-2.22 may be regarded as a better solution than the 2L-BTB topology, offering capabilities of higher output voltage levels, higher voltage amplitude and larger output power [45][46]. Three classifications of the multilevel converters as shown in Figures 2.19-2.22 have been identified [46][47][48]: neutral –point diode clamped structure, flying capacitor clamped structure and cascaded converter cells structure. The multilevel converter has been considered cost-effective when used in the 3MW-7MW range [40]. The Three level neutral point diode clamped back to back (3L-NPC BTB) shown in Figure 2.19 is a readily available version in the wind turbine market today, similar to the 2L-BTB in terms of the back to back design.

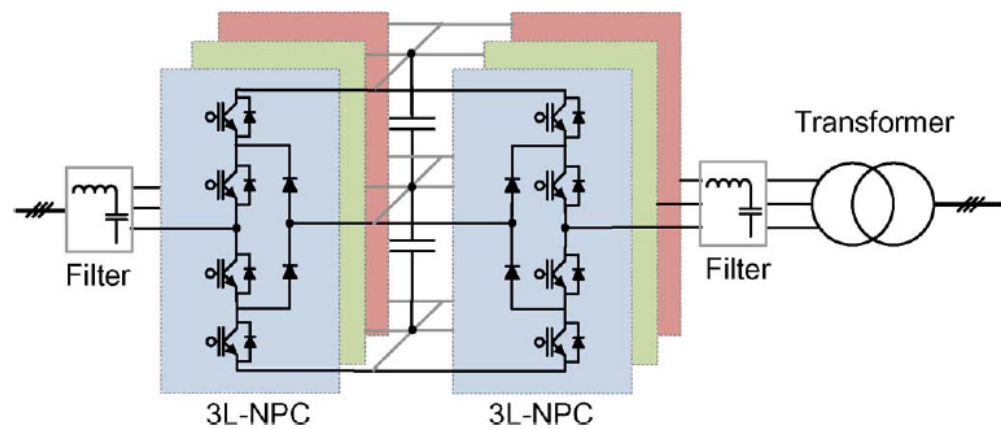


Figure 2.19: Three- level neutral- point diode clamped back-to-back converter [40]

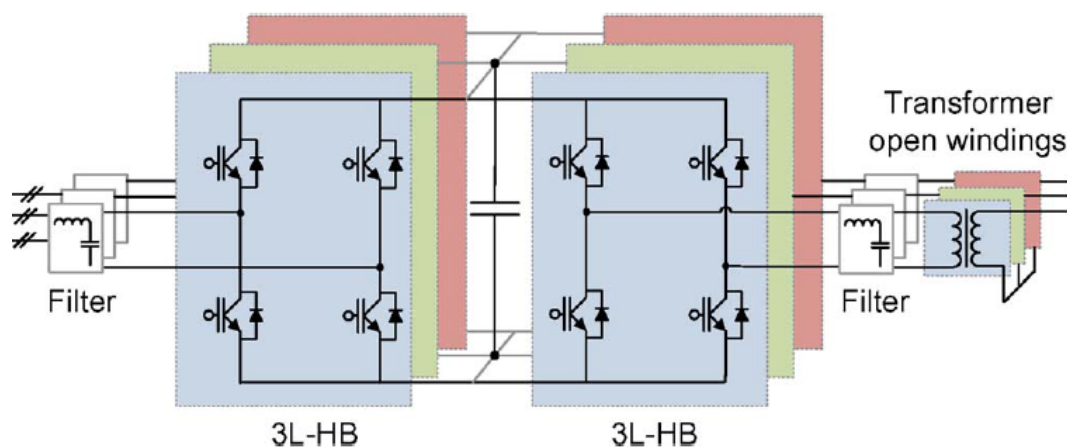


Figure 2.20: Three- level H-bridge back-to-back converter [40]

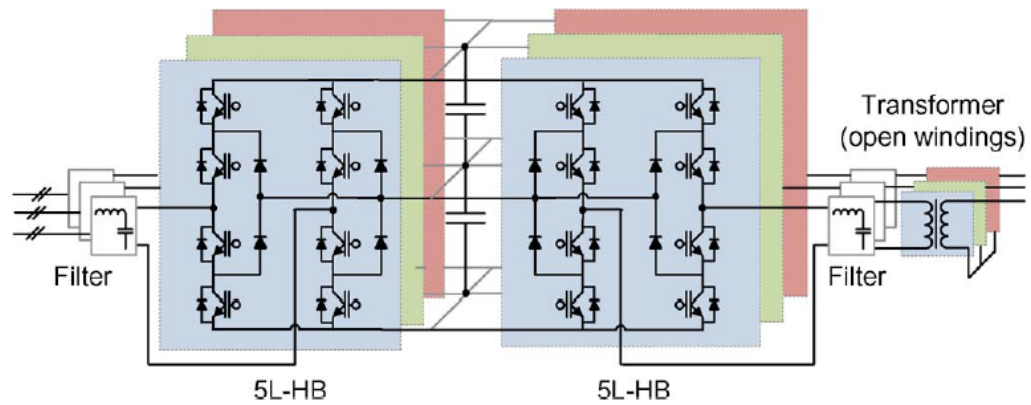


Figure 2.21: Five-level H-bridge back-to-back converter [40]

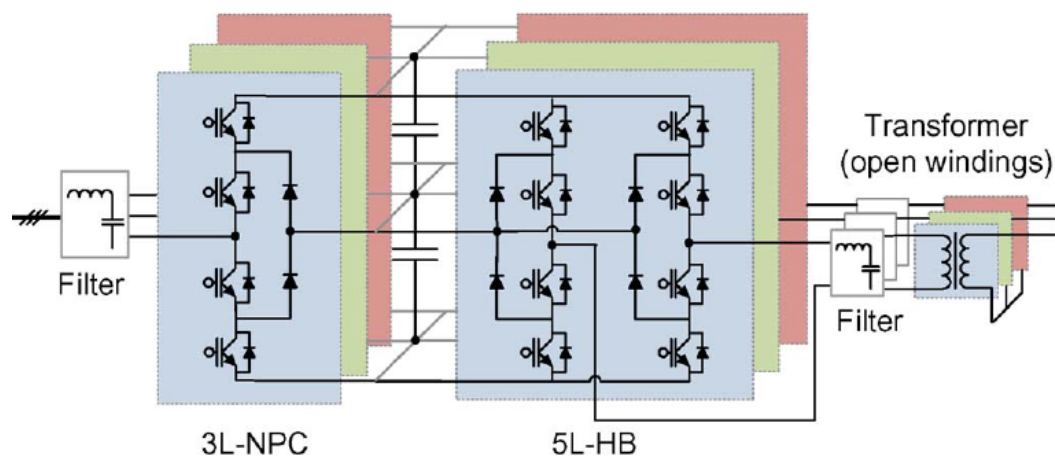


Figure 2.22: Three-level neutral-point clamped and five-level H-bridge converter [40]

Other promising multilevel topologies include: Three level H-bridge back to back (3L-HB BTB) shown (in Figure 2.20), Five level H-bridge back to back (5L-HB BTB) which is an extension of the 3L-HB BTB and the Three level neutral point diode clamped 3L-NPC BTB) for generator side and Five level H-bridge (5L-HB BTB) for grid side. It has been observed that increase in number of levels introduces additional switching components which may be inimical to the required total system reliability coupled with extra cost and weight challenges. In [40] the comparison between each multilevel converter was discussed with credit given to the 3L-HB and 5L-HB for their fault tolerant capability which may be seen as welcoming requirement worth introducing in the design of offshore wind turbine converters. This may enhance the availability of the offshore wind turbine power converter whose failure rate is obviously significant.

It is noted that almost all modern wind turbines use some form of power converter, allowing variable speed operation of the generator and also to more easily meet grid requirements. There continues to be development in the state of the art as turbines increase in power rating and voltage rating. At the same time, power converters have a relatively high failure rate compared to other powertrain components, raising concern among wind turbine developers [27][49]. As the wind turbine industry grows and concentrates on turbine development for offshore, the design of the power converter should meet criteria such as reliability, availability, cost effectiveness and efficiency.

2.6 Comparison of different wind turbine powertrains

Different powertrain arrangements have been adopted in wind turbine systems, using combinations of gearbox, generator and power converters as described in Sections 2.3-2.5. The nomenclature of each powertrain is principally based on the type of generator and gear system used. In [50] the wind turbine powertrain was classified based on the gearing system namely: geared (single stage and three stage) and direct drive concepts, investigating seven variable speed constant frequency wind turbine generator systems. Nomenclatures such as doubly fed induction generators with three stages (DFIG3G), Direct drive synchronous generators (DDSG), Direct drive permanent generators (DDPMG), Permanent magnet generators with single stage gearbox (PMG1G), Doubly fed induction with single stage (DFIG1G) have also been used to classify generators connection to the gearbox [21]. In [32][51] another description was made based on the generator connection to the grid shown in Figure 2.23. Most of the direct drive generators use the ‘type 4’ configuration having a full range of variable shaft speed operation and allows maximum power tracking of the wind velocity. The converter is rated at the full power of the generator as against ‘type 3’, DFIG, with the converter being rated at the slip power i.e. at 30% of the generator rated power. A version of ‘type 2’ connection was applied in the Optislip technology by Vestas [39] in the early years of wind turbine development, allowing a certain range of rotor speed variations by the rotor resistance control.

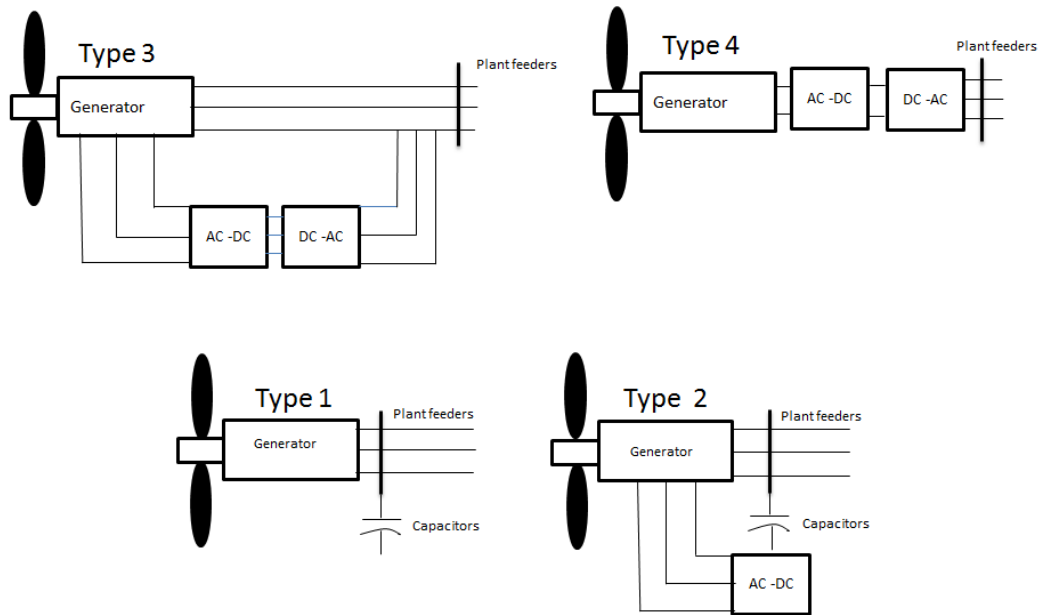


Figure 2.23: Generators type based on grid connection [32]

In the light of the various range of powertrain commercially available in the wind industry, a critical comparison of wind turbines configurations has been made according to [21][50]:

➤ DFIG3G

In this configuration, the output of the gearbox is connected to a doubly fed induction generator. The doubly fed induction generator has reactive and real power flow control and it is possible to obtain a wide range variable speed with a reduced static converter size and acceptable power production. The gearbox which consists of three stage system uses the planetary and spur gears. The DFIG3G is the lightest, lowest of the powertrain in terms of cost but with relatively low annual energy yield due to high copper, iron and gearbox losses [21]. This configuration uses a partial rated power converter to vary the electrical frequency on the generator rotor and hence provide variable speed operation.

➤ DDSG

In this powertrain, the synchronous generator is directly coupled to the turbine rotor shaft with complete elimination of the gearbox. This implies that the generator is at the same speed with the rotor speed. There is zero loss due to gearbox, also increasing the reliability of the powertrain. However, there is

excitation loss in the system. According to [2.21], this will result to a heavier and very expensive machine. In terms of weight and cost, this powertrain appears to be the heaviest and most expensive. This configuration uses a fully rated converter.

➤ DDPMG)

In this design, permanent magnets are used, hence reducing the loss as there is no rotor current. An increased number of poles allows for thinner, lighter yoke. With a higher frequency than the DDSG, iron losses can be higher than copper losses and account for over 15% of the annual dissipation in the generator system [21]. There is zero loss due to gearbox. This configuration uses a fully rated power converter.

➤ PMG1G)

This design has permanent magnet generator coupled to a single stage gearbox. The machine has a smaller torque rating than the DDPMG and is smaller, cheaper and more efficient; this improvement is traded off against an increase in size, cost and losses in the gearbox. This configuration uses a fully rated power converter.

➤ DFIG1G)

This machine is larger than a conventional DFIG because of the significantly higher torque rating. This configuration uses a partially rated converter.

Interestingly, the result of the comparison has shown close similarities with the DFIG1G appearing as the most attractive in terms of energy yield per cost [21]. This is due to the lower rating of the converter and subsequent reduction of the cost and losses. In [50], the comparison was based on the annual energy production per cost proposing single stage gearbox with DFIG1G has been more attractive having the lowest cost solution at the small and medium rated powers. A similar comparison was made in [21] based on cost and energy yield, identifying DFIG3G as the cheapest solution and DDPMG as having the highest energy yield. However, DFIG1G was concluded to be the most attractive in terms of energy yield per cost. It should be noted that energy yield per cost is analogous to payback period and the metric of cost of energy pay favour a different powertrain. The conclusions to [21] discuss the

importance of reliability and its likely impact on the cost of energy. Recent studies also show that powertrain with permanent magnet generators have higher availability, lowest O&M cost and *CoE* compared to DFIG. However, in the PM class, DDPMG has the lowest compared to those with gearboxes [52].

2.7 Reliability

Reliability is the probability of a component or system to perform its intended function during the stipulated design time under certain prescribed conditions. Reliability indices are certain measures, criteria and parameters used in evaluating and assessing the reliability behaviour of different systems. They serve as a guide for acceptable values in the reliability assessment. Some important indices have been identified as: expected number of failures within a period of time, mean time between failure (MTBF), mean time to repair (MTTR), and expected loss of output due to failure [53]. A holistic metric is “availability” which can be interpreted to mean the probability of the system continuing to function in its operating state at some time in the future.

2.7.1 Reliability and Availability parameters

The term “mean time to failure”, MTTF, is the expected time for a system to fail. For a repairable system, the failure of a component requires an immediate action to repair the system and get it operational again [27][53].

The time taken to execute the repairs and get the system functional again is regarded as the “MTTR”, of the system. In some sources, this “mean time to repair” includes both the repair operation time and the logistics delay time (LDT) (i.e. the delay time in getting to the turbine in order to initiate the repair process). It was not clear from the data source used in this thesis if MTTR included LDT. Hence MTTR was assumed to mean time used for repair of parallel powertrain. In some cases, downtime was assumed as MTTR. In other sources the LDT is expressed separately in the calculation of the total time which the system is out of service, sometimes referred to as the total outage time or ‘downtime’ due to a failure event [53],

$$\text{Downtime} = \text{MTTR} + \text{LDT} \quad (2.13)$$

The “mean time between failures”, MTBF, then is given by,

$$\text{MTBF} = \text{MTTF} + \text{MTTR} \quad (2.14)$$

The failure rate λ is the number of failures per unit time (where time units are defined in MTBF),

$$\lambda = \frac{1}{\text{MTBF}} \quad (2.15)$$

Similarly, the repair rate μ is the number of repairs per unit time (where time units are defined in MTTR),

$$\mu = \frac{1}{\text{MTTR}} \quad (2.16)$$

Equation (2.16) can be recast in terms of failure and repair rates,

$$\text{MTBF} = \frac{1}{\mu} + \frac{1}{\lambda} \quad (2.17)$$

These indices can be used to describe the system availability. In simple terms, availability A is described as the ratio of actual time when the system is functional to the expected service time of that system [27][31][53].

$$A = \frac{\text{actual operating time}}{\text{expected operating time}} = \frac{\text{MTBF}}{(\text{MTBF} + \text{MTTR})} = \frac{\mu}{(\mu + \lambda)} \quad (2.18)$$

2.7.2 Bathtub curve

The failure rate described above is assumed constant. However, experience has suggested that the failure rate changes with time. In analysing the reliability of systems, the bathtub curve shown in Figure 2.24 has been developed to describe the hazard function of the system and has been used to describe the reliability of wind turbines [27]. The shape of the curve describes the features of the physical components of systems such as electronic devices, computers components and other engineering components [53]. The characteristics of the systems are best understood by dividing the curve into three sections namely: early failures, random failure and the wear out failures [27]. The early life of components is associated with decreasing failure rate as early manufacturing defects and errors are identified through quality control checks

and testing. As a result, the initial high failure is reduced immediately. This stage is also known as infant mortality phase of the system. The random failure stage is known to have a low or constant failure rate and it happens when the product is put to use or in operation by the consumers. During this period, failures happen by chance. The exponential distribution function is valid during this region. As the system approaches the peak of its useful life, failures are seen to occur more frequently, signifying increased failure rate due to aging and wear out.

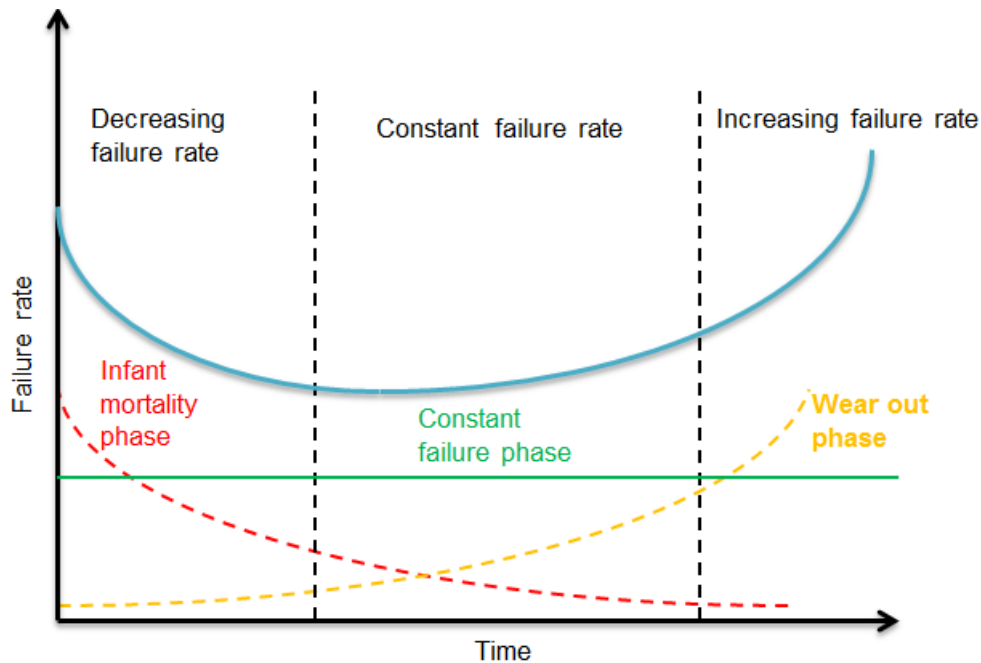


Figure 2.24: Bathtub Curve showing phases of life cycle of a component [27]

2.7.3 Reliability of wind turbines

Wind turbines constitute an engineering system which requires an extensive understanding of its characteristics in order to assess and evaluate its reliability. Like other systems, wind turbines are susceptible to failure leading to its stoppages. Though not all outages in wind turbine are regarded as failure, an automatic or manual restart maybe all that is needed to return to operational state. An in-depth understanding of the categories of stoppages and failure rates encountered by wind turbine systems is needed to fully evaluate the reliability of wind turbines [27]. An awareness of the failure rates gives an idea of the mean time between failures MTBF while evaluating the availability involves the understanding of the downtime.

The knowledge of wind turbine failure rates allows comparison of reliability performance, improvement in design and future maintenance plans for sub-assemblies with high failure rate. Similarly, it is important to understand the likely downtime per failure as availability – as defined in equation 2.18 – can be increased by both reducing failure rate and by increasing repair rate. The importance of failure and repair data for evaluation of wind turbine reliability and availability has led to several surveys and research in recent times [54][55][56][57]. The essence of the studies is to obtain information and data on the reliability of wind turbine from commercial and public sources for comprehensive statistical analysis of existing wind turbines for future improvement. Some of the surveys reveal information on failure rates of different wind turbines (fixed speed or variable speed). In-depth understanding of failure rates of different wind turbines and their sub-systems will improve future design strategies and maintenance activity. In this way, the reliability and availability of the wind turbine, sub-system and the components will increase.

The reliability of the onshore wind farm has been known to some extent, with a failure rate of 1-3 failures per turbine per year been predicted [27]. For the offshore wind site, it is likely that both failure and repair rates will be different to onshore should a common turbine model be used. High availability, low cost of operation and O&M are key to driving down the cost of energy of offshore wind farms. Achieving this may require designs of the wind turbine with failure rates likely to be around 0.5 failure/turbine/year, since planned maintenance is expected to be as low as one visit per year [27]. To further understand the reliability of wind turbines, another strategy adopted in some reports involves the breaking down of the whole wind turbine assembly into sub-systems (gearbox, rotor hub, shaft, generator), assemblies (gearbox), subassemblies (high-speed shaft) and then components (generator windings) [58]. This has the advantage of drilling down to the very specific location of the reported fault creating better and concentrated maintenance activity.

The report from WSD, WSDK and LWK in [27] has been identified to have some limitations in terms of population size, differences in data collection periods, non-uniformity in the age of wind turbine [55]. Irrespective of the discrepancies observed in some of the surveys, there seem to be some useful results indicating uniform

convergence in relation to wind turbine sub-assemblies and components with significant failure rate, MTTR and downtime [59].

Effort has been placed on the approach for collecting reliability data for wind turbines. Some of the methods include: Supervisory Control and Data Acquisition (SCADA) data, maintainers' report logging and operators report. The importance of a standardised mode of wind turbine data collection has been emphasized as revealing the actual location of failure and the sub-assembly affected [27]. Such information will improve maintenance planned to maximise availability. Modern wind turbines now have SCADA and CMS system installed in the wind turbine to enhance information collection and data gathering. The motivation of this effort is geared towards better reliability and availability improvement of the wind turbine.

Some authors have attempted using WindStat data to predict the reliability of large offshore wind turbines, proposing that offshore wind turbine should be subjected to more intensive reliability improvement with a focus on generator and power converters whose reliability is presently below that of other industries [31][54][60]. Similar results taken from LWK data shows that the gearbox, electrical system and generators have high MTTR [31][55][61]. This high MTTR encourages future research in terms of redundancy in the powertrain of offshore wind turbines.

2.7.4 Reliability of powertrains

The reliability of a system, wind turbine or the powertrain is a function of the failure rates. Present day changes in turbine designs are focussed more on the powertrain configurations as this affects reliability greatly [21][59][60]. Though some powertrain have been considered as being more reliable than others, it is well known and accepted that this also depends on how the powertrain components are manufactured, assembled, installed and maintained. In [58] the different electrical configurations of the current wind turbines were summarised. Some of the wind turbine configuration dominant in the wind farms today are: the geared high-speed asynchronous generator using a partial rated converter and gearless, low-speed synchronous generator with fully rated converter [41]. Benefits associated with this design have been discussed extensively by several authors [21][41][62] with high-reliability potential credited to

the gearless design due to the removal of losses emanating from the gearing system. However, in [59] the reliability analysis reveals that the direct drive wind turbine may not have better reliability than the geared concept but rather have better potential for improvement with time.

Table 2.3: Failure rate of powertrain components [60]

Subassembly	Failure rate (failures per item per year)	MTBF in years
Generator	0.0315-0.0707	~14-32
Gearbox	0.155	~6
Converter	0.045-0.2	~5-2

Similar results were made in [31] during WMEP studies and analysis showing results below in Figure 2.25.

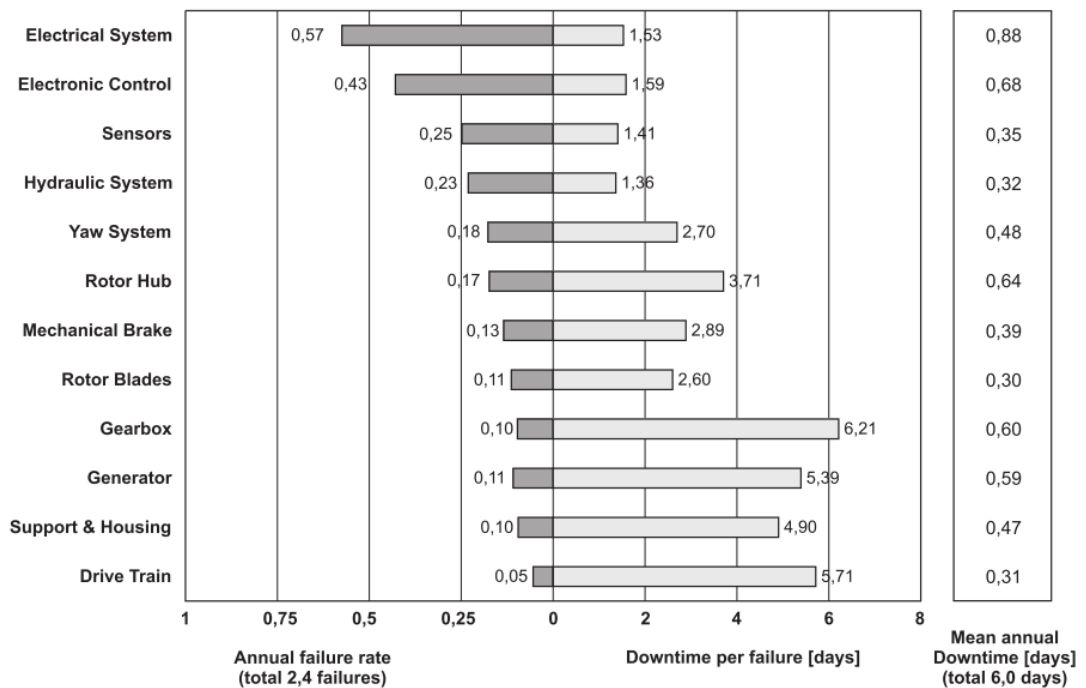


Figure 2.25: Reliability characteristics of wind turbine of sub-assemblies [31][60]

2.7.5 Condition monitoring system

Condition monitoring involves health checks on the status of equipment to predetermine or predict if any failure is in the offing for arrangement of proactive maintenance. Historically, this strategy has been applied in the oil and gas industry, aviation sector and manufacturing companies. Currently, lots of research has been made in the wind energy industry for health checks of wind turbine components with

a high risk of failure. Results from such studies reveal the need for CM as a method to reduce failures in the gearbox and other powertrain components [27][63]. Generally, it has been reported that CM helps improve the reliability, increase availability and reduce cost of energy for wind turbine systems [64].

Some of the suggested CMS techniques include: vibrational analysis, use of low and high-frequency accelerometers, wavelet techniques, oil lubricant analysis, strain measurements and electrical signal diagnosis [65][66].

Prior to the deployment of CMS, one of the monitoring systems used was SCADA which has now evolved into industrial control system (ICS) and distributed control system (DCS). It was designed for data acquisition and controlled by precise measurement of the status of process components such as pumps, valves, separators, surge vessels etc. The combination of the two monitoring systems (CMS and SCADA) is predicted to offer good detection, diagnosis and prediction of failure types in the wind turbine powertrain [27]. Although, SCADA system gives cheaper option but it lacks in-depth coverage of analysis when compared to CMS.

2.8 Redundancy in wind turbine powertrains

2.8.1 Introduction to fault tolerance

Fault tolerance has been described in [67][68] as the ability of the system to continue operating in the event of a sub-component failure, until a replacement is possible. Although the power level is expected to reduce below the expected or healthy capacity, the penalty of the failure would be reduced.

Different aspects of fault tolerance have been recommended by Heimerdinger and Weinstock as necessary steps during the design of systems to achieve high availability and reliability [69]: This involve fault avoidance, fault removal, fault forecasting, fault tolerance, fault repair, fault detection, fault isolation and control adaptation. It is suggested that components of the system should be designed with a high level of reliability to avoid failure by using quality materials during manufacturing. For the offshore wind turbine where access time is unpredictable, it is imperative that priority be given to these important criteria. In wind turbine, some of these methods have been

developed and utilised for improve the reliability and availability of the wind turbine components.

One major challenge worth addressing in modern wind turbines is the loss in power generation due to a failure of one component of the powertrain. Incorporating fault tolerant design allows the system to continue operation in the event of a failure [67]. As the wind turbine industry is increasingly designing new turbines for the offshore environment, the need to design their powertrain components with some level of fault tolerance has become necessary.

Historically, fault tolerance has been adopted in information technology, aviation and medical industries where systems are expected to run continuously and safely [69][70][71]. In these industries, some of the elements of the system are considered as being very critical, demanding a high level of safety. Looking at the trend in terms of access in the offshore environment, certain wind turbine components could be described as being very critical such as generators, gearboxes and converters due to their high failure rate. Integrating fault tolerance in these components may keep the turbine working until an available window for repairs is gained.

It has been reported that a dependable fault tolerance system must be available, reliable, safe and secure [71]. In the wind turbine, high reliability is expected if the goal of increasing availability is to be met, especially in the powertrain where the failure rate is found to be high.

2.8.2 Fault tolerance in generators

It has become necessary to consider the possibilities of integrating fault tolerance into the electrical machines for the offshore wind turbine. Strategies to achieve fault tolerance in electrical machines for other applications has been researched and presented. Though not much application made to the wind turbines environment, the strategies already identified to fault tolerance are: (1) fault tolerance by increasing the number of phases (2) fault tolerance of switched reluctance machines and (3) design of fault tolerance of PM machines and their power converters. Increasing the number of phases of the wind turbine generator to achieve fault tolerance seems possible without a significant rise in cost and part count of components. In [72], fault tolerance

was reported as a means of increasing the availability of wind turbine generators systems.

2.8.2.1 Fault tolerance by increasing the number of phases

This type of fault tolerance strategy involves designing the machines with multiple phases so that if one phase fails due to a fault, the others can continue to operate. This method – sometimes described as phase redundancy – involves or is based on the concept of parallel redundancy and has been used in UPS. It is based on the possibility of an n -phase machine continuing operation with $(n-1)$ or less of its stator phases out of operation. In [73] the phase redundancy concept was analysed and tested using a 5-hp six phase induction motor. It was suggested to use full bridge converter in each phase of the machine so that if one phase fails the other others will continue to operate or if one set of the three phase fails, the other phases will continue. The result of this is that there will be a reduction in power while the currents will become asymmetric leading to pulsation in torque and losses. Failure of one set of three phases will result in larger reduction in power and symmetric current and no additional losses and pulsation torque. Hence, the phase redundancy method will result in reduction in power and can deal with power converters fault and open circuit faults. The advantage of multiphase machine includes high reliability and fault tolerance potential.

The design of multiphase generators for fault tolerance was examined and analysed for the marine turbine application [74]. It is stated that one of the advantages of multiphase generators is higher reliability.

Details of the construction and arrangement of this type of machine is given in [75]. The objective of fault tolerance using multiphase machines can be achieved without adding more components into the design [76]. Converters with higher power ratings normally are designed to have parallel units as it is for high power machines with windings consisting of a number of parallel coils.

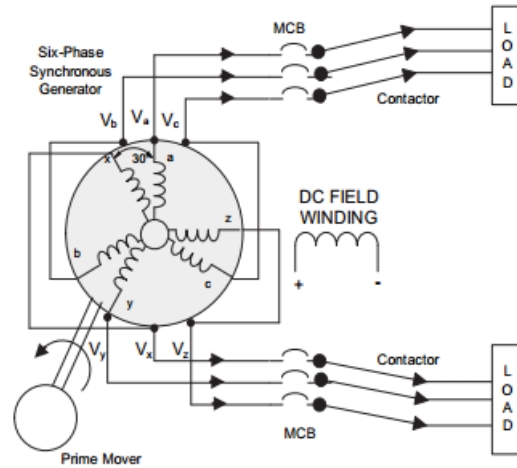


Figure 2.26: Six phase synchronous generator system [77]

2.8.2.2 Fault tolerance by using switched reluctance machines

The SRM has salient (protruding structure from the yoke into the air gap) pole stator and rotor both constructed from laminated steel. Only the stator has concentrated windings while the rotor has no windings or magnets. The connection of the stator windings is made in series to the opposite stators pole to form a phase, though some arrangements can have more than two opposite poles forming a phase.

The potential of the SRM to offer fault tolerant capability emanates from the construction of the rotor and stator creating phases that are electrically and magnetically separated. Failure of one of the phases can keep the machine operational since the other phases are intact. It has been reported that SRM has found application in aircraft sector as starter/generators though proposed for the wind turbine but yet to be fully applied maybe for the existence of alternatives generators with higher torque densities [78].

2.8.2.3 Permanent magnet machine design for fault tolerance capability

Possible faults in the electrical machine may include: open and short circuit winding faults, inter-turn short circuits, inter-phase short circuits, active switch open circuits,

diode open and short circuits, DC link capacitor failures, bearing damages, stator or armature faults, broken rotor bars, faulty end rings and eccentricity-related faults [76][79]. These faults may result in decreased efficiency, decreased torque, overheating, unbalanced voltages and line currents. PM machines may be designed with the converters to handle some of these faults and continue operation. This can be achieved by adopting the single-layer fractional-pitch windings in the stator circuit, with a low mutual inductance and a self-inductance of 1pu between the phases. The result can be an electrical machine with a low power factor and a larger power converter. When compared to the conventional PM without fault tolerance, machines designed with fault tolerance may attract an extra cost of about 10% [76].

Designs of wind turbine generators were investigated with the conclusion that the 6/4 (6 slots in each stator module corresponding to 4 rotor poles) module is promising for the wind generator design in terms of weight reduction of a module, electromagnetic performance and good vibration performance [80][81].

2.8.2.4 Fault tolerance in power converters

There is a high possibility of integrating fault tolerance in power converters. The probability of different failures of converters has been considered as well as their reliabilities. Strategies to achieve fault tolerance in converters have been researched and presented in [82]. To do this, more power electronic converters components are added to make the converter fault tolerant. It has been reported that amongst the various powertrain components, the power converter has a higher failure rate than the electrical machine [56][58][61]. Therefore, applying the fault tolerance converter to the system will make sense. Some examples of fault tolerant converter have been reported in [76].

Short circuit faults are difficult to manage in terms of fault tolerance as they give rise to large currents, temperatures and torques. Consequently, the fault tolerance capabilities of the converter system mentioned earlier can deal with open circuit faults in the machine. Another observation is that the increased semiconductor component count can make for a more complex system, increasing the number of faults. This arises from the fact that fault tolerant design was applied to safety critical devices, for

instance in aerospace (mission oriented system) where stoppages are intolerable. In certain application, stops with a short duration may be allowed as availability is the key objective of such a system, rather than safety criticality. With this, some of the components may be removed to make the converter more suitable for the proposed application with less cost.

In wind turbine, this strategy has been adopted in the design of the 4.5MW wind turbine by Gamesa and the Clipper turbines with multiple generators. The significant difference is the use of parallel phases in one single generator of Gamesa but the use of more than one generator in the Clipper design. It is not yet clear which technology has better advantage in terms of availability, energy production yield and *CoE* improvement. The use of separate generators may attract more cost, but it may be easy to replace during maintenance.

A quantitative analysis of power electronic converters of wind turbine generator systems has shown that after a certain limit, a further increase in the number of converter modules only offers a fractional benefit in availability [72].

2.9 Wind turbine parallel powertrains

The conventional wind turbine system consists of a gearbox connected to the generator and a power converter. With this arrangement, the single generator is rated at the total power of the wind turbine so that failure of the generator means total power loss i.e. a halt in energy production. An alternative configuration with more than one generator has been proposed where the gearbox is connected to multiple smaller generator units. The NREL carried out an investigation to assess the conventional and innovative wind drive technology with the aim of pinpointing the most viable technology. The aim of the project was to investigate, identify, design, explore, implement and test a megawatt scale powertrain topology to know which amongst the powertrain offers the best and most efficient overall life cycle cost advantage. The choice for the best powertrain led the team to identify and conduct a comprehensive assessment of the following powertrain configurations [15]:

- The baseline geared powertrain using doubly fed induction generator
- Medium speed geared single output powertrain MS-1

- Gearless/Direct Drive Permanent generator powertrain
- Medium speed geared six output powertrain MS-6 (multiple output powertrain)

Much research have been made on the first three powertrain stated above with greater percentage of the commercial available wind turbines utilising such technology [83][84][85]. The multiple output powertrain is made of a gearbox having large diameter gear with pinions, which interfaces with generators. The number of generators will determine the size of the gear and the number of pinions to be used in the powertrain. As shown in Figure 2.27 below, the six generators multiple output powertrain evaluated by NREL in [15], has a main bearing, bull gear, six pinions, spindles, generators, brake systems and so on.



Figure 2.27: A 1.5MW single output and multiple output powertrain [15]

This multiple path powertrain configuration can adopt multiple low speed paths with multiple generators driven by a single stage gear system or multiple high speed generators driven by multiple separate gear paths. Any number of generators ranging from two can be used connected to their own power converters in the output of the generator to allow for variable speed control operation. The control operation could add more generators at higher wind speed and shut down some of the generators at low wind speed.

The Liberty 2.5MW wind turbine was designed with distributed powertrain having two stage helical gearboxes and four separate synchronous permanent magnet generators [86]. The generators were fed from four high speed shafts to distribute torque to the four generators. The designers claimed that this torque splitting gearbox arrangement would eliminate early bearing failure, reduce the mean time to repair, and the maintenance cost associated with generators repairs [87].

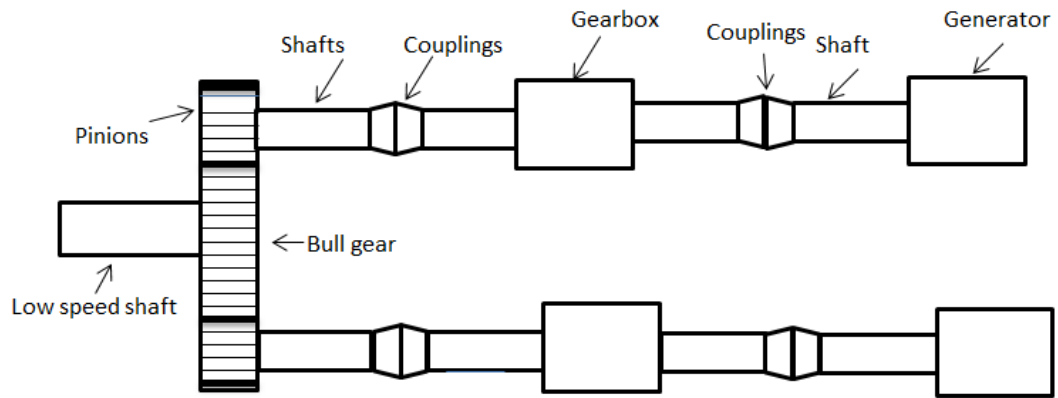


Figure 2.28: Schematic of multiple output powertrain [86]

As shown in Figure 2.28, the input torque from the low speed shaft (LSS) is divided by turning pinions around the bull gear, which is mounted on the input shaft. The input torque is then translated through shafts and couplings into multiple gearboxes that function independently (aside from a common input). The small multiple generators are coupled to the multiple gearboxes using the couplings and shafts. The bull gear and the pinions form the first stage to the gearbox functioning as a torque splitter by dividing the load between the pinions and distributing the contact load between the teeth of the pinions. The multiple parallel gearboxes could be regarded as second stage. The innovative design using torque splitting distributed gearbox multiple output powertrain over conventional power train with one single gearbox and generator offers advantages, claimed in [87] as:

- A significant form of redundancy is seen in the parallel powertrain since a single point failure of one gearbox and generator incapacitating the entire system – as in conventional system – is eliminated. With parallel powertrains, the failure of one generator or small independent gearbox will enable the system to continue operating albeit at a reduced power capacity.
- Generally, generators are designed to operate at maximum efficiency when delivering near nominal power input. At low wind speeds, a single generator may have to operate at reduced efficiency since it is not generating at full capacity. With parallel powertrains, there is a possibility of taking some of the generators offline at low wind speed conditions, adding them back into operation at higher efficiency at higher wind speeds.

- It may be easy to design robust smaller generating power trains units with strong assurance of performance reducing failures and maintenance time.
- This torque splitting gearbox arrangement eliminates early bearing failure, reduces the mean time to repair, maintenance cost associated with generators repairs.
- Replacement of a single heavy generator and gearbox during maintenance could cost a large sum of money. Having to replace the compact small generators and gearbox with on-board hoist instead of the heavy and expensive ground based or heavy lifting vessel crane could save O & M cost. The use of high-speed gear sets in form of cartridge can be easy for the personnel to replace using on-board hoist rather than heavy cranes. In this case, the number of technicians involved may be reduced also.

In similar studies using distributed powertrain with eight multiple generators, it was reported that the final system design demonstrated a 35 percent cost improvement compared with conventional 1.5 MW gearbox designs [88]. The report of the Northern team's studies in [15], reveals that the MS-6 configurations did not show any competitiveness because of high O&M cost. The use of large number of generators and power converters in the design was adduced as the reason for the high cost. The cost may be reduced if the concept of nine-switch topology for converters is applied [89]. In this case, the six outputs of the generators feeding the converters could be paired, permitting the application of three instead of six converters. This will translate into a significant decrease in the cost of converters and reduction in the total cost of the powertrain.

The high cost and other downside of the multiple powertrains inferred by the Northern team in [15] seem to juxtapose the results from other studies in [23][87][88][90] stating an expected reduction in the cost of this innovative powertrain. So, these two different viewpoints, one concluding that there are benefits, and the other saying that there are not, both lack clarity about CAPEX, OPEX e.g. operation and maintenance cost, availability. There was no analysis to fully understand the optimum number of parallel powertrain modules to strike a balance. It is also noted that a simplified approach was taken for the annual energy production in that analysis which creates a gap for further studies. Consequently, it is worthwhile for advanced research to be carried out to

validate the potential of parallel powertrain in reducing the cost of energy predicating on the expected availability increase for the offshore wind site, extra energy from the failure states etc.

Halting the further operation of the offshore wind turbine due to fault for a considerable time will definitely increase the *CoE* while reducing the *AEP*. Circumventing such scenario of complete zero energy or power production has necessitated the need for a powertrain design that will remain operational during failure of any generator or gearbox components. The nearest powertrain option to this condition which could possibly proffer solution is the multiple output powertrain design. Therefore, this work looks at the cost of energy analysis from a holistic point of view, making an adequate evaluation of the *CoE* elements in terms of modelling availability, annual energy production, operation and maintenance cost, for a fair comparison between the non-parallel and parallel powertrain.

Chapter 3 Reliability survey of failure and repair rate of powertrain equipment for parallel powertrain

3.1 Introduction

In this chapter, a comprehensive survey has been made to collate wind turbine powertrain reliability data from various sources, including databases in the public domain. In the context of parallel powertrains, it will be necessary to understand whether component failure rates vary with machine power or torque rating, size or number of sub-components. If there is a relationship, it would be useful to uncover the nature of such relationships so that it can be applied to powertrain components which will be rated at a power rating lower than the turbine's rating.

Section 3.2 presents reliability data from different sources. Section 3.3 shows the numerical relationships between ratings of powertrain and their failure and repair rates. Section 3.4 shows a representation of wind turbine sub-assemblies using reliability blocks. Section 3.5 illustrates Failure mode and effect analysis of wind turbine systems. Finally, the chapter draws conclusions on the findings made.

The following secondary research question has been set out to be answered in this chapter.

How do failure and repair rates of powertrain equipment vary with size and power?

3.2 Powertrain failure rate data

3.2.1 Failure rate of electrical machines from other industries

Data from industry shows that failure rate and repair rates of electrical machines vary with their size [91][92]. Table 3.1 shows the failure rate data from industry on the

population of electric motors of different sizes and power ratings. The third size category (3.73-7.46MW; 5001-10 000 hp) shows a relatively high failure rate although this was reported to be based on a small population in sample size. Generally, there is an increase in failure rate as the size and ratings of the machines increase. Similar results show that large AC motors used in the military warships have higher failure rate than the small rated type [93].

Table 3.1: Reliability data from other industry based on power ratings of motors [94]

Industry	Power ratings (MW)	Failure rate/year
All	0.15-0.37	0.0681
All	0.37-3.73	0.0730
All	3.73-7.46	0.2169

Larger power ratings are correlated with larger torque ratings, particularly in most industrial applications where electrical machine speeds are often clustered at specific speed points (1500rpm and 3000rpm). An increased torque rating could influence the failure rate in a number of ways:

- Loads on the electrical machines are larger. The total torque load on the mechanical parts is larger, so there may be an increased risk of mechanical failures.
- Electrical machines with larger ratings tend to be more sophisticated. Larger machines may warrant additional investment in cooling to improve efficiency. This may lead to additional components that may increase electrical machine failure rates.
- Larger torque ratings mean physically larger machines with increased component count. The relationship between volume and torque (assuming a maximum shear stress) is linear, so a higher torque rating will result in a higher volume. This can either lead to either an increase in part numbers (e.g. more rotor poles in direct drive machines) or increased size in parts (e.g. more turns per phase).

3.2.2 Onshore and offshore failure rate of wind turbine powertrain from wind turbine manufacturer

Table 3.2 shows the failure rates for PMGs and DFIGs used in offshore and onshore wind turbines. Comparing the failure rates based on these locations show that the wind turbine generator in the offshore location has a higher failure rate than the one in the onshore location. Potential causes for this are:

- that the loads and environment factors offshore are generally more challenging than on onshore
- that the turbines' power rating is higher and so there are more failures
- that there are fewer opportunities to carry out preventative maintenance actions offshore
- that the offshore turbines are generally younger than the onshore turbines and so might be in a different part of the failures with age characteristic

Table 3.2: Failure rate for generators and power converter

Powertrain	Ratings (MW)	Type	Failure/year	Location	Reference
Generator	3	DFIG	0.999	Offshore	[95]
Power converter	3	FRC	0.180	Offshore	[95]
Generator	2	DFIG	0.123	Onshore	[57]
Power converter	2	PRC	0.107	Onshore	[57]
Generator	2	PMG	0.076	Onshore	[57]
Power converter	2	FRC	0.593	Onshore	[57]

Looking at failure rates of 0.123 for the DFIG and 0.076 for the PMG, the failures include those of the generator auxiliary systems, such as cooling and lubrication. The lower failure rate could possibly come from the reduction in failure modes in the PMG, e.g. lack of brush gear and slip rings and rotor windings. This suggests that powertrains with complex and larger number of components will have more failure modes and a higher failure rate.

In terms of ratings, it is observed that generators with higher ratings will fail more than the ones with smaller ratings. This is similar to the trend in Section 3.2.1. In the data in Table 3.2, the failure rate of 0.999 is about 8 times that of the small MW level with failure rate of 0.123.

When the location/sites are considered, it could be seen that generators in the offshore have higher failure rates compared to onshore. One possible explanation for this is that the offshore sites have a higher average wind speed than the onshore sites. It has been reported in [57] that higher wind speeds have a greater impact on failure rates offshore compared to onshore. There is also the case of the harsher environment in the offshore sites which may affect the powertrain components in the nacelle especially when they are opened during repair events.

The DFIG generators use PRC while PMG utilizes FRC leading to higher losses, causing cooling issues and the greater stress on the converters. According to [96], the converter module used in the FRC is roughly three times the size of the converter module in the PRC. Assuming that this means that the number of components also increases, and that individual component failure rate is constant, then it is unsurprising that there is a higher frequency of converter sub-system failure. This does not account for all the difference in failure rate, suggesting that there are other reasons for the variation in failure rate.

A comparison of generator types shows that the PMG seems to have better reliability than DFIG of similar size and ratings. Data from Table 3.2 shows a failure rate data of about 5 times that of DFIG for the PMG. However, when considered in conjunction with the converter, the reverse becomes the case, i.e. DFIG configuration has the lower failure rate. Because of the different downtime consequence for failures in a machine or in a power converter, it has been shown that there are higher availability and lower O&M in the PMG configurations [95].

3.2.3 Failure data for German and Danish wind turbines

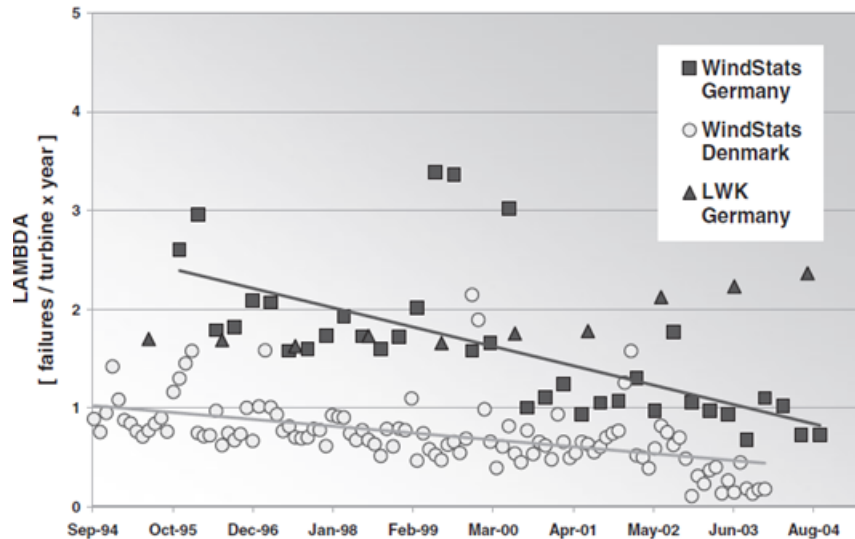


Figure 3.1: Failure rate data from turbine in Denmark and Germany [97]

Figure 3.1 shows failure rates for wind turbine in Denmark and Germany, first analysed in [97]. A survey of reliability data was carried out on German and Danish turbines and the results show higher failure rate for German turbines (typically larger sized turbines) than for the Danish turbines (smaller sized turbines) [97].

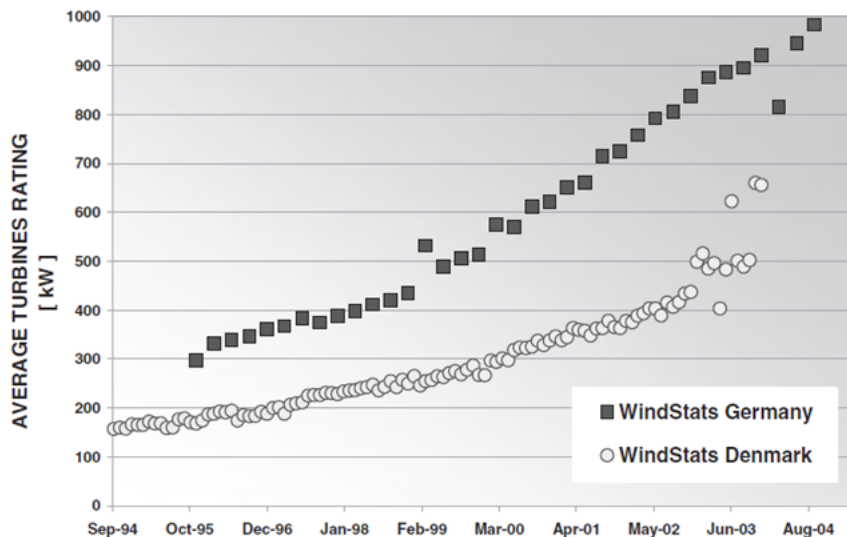


Figure 3.2: Growth of wind turbine sizes in the Danish and German population [97]

Figure 3.2, shows the difference in size between the two populations, with the Danish turbines (lower failure rate) rated at about half that of the German turbines (higher failure rate) on average. Although size of turbines as a key determinant of failure rate might be deduced from offset (in terms of failure rate) of the curves in Figures 3.1 and 3.2, the shape of those curves would suggest a different story. As the turbines increase in size through time (Figure 3.2), the subpopulation failure rates are falling with time. This suggests that size is not the only determining factor. Indeed in [97] and elsewhere there are discussions about changing failure rates due to different technologies and operating experience. Another author reported that failure rates of power converter components are tightly related to capacities of wind turbines and wind speeds [98]. Tavner in summarizing the current trend and knowledge of wind turbine reliability had surmised that failure rates of wind turbine generally increase with the design sizes due to the associated increase in the complexity of the new and larger design [27].

The data in Table 3.3 below is statistical data from Germany's '250 MW Wind' programme, evaluated by IWES [31]. The population comes from 1500 onshore WT with 64,000 maintenance and repair reports collected and analysed. The study used existing onshore experience to discuss the frequency of failures and the duration of downtimes for the different wind turbines sub-assemblies so that a fair prediction could be made of what is expected when turbines are deployed offshore.

From the table, it is observed that even though the electrical and electronic subassemblies fail more frequently than mechanical ones, the mechanical and electromechanical subassemblies experience longer downtimes. In terms of location, the analysis in [31] shows that turbines located near the coast and in the highlands suffer higher failure rates which gives a fair prediction of what is expected for an offshore wind turbine. In such sites, the downtime will also be increased due to limited accessibility, resulting in lower availability.

Table 3.3: Reliability characteristics for different subassemblies in the WMEP programme [31]

WT subassemblies	Failure rate/year	Downtime per failure (days)	Mean annual downtime (days)
Electrical system	0.57	1.53	0.88
Electronic control	0.43	1.59	0.68
Sensors	0.25	1.41	0.35
Hydraulic system	0.23	1.36	0.32
Yaw system	0.18	2.70	0.48
Rotor Hub	0.17	3.71	0.64
Mechanical brake	0.13	2.89	0.39
Rotor blades	0.11	2.60	0.30
Gearbox	0.10	6.21	0.60
Generator	0.11	5.39	0.59
Support & housing	0.10	4.90	0.47
Drive train	0.05	5.71	0.31

Table 3.4 shows results from a survey performed by the LWK, in Schleswig Holstein, Germany. The wind turbine subpopulations have small and large wind turbines of around 15 years include fixed and variable speed configurations, both with geared and direct drive concept. In Table 3.4, the comparison between failure rate field data of a small wind turbine of 300 kW, and a 1 MW wind turbine main assembly are shown. The gearbox, yaw system, blade and generator top the list of assemblies that are prone to more failure. For the smaller wind turbines, the failure rates are quite low with the least failure occurring in shaft/ bearing. It is noticed that for the larger turbines, there is a significant increase in the failure rate at the MW level. Comparing the same assembly at the two MW power rating level indicates well over 100% increase in failure rate as the turbine sizes changes from the 0.3MW to 1MW.

Table 3.4: Typical comparison between reliability field data of a 0.3MW and a 1MW wind turbine main assembly failure rates [99][100].

Wind turbine assemblies	Failure rate of LWK WTs (Failure per turbine per year)	
	300 kW WT	1MW WT
Generator	0.059	0.126
Brake	0.029	0.056
Hydraulics	0.039	0.096
Yaw system	0.079	0.152
Sensors	0.037	0.151
Pitch system	0.034	0.237
Blade	0.078	0.308
Gearbox	0.079	0.255
Shaft/bearings	0.002	0.046

3.2.4 Failure data for Swedish wind turbines

A survey of reliability for a population of turbines in Sweden shows similar trends as other data earlier stated. Figure 3.4 shows that turbines rated below 0.5MW and 0.5MW – 1MW show slight increase in failures during the first three years of operation and an annual failure rate decrease after five years. One significant result is that the turbines rated above 1MW have a higher annual failure rate than smaller turbines. It is also seen that for the turbines rated above 1MW, the failure rate appears to increase, rather than decrease or remain constant.

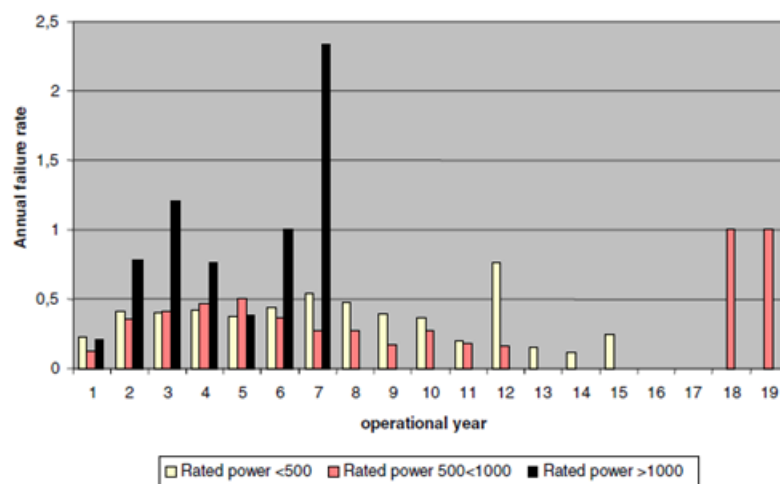


Figure 3.3: Failure rate based on Swedish wind turbines [101]

Although the data on real wind turbines is not always clear – as there are other factors that vary – generally it can be seen that there is a trend showing that as wind turbine and powertrain ratings increase, so does the failure rate. This will be an important aspect that will need to be captured in any modelling of parallel powertrains. The caveats – of changing technology, variations in design and location also being factors – should also be noted for the rest of this thesis.

3.3 Deriving useful relationships between ratings and powertrain failure and repair rates

The rest of this thesis will look at availability and costs of parallel and non-parallel powertrains. These models will require relationships between failure and repair rates to be established. This section will attempt to derive numerical relationships for ratings of electrical machines and power converters and their failure and repair rate.

Considering the insufficiency of reliability data for all sizes and ratings of existing powertrains, an extrapolation method was adopted by plotting the failure rates against power in order to establish the relationship of subsystem failure rate as a function of power rating.

Table 3.5 gives some examples of the varying failure rate λ . The generators include a mixture of electrical machine types, and the failure rate given is a composite of the different generators from each source. The lower power ratings tend to be dominated by constant speed stall regulated turbines, whereas the higher ratings are variable speed pitch regulated machines. The final population has the largest turbines and they are all offshore between 3 and 10 years old, from between 5 and 10 wind farms throughout Europe. This population consist of ~350 offshore wind turbines from a leading manufacturer with over 1768 turbine years of operational data. This population has the highest failure rate.

The data in the fourth column of Table 3.5 was based on 2222 onshore wind turbines from a leading manufacturer, and is composed of failure rate of two different generator and converter types. All turbine generators and converters are in their first five years of operation and from wind farms throughout Europe. The full dataset consists of over 34 000 000 turbine hours (3881 years) of data.

It is noted that this large and modern population of wind turbine provides up to date and reliable failure rates, which are lacking in the public domain and was therefore considered to be useful for the analysis and modelling in this thesis.

Table 3.5: Failure rate of wind turbine powertrain components based on power rating [57][95][100][102]

Wind turbine rating (MW)	≤ 0.3	0.6	≥ 1	2	3
Wind turbine Population	83	202	38	2222	350
	[100][102]			[57]	[95]
Generator λ (/year)	0.10	0.55	0.25	0.102	1.00
Squirrel Cage Induction	Yes	Yes	Yes	-	-
Direct Drive Synchronous	-	Yes	Yes	-	-
Doubly Fed Induction	-	-	Yes	Yes	Yes
PM Synchronous	-	-	-	Yes	-
Power converter λ (/year)	-	0.01	-	0.35	0.18

Table 3.6: Downtime and repair time of wind turbine powertrain components based on powertrain rating [95][100][102][103-104]

Wind turbine rating (MW)	≤ 0.3	0.6	≥ 1	3	
	[100][102][103]			Repair time [95]	Downtime [104]
Wind turbine Population	83	202	38	350	350
Generator (hours)	40	52	70	-	147
Power converter (hours)	-	15	23	12	-

By taking in all of the wind turbine generator and power converter failure rate data from Table 3.5, it is possible to characterize a generic powertrain, i.e. one which is independent of a particular turbine powertrain type. In this case, ‘powertrain’ refers to the generator and power converter. The data points were weighted based on the

population of the wind turbines in that category of power rating (i.e. the population numbers given in table 3.5). Different trendlines could be fitted to the data including exponential, logarithmic, power function. This was done and the quality of fit (given by R^2 value) is shown on Table 3.7. Taking the linear by way of examples and plotting the failure rates against power, the relationship of subsystem failure rate as a function of power rating is found to be

$$\lambda_{\text{subsystem}} = m_{\lambda} P_{\text{subsystem}} + c_{\lambda} \quad (3.1)$$

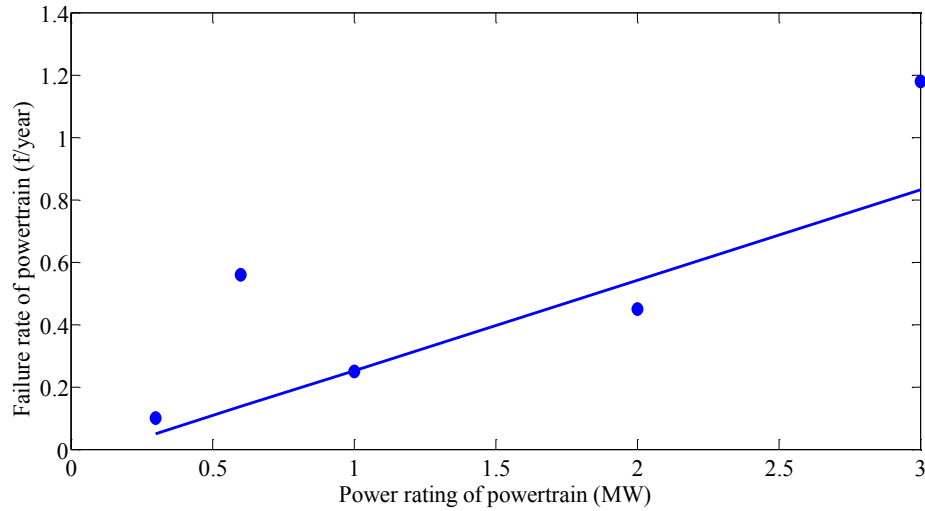


Figure 3.4: Failure rate versus rating of powertrain

In the case of Figure 3.4, $m_{\lambda} = 0.357$ powertrain subsystem failures per year per MW when $c_{\lambda} = 0$ powertrain subsystem failures per year (i.e. if the powertrain subsystem is rated at 0MW there are no failures). When the intercept is not fixed i.e. non-zero value, of c_{λ} an offset of $c_{\lambda} = -0.037$ gives the best fit $m_{\lambda} = 0.289$ with an offset of -0.037 . This would mean that the failure rate is negative when the power is close to 0. This is clearly unreasonable. Instead the case with $c_{\lambda} = 0$ was considered.

Although some trendlines give slightly better fit than the linear (as shown in Table 3.7) the linear trendline is relatively good and has the benefit of being simple and has a useful form, allowing simple integration into the mathematical analysis that will be shown in chapter 4 and 5.

Table 3.7: Other trendlines and the R^2 .

Trendline shape	Failure rate versus power rating		$MTTR$ versus power rating	
	R^2	offset	R^2	offset
Linear	0.46	-0.038	0.979	0.0049
Exponential	0.51	-	0.918	-
Logarithmic	0.22	0.379	0.998	0.011
Power	0.39	-	0.988	-

The same approach was taken for the $MTTR$ data.

Table 3.6 shows how the repair time and downtime (and hence repair rate μ) can vary. The repair time is likely to increase with larger units of the parallel powertrain as component sizes and numbers increase. Wind turbine generator and power converter downtimes based on Table 3.6 were analysed to give subsystem $MTTR$ as a function of power rating for a generic powertrain,

$$MTTR_{\text{subsystem}} = m_{MTTR} P_{\text{subsystem}} + c_{MTTR} \quad (3.2)$$

These data points have been plotted in Figure 3.5, where $m_{MTTR} = 0.004$ years per powertrain subsystem repair per MW has been found.

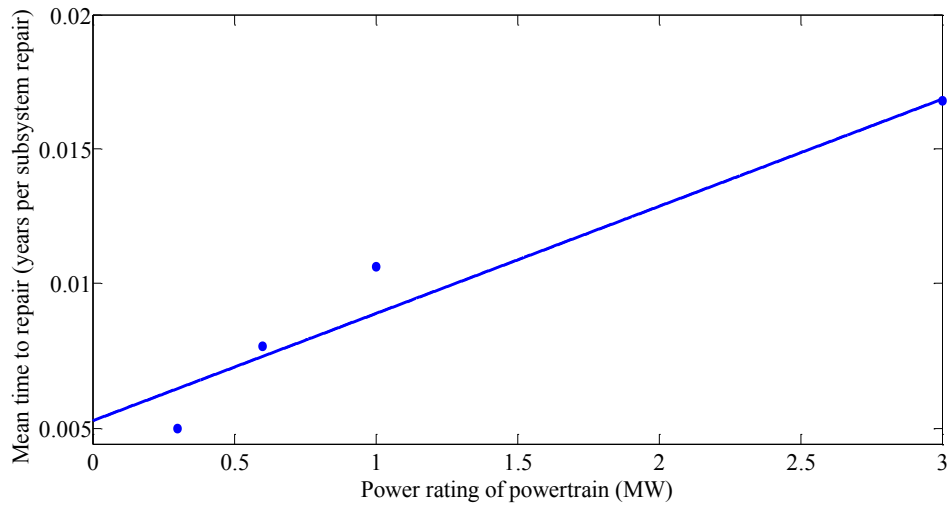


Figure 3.5: Mean time to repair versus rating of powertrain showing the linear regression type for the powertrain

For offshore sites, there is likely to be some delay, which is independent of the power rating, e.g. delays taken up by travel time, waiting for weather to allow access and so on. This can be seen in the final columns of Table 3.6, which show the difference in time spent in the turbine and the total downtime for each failure. However, in order to

simplify the model, it was assumed that $c_{MTTR} = 0$ years, i.e. if the subsystem is rated at 0MW then the subsystem takes no time to repair. To find the repair rate from equation (3.3), one notes that $\mu = 1/MTTR$ and so,

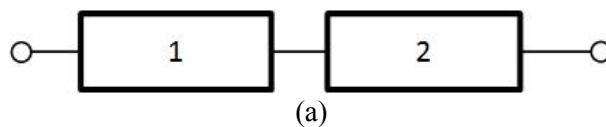
$$\mu_{\text{subsystem}} = \frac{1}{m_{MTTR} P_{\text{subsystem}} + c_{MTTR}}. \quad (3.3)$$

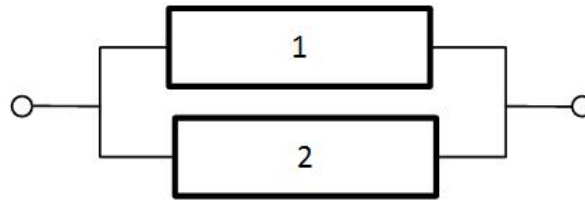
From a population level analysis, there are now numerical relationships between power rating and failure and repair rates. To understand why failure and repair rates might be linked to turbine rating, it is important to explore this more systematically. The following two sections will explore reliability block diagrams and failure modes and effects analysis to understand powertrain failures in a little more detail.

The reliability data used in this thesis follows from the published part of the author's work stated in section 1.5. It is also noted that there are limitations in the use of disparate onshore and offshore generator and power converter failure rate and repair rate data from a number of published sources with some assumptions and estimation made. The failure rate, and repair rate data were assumed from a baseline generic powertrain. The parallel module failure rate, and repair rate were also assumed to scale with the rating of the subsystem, $P_{\text{subsystem}}$. In reality, these may not scale linearly with the power ratings as N increases. However, the models themselves and the methodologies are effective for any available input data and independent of the data quality.

3.4 Reliability block diagrams

Individual sub-assemblies of a wind turbine can be represented by a set of blocks which are connected together either in series or parallel to represent their functionality. Figure 3.6 shows two representations of reliability diagrams for two different systems. When the blocks are joined in series, it is expected that all the sub-assemblies or units that make up the system must be operational or work together for the whole system to function.





(b)

Figure 3.6: Reliability block diagram for (a) series and (b) parallel arrangement of system components

The generalized form of the equation describing any number of sub-assemblies or components, n in series is

$$R_S = \prod_{i=1}^n R_i \quad (3.4)$$

It can be seen from equation (3.4), that for powertrain components such as power converters – where all components must function for the sub-system to function – that if we have to increase the number of components n in order to achieve new power or torque levels then the sub-system reliability will fall.

On the other hand, if the components are regarded to be in parallel, the failure of one part does not affect the whole system. In that case, only one of the units of the whole system is required to be functional for the system to be successful. The reliability of the parallel system R_p becomes,

$$R_p = 1 - Q_1 Q_2 = R_1 + R_2 - R_1 R_2 \quad (3.5)$$

where, $Q_1 Q_2$ are the probability of failure (unreliability) of the components 1 and 2. The generalized form of equation (3.5) above for any number of sub-assemblies or components, n becomes,

$$R_p = 1 - \prod_{i=1}^n Q_i = R_1 + \dots + R_n - \prod_{i=1}^n R_i \quad (3.6)$$

Equation (3.6) shows that having more parallel subsystems (i.e. n increases) will increase reliability.

3.5 Failure mode and effect analysis

The FMEA is a design stage reliability analysis tool and has been used in many power generation engineering systems. It is useful in carrying out the root cause and failure modes aimed at risk estimation, elimination or reduction within a design. Due to its wide industrial application, specific standards have been developed for its application. The common practice is to outline the severity, occurrence and detection rating scales in addition to a spreadsheet layout. A more detailed process of FMEA is given in [105]. One useful approach to adopt when assessing the reliability of a complex system such as a wind turbine is to carry FMEA on the system by breaking down into a number of sub-systems and components. In this case, we can use elements of FMEA to:

- understand how these failure rates of different failure modes might vary with power rating
- understand the various consequences – in terms of downtime – of different failure modes within the powertrain, and how the repair time might vary with power rating

The first step is to identify the failure rates of the components in the powertrain sub-systems as shown in Figure 3.7.

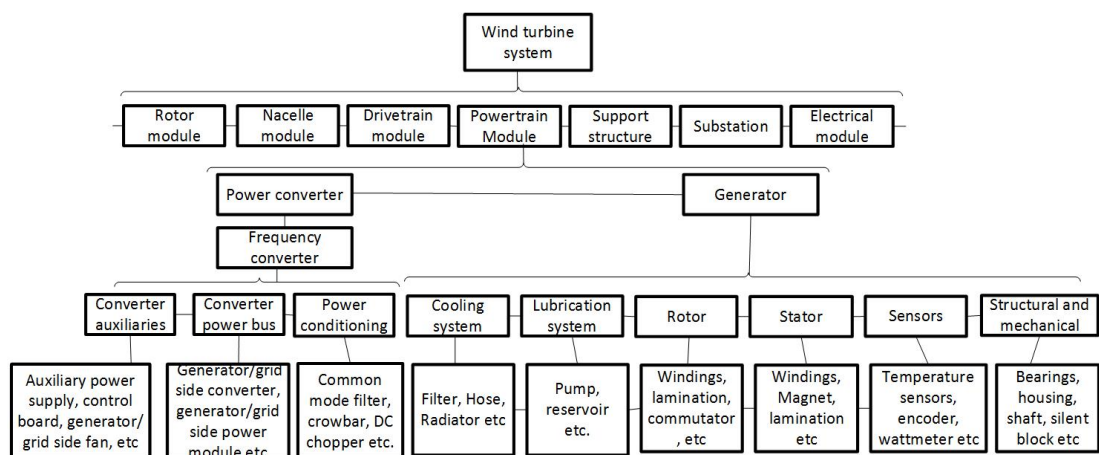


Figure 3.7: Breakdown of wind turbine powertrain sub assembly and components

Although the breakdown structure shown in the Figure 3.7 above will help identify the location of the failure, clear understanding of the root cause and failure mode will give insight into the failure mechanism. In the Reliawind project, the most unreliable sub-assemblies and the failure modes were identified using FMEA [27]. The failure modes

for generator and converter from that report or studies is shown in Table 3.8 include: worn slip ring brush, stator winding, encoder failure, bearing failure and external fan failure.

Table 3.8: Failure modes of powertrain modules identified through FMEA [27]

Failure modes	WT sub-system/assembly	
	Generator	Power converter
Failure mode 1	worn slip ring brush	Generator- or grid-side inverter failure
Failure mode 2	stator winding	Loss of generator speed signal
Failure mode 3	encoder failure	Crowbar failure
Failure mode 4	bearing failure	Converter cooling failure
Failure mode 5	external fan failure	Control board failure

The failure modes shown are traceable to the components of the breakdown/taxonomy structure of Figure 3.7. It is noted that through FMEA, the failure modes causing the unreliability or failure of powertrain sub-assemblies can be identified.

The data in Table 3.9 is based on the failure rate data for a 3MW generator from [95]. The percentage contribution to the failure rate of the sub-assemblies taken from [27] was used to estimate the expected failure rate based on the size of the generator from [95]. A similar approach was used for the power converter.

Table 3.9: Sub-system Failure Rate estimation (failures/year) for conventional turbine

Generator		Power converter	
Sub-assemblies	Failure rate	Sub-assemblies	Failure rate
Cooling system	0.00999	Converter auxiliaries	0.0170
Lubrication system	0.01998	Converter power bus	0.1145
Rotor	0.02997	Power conditioning	0.0377
Stator	0.14985		
Sensors	0.01998		
Structural and mechanical, including bearing	0.56943		

One would expect that components on the rotor and stator, for example, would vary with generator size (correlated with torque rating) as there will be a greater surface area and hence failure rates. Some failure rates of sub-assemblies are likely to be approximately constant, such as sensor failure rates, as there may be the same number

of sensors and a constant sensor failure rate. Other sub-assembly failure rates may depend more on loading which might change with power rating, e.g. cooling, lubrication and bearing loading. This suggests that the failure rate and power rating relationship derived in Section 3.3 are a simplification.

In terms of consequence – here meaning time to repair – it is likely that some of these failures will take longer to repair in larger powertrains and that some of these failures will have fairly constant repair rates. For example, as the machine rating increases, the time to remove and replace a whole machine (e.g. some failures on the rotor, stator and structures) will likely take longer with larger and heavier machines. On the other hand, replacement or repair of sensors and other auxiliary systems is more likely to be independent of the power rating. Again, in terms of the relationship between repair rate and power rating derived in Section 3.3, it can be seen that it is only a simplification. A parallel powertrain is interesting in this consequence as the sub-system repair rate might be higher and the consequence in terms of lost energy capture will also be smaller as compared to conventional powertrains.

With the application of FMEA to the powertrain design process, there is an interesting relationship between the consequence of a fault, detection of faults and occurrence of faults. In order to reduce the consequence or severity of a fault, it is logical to add in additional monitoring mechanisms to increase the detectability. For example, one could shut down the turbine when winding temperatures rises above a certain threshold if one monitors temperatures and this might allow a major failure to be avoided. In so doing, this may end up driving up the failure rate. This trend for additional detection is likely to grow offshore and with larger turbines, where the cost consequence of failures is more severe. A further insight from the FMEA process is that many of the identified powertrain failures will result in a wind turbine shutdown. This is particularly true for those turbines that are heavily monitored, including the monitoring of auxiliary systems such as cooling systems. Parallel powertrains may help to avoid additional full shutdowns, whilst reducing the risk of very severe consequences.

3.6 Chapter conclusion

This chapter investigated the relationship between a turbine or sub-system's power rating and its failure and repair rates. These relationships were noted when examining failure rates from electrical machines in industry generally and the wind industry more specifically. Numerical coefficients were found for combined data (generator and power converter from different powertrains) for failure and repair rates that can be used elsewhere in the thesis for modelling parallel powertrains. A hypothesis was developed to explain this using reliability block diagrams. A deeper investigation of failure rates suggests that these relationships are simplifications and hold for some of the failure modes but not all. Both reliability block diagrams and FMEAs suggest that parallel powertrains may be useful for reducing turbine downtime and O&M costs.

In conclusion to the investigation and analysis carried out in this chapter, the first step towards the novelty of the research carried out in this thesis has been shown and the first primary research question "How do failure and repair rates of powertrain equipment vary with size and power"? which was set out at the beginning of this chapter has been moderately answered.

The results based on data from wind turbine industry and other industries show that failure and repair rates of electrical machines and powertrain components vary with their size and power rating. There is an increase in failure rate for higher sizes and power ratings while the repair rate (quick repair time) tends to reduce.

Chapter 4 MARKOV State space models for availability

4.1 Introduction

One of the methods to increase the availability of generators which has been adopted in the wind turbine industry by some manufacturers is to equip it with a comprehensive range of monitoring equipment such as temperature sensors and brush wear monitoring. Sensors for vibration, leakage or other measured variables are optionally available. Another review suggested that to increase the availability of wind turbine generator systems, design for component reliability, active control for reliability and design for fault tolerance can be used [106].

Considering the trend of the reliability data surveyed in chapter 3 from different operational wind turbines, further analysis was carried out using the failure and repair rate data in relation to the powertrain sizes. The novelty of the work in this chapter lies in the modelling of the availability of a wind turbine parallel powertrain using a MSSM approach. This work finds that equivalent availability can be increased when using a parallel powertrain. It is noteworthy that this improvement is not inherent to the parallel nature of the powertrain but rather it comes about because the parallel powertrain employs smaller units of powertrain (which tend to have lower failure rates and higher repair rates) and because these units can be over-rated thereby reducing the energy loss consequence of a powertrain failure.

This research examines the use of parallel generators and power converter units in offshore wind turbines and how they can be designed to maximize the wind turbine's energy production. Section 4.2 describes the development of MSSM and their use to find a figure of effective availability. This is done for a simplified case and then a more realistic case so that effective availability can be found for any N parallel powertrains, where each parallel powertrain is rated at P/N (where P is the wind turbine's power rating).

A further development comes from the fact that as N increases, the size of the equipment in each parallel powertrain becomes smaller and so the failure rate and

repair rate may change, as derived in Chapter 3. These effects are introduced into the model. As a final extension, the research examines the power rating of the parallel powertrain units, developing the model allowing the power rating of the generator and converter to vary between P/N and P . Section 4.3 presents the results for these models. Section 4.4 discusses these results and interprets them in the context of an offshore wind turbine of 3MW power rating. Finally, the chapter draws conclusions and highlights some of the limitations of the methodology.

The following secondary research questions have been set out to be answered in this chapter.

- Is any improvement in availability possible using parallel powertrain?
- What degree of parallelism, N is most effective in terms of availability improvement?
- What strategy is best to introduce parallelism in terms of availability improvement?

This is aimed at determining the improvement in the availability of powertrains with parallelism compared to the baseline powertrain's availability.

This was done based using two different ways:

- (a) Use of MSSM to model the equivalent availability at constant and varying failure and repair rate of turbines powertrain with different parallelism topologies
- (b) Use of MSSM to model the equivalent availability with varying parallel powertrain subsystem power rating

4.2 Methodology

4.2.1 Markov state space modelling

The MSSM involves the transition of components between states, with failure rates and repair rates being used to calculate the probability of being in these different states. MSSM has been used for many years now in the evaluation of reliability [53]. In [107] it was used to model the reliability of power converters more effectively than other reliability modelling tools. Although many papers using MSSM have been published,

it has not yet been used to evaluate the equivalent availability of parallel powertrains of wind turbines.

In a simple case, shown in Fig. 4.2, a 3MW turbine system can either be in an operating state (“Up”) or a failed state (“Down”). When operating, the turbine can produce up to 3MW (depending on the wind speed); when in the failed state the turbine produces 0MW.

In this chapter, systems with N parallel components are considered; the power output is reduced depending on the number of parallel components in the system. The failure and operating transition of the system are modelled using the failure rates, λ , and repair rates, μ , of the system. The limiting state probability of the system is derived using the transitional probability matrix equation of the MSSM.

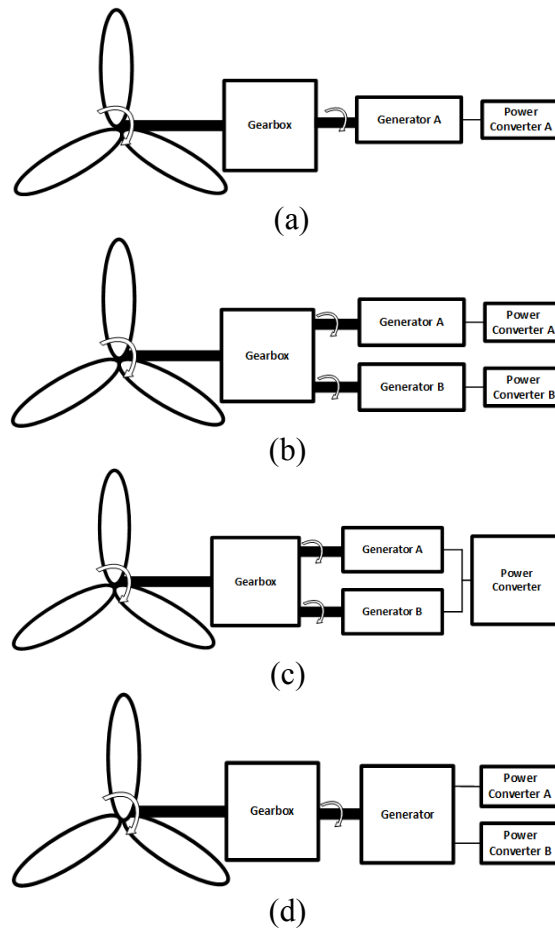


Figure 4.1: Wind turbine powertrains: (a) Single-input-single-output system, $N = 1$ (b) Powertrain system with both generator and power converter in parallel, $N = 2$ (c) Powertrain system with only generator in parallel, $N = 2$ (d) Powertrain system with only power converter in parallel, $N = 2$

Fig. 4.1(a) shows a wind turbine powertrain with a single gearbox, single generator and single power converter; Fig. 4.1(b) shows the same turbine powertrain with a single gearbox with $N = 2$ (two parallel generators and power converters). Each generator is connected to the power converter; hence, a combined failure and repair rate is used for the two components. The availability of the system was analysed using failure and repair data from the wind turbine industry. The parallel powertrain was also considered for separate cases where the powertrain consists of parallel generators only (Fig. 4.1(c)) and then only power converters in parallel (Fig. 4.1(d)).

4.2.2 Simple Markov model for $N=1$

The conventional baseline wind turbine has a gearbox connected to the generator and the converter which could be described as a series model of the system as shown in Figure 4.1(a). As indicated in the state space model, this series model has no intermediate state space levels meaning that it can only produce power at 3MW depending on available wind speeds or no power (0MW). The symbol λ represents the failure rate and implies the system going from being “Up” (State 1) to “Down” (State 2) while μ symbolizes the repair rate meaning transition from “Down” to “Up”.

In matrix form, the limiting state probabilities of being in State 1, p_1 , and State 2, p_2 , are represented as,

$$[p_1 \quad p_2] \begin{bmatrix} p_{11} & p_{12} \\ p_{21} & p_{22} \end{bmatrix} = [p_1 \quad p_2] \quad (4.1)$$

where $\begin{bmatrix} p_{11} & p_{12} \\ p_{21} & p_{22} \end{bmatrix} = \begin{bmatrix} 1-\lambda & \lambda \\ \mu & 1-\mu \end{bmatrix} = P$ is the transitional probability matrix and p_{11} describes the probability when in State 1 of remaining in State 1, p_{12} describes the probability of transitioning from State 1 to State 2, p_{22} describes the probability when in State 2 of remaining in State 2 and p_{21} describes the probability of transitioning from State 2 to State 1. This can be done more generally for any N . Knowing that the probabilities sum to unity, i.e $p_1 + p_2 + \dots + p_{N+1} = 1$, then (4.1) can be interpreted as

$$AX = b \quad (4.2)$$

where $b = \begin{bmatrix} 0 \\ 0 \\ \vdots \\ 1 \end{bmatrix}$, $X = \begin{bmatrix} p_1 \\ p_2 \\ \vdots \\ p_{N+1} \end{bmatrix}$ and A is the coefficient matrix derived from the set of

simultaneous equations. Then X can be solved by using $X = A^{-1}b$ i.e. multiplying the column vector b by the inverse of coefficient matrix A to get the probabilities at State 1 and 2 as,

$$p_1 = \frac{\mu}{(\mu + \lambda)}, \quad (4.3)$$

$$p_2 = \frac{\lambda}{(\mu + \lambda)}. \quad (4.4)$$

When in State 1 – and the wind speed is between rated wind speed and cut-out wind speed – the powertrain power is the rated wind turbine power, $P_1 = P$ (in this case 3MW). When in State 2, the powertrain power is 0. The simple availability of the powertrain system is given by p_1 . In order to compare this with the availability of systems with $N > 1$, a concept of “equivalent availability” is introduced. This is the sum of the products of power and probability for all $N+1$ states divided by the rated power,

$$A_{eq} = \frac{\sum_{x=1}^{x=N+1} P_x p_x}{P}. \quad (4.5)$$

Substituting the probabilities and power at each state into (4.5) gives the equivalent availability for $N = 1$,

$$A_{eq,N=1} = \frac{P_1 p_1 + P_2 p_2}{P} = \frac{\mu}{(\mu + \lambda)}. \quad (4.6)$$

Equation (4.6) then gives the availability of the baseline powertrain, i.e. with a simple series connection. The next subsection will develop expressions for equivalent availability for $N = 2$ and then more generally N .

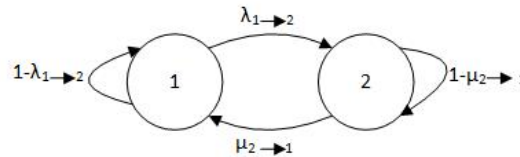
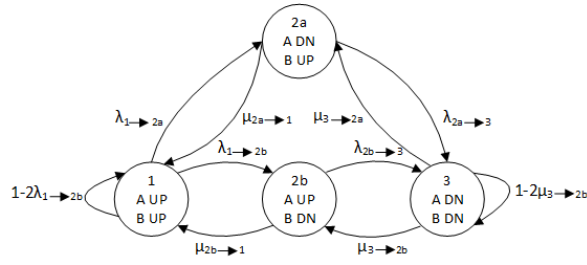
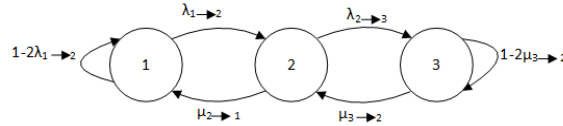


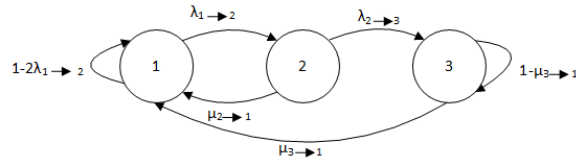
Figure 4.2: State space model of a single component, $N = 1$ system



(a)



(b)



(c)

Figure 4.3: State space model of two parallel components, $N = 2$ system: (a) Simplified model with four states (b) Simplified model with reduced states (c) Simplified model with alternative repair path.

4.2.3 Simple Markov model for $N=2$

Figure 4.3(a) gives the Markov state space diagram for $N = 2$, shown in Figure 4.1(b). State 1 is when both subsystem A (i.e. Generator A and Power Converter A) and subsystem B are “Up”; State 3 is when both subsystems are “Down”. State 2a and 2b are equivalent as they both represent the case when one of the parallel subsystems is “Down” and lead to power output reducing to 50%. Assuming that the failure rates are equal ($\lambda_A = \lambda_B = \lambda$) and the repair rates are equal ($\mu_A = \mu_B = \mu$) then the probability of being in states 2a and 2b are equal, and they can be combined to give State 2 in a simplified diagram in Figure 4.3(b).

In matrix form, the limiting state probabilities are represented as,

$$[p_1 \quad p_2 \quad p_3] \begin{bmatrix} p_{11} & p_{12} & p_{13} \\ p_{21} & p_{22} & p_{23} \\ p_{31} & p_{32} & p_{33} \end{bmatrix} = [p_1 \quad p_2 \quad p_3] \quad (4.7)$$

where $\begin{bmatrix} p_{11} & p_{12} & p_{13} \\ p_{21} & p_{22} & p_{23} \\ p_{31} & p_{32} & p_{33} \end{bmatrix} = \begin{bmatrix} 1 - 2\lambda & 2\lambda & 0 \\ \mu & 1 - \mu - \lambda & \lambda \\ 0 & 2\mu & 1 - 2\mu \end{bmatrix}$. For two parallel components, the probabilities of States 1, 2 and 3 can be found by using straightforward substitution or matrix techniques and are,

$$p_1 = \frac{\mu^2}{(\mu + \lambda)^2}, \quad (4.8)$$

$$p_2 = \frac{2\mu\lambda}{(\mu + \lambda)^2}, \quad (4.9)$$

$$p_3 = \frac{\lambda^2}{(\mu + \lambda)^2}. \quad (4.10)$$

The denominator for each is $(\mu + \lambda)^2$ and the numerator for each probability can be found using the binomial expansions, for $N = 2$,

$$(\mu + \lambda)^2 = \binom{2}{2}\mu^2 + \binom{2}{1}\mu\lambda^{2-1} + \binom{2}{0}\lambda^2, \quad (4.11)$$

$$\text{where } \binom{N}{r} = \frac{N!}{r!(N-r)!}.$$

For $N = 2$, when the wind speed is between rated wind speed and cut-out wind speed, the power output for State 1 is $P_1 = P$, for State 2 it is $P_2 = P/2$ and for State 3 it is $P_3 = 0$. Using equation (4.5), the equivalent availability A_{eq} of the two parallel powertrain model can then be evaluated as,

$$A_{eq,N=2} = \frac{Pp_1 + \frac{P}{2}p_2}{P} = \frac{\mu(\mu + \lambda)}{(\mu + \lambda)^2} = \frac{\mu}{(\mu + \lambda)}. \quad (4.12)$$

It is worthy of remark that the equivalent availability is the same for $N = 2$ as it is for $N = 1$ (given by (4.6)).

4.2.4 Simple Markov model for N

The simple model can be extended for any N . The more general form of the binomial expansion for N leads to,

$$(\mu + \lambda)^N = \binom{N}{N} \mu^N \lambda^0 + \binom{N}{N-1} \mu^{N-1} \lambda^1 + \dots + \binom{N}{1} \mu^1 \lambda^{N-1} + \binom{N}{0} \mu^0 \lambda^N. \quad (4.13)$$

From this the probabilities of states of the first two and the last two states are

$$p_1 = \frac{\binom{N}{N} \mu^N}{(\mu + \lambda)^N} \quad (4.14)$$

$$p_2 = \frac{\binom{N}{N-1} \mu^{N-1} \lambda}{(\mu + \lambda)^N} \quad (4.15)$$

$$p_3 = \frac{\binom{N}{1} \mu^1 \lambda^{N-1}}{(\mu + \lambda)^N} \quad (4.16)$$

$$p_4 = \frac{\binom{N}{0} \lambda^N}{(\mu + \lambda)^N}. \quad (4.17)$$

The reader should note that States 3, 4, ..., $N-2$ has been omitted for brevity. The power output of the states are $P_1 = P$, $P_2 = P(N-1)/N$, ..., $P_{N-1} = P/N$, $P_N = 0$. Combining this with (4.14-4.17) and applying (4.5) leads to a general result for any N ,

$$A_{\text{eq},N} = \frac{Pp_1 + P \frac{N-1}{N} p_2 + \dots + P \frac{1}{N} p_{N-1}}{P} = \frac{\mu(\mu + \lambda)^{N-1}}{(\mu + \lambda)^N} \quad 4.18$$

$$= \frac{\mu}{(\mu + \lambda)}.$$

i.e. the equivalent availability in this simplified model is independent of the number of parallel subsystems, N . This is an interesting result which suggests that parallel powertrains do not automatically lead to improved availability. It should be noted that the power rating of each parallel powertrain sub-system has been assumed to be P/N . The influence of N may be felt when the failure and repair rates vary with N , as found in Chapter 3.

4.2.5 Developed case with more realistic repair transition paths

The simple model in subsections 4.2.2-4.2.4 is reasonable in that it assumes that failure transitions are independent, however it is limited by the repair transition paths. The model present in Figure 4.3(b) is not very realistic, as it is likely that if the wind turbine powertrain was in State 3, repair would be carried out on two of the subsystems (i.e. returning the system to State 1), rather than just one subsystem (i.e. returning the system to State 2). Indeed, the repair rate for $\mu_{2 \rightarrow 1}$ and $\mu_{3 \rightarrow 1}$ are likely to be approximately the same once logistic and weather window delays are taken into account. Figure 4.3(c) shows the developed case, where the repair transition paths have been updated. It is assumed that $\mu_{N \rightarrow 1} = \mu_{3 \rightarrow 1} = \mu_{2 \rightarrow 1} = \mu$. The transitional probability matrix for the developed state space model for $N=2$ parallel subsystems then becomes

$$\begin{bmatrix} p_{11} & p_{12} & p_{13} \\ p_{21} & p_{22} & p_{23} \\ p_{31} & p_{32} & p_{33} \end{bmatrix} = \begin{bmatrix} 1 - 2\lambda & 2\lambda & 0 \\ \mu & 1 - \mu - \lambda & \lambda \\ \mu & 0 & 1 - \mu \end{bmatrix} \quad (4.19)$$

The probabilities of being in States 1 to 3 are,

$$p_1 = \frac{\mu(\mu + \lambda)}{(\mu + 2\lambda)(\mu + \lambda)} = \frac{\mu}{(\mu + 2\lambda)} \quad (4.20)$$

$$p_2 = \frac{2\mu\lambda}{(\mu + 2\lambda)(\mu + \lambda)} \quad (4.21)$$

$$p_3 = \frac{2\lambda^2}{(\mu + 2\lambda)(\mu + \lambda)} \quad (4.22)$$

Generally the denominator for these probabilities is given by $(\mu + N\lambda)(\mu + (N-1)\lambda) \dots (\mu + \lambda)$ for N parallel subsystems. Applying (4.5) with probabilities given by (4.20-4.22) leads to,

$$A_{\text{eq},N=2} = \frac{Pp_1 + \frac{P}{2}p_2}{P} = \frac{\mu(\mu + \lambda) + \mu\lambda}{(\mu + 2\lambda)(\mu + \lambda)} = \frac{\mu}{(\mu + \lambda)}. \quad (4.23)$$

The reader should note that this is the same equivalent availability as given by the simple model. Higher values of N were evaluated using symbolic computation software (Maple). In every case, the same equivalent availability was observed.

4.2.6 Case with failure and repair rates changing with N

In Sections 4.2.2-4.2.5, a constant failure rate was assumed for the parallel powertrain subsystems, regardless of the power rating and physical size. However, Chapter 3 showed that both failure and repair rates appear to vary with power rating, and therefore the number of parallel powertrains.

In general, this change in failure rate from the assumed baseline failure rate can be taken into account using a modifying coefficient, a . For example, the failure rate of a subsystem in a $N = 2$ system is given by $\lambda_2 = a_2\lambda$ where λ is the baseline (i.e. $N = 1$) failure rate and a_2 is the modifying coefficient for when $N = 2$. When $a < 1$ it implies that the subsystem failure rate is less than the baseline and when $a > 1$ it implies that the failure rate is greater than the baseline. By substituting $\lambda_N = a_N\lambda$ into (4.18) it is possible to see the effect that this has on the equivalent availability,

$$A_{\text{eq},N} = \frac{\mu}{(\mu + a_N\lambda)}. \quad (4.24)$$

In Chapter 3, by plotting the failure rates against power, the relationship of subsystem failure rate as a function of power rating was established as shown in (3.1) where $m_\lambda = 0.357$ powertrain subsystem failures per year per MW when $c_\lambda = 0$ powertrain subsystem failures per year (i.e. if the powertrain subsystem is rated at 0MW there are no failures). If the baseline ($N=1$) failure rate is $\lambda = m_\lambda P$ and with $P_{\text{subsystem}} = P/N$ it can be seen that $a_N = 1/N$. As N increases then the equivalent availability increases. Therefore, using equation 3.1, the failure rates for the parallel powertrain subsystems for $N > 1$ was estimated and used as input data for all cases of parallel powertrain in this thesis.

A similar process can be used to modify the repair rate using a modifying coefficient, b . When $b < 1$ it implies that the subsystem takes longer to repair than the baseline and when $b > 1$ it implies that the subsystem repair process is quicker than the baseline. By substituting $\mu_N = b_N\mu$ into (4.24) it is possible to see the effect that this has on the equivalent availability,

$$A_{eq,N} = \frac{b_N \mu}{(b_N \mu + a_N \lambda)} \quad (4.25)$$

where a_N and b_N are the modifying coefficients of the failure and repair rate for any N subsystem. The repair time is likely to increase with larger units of the parallel powertrain as component sizes and numbers increase. In Chapter 3, wind turbine generator and power converter downtimes were analysed to give subsystem $MTTR$ as a function of power rating for a generic powertrain as shown in equation 3.2,

If the baseline repair rate is $\mu = 1/(m_{MTTR} P_{\text{subsystem}})$ and with $P_{\text{subsystem}} = P/N$ it can be seen that $b_N = N$. As N increases then the equivalent availability increases because of the improved repair rate.

Therefore, using equation 3.2 and 3.3, the $MTTR$ and repair rates for the parallel powertrain subsystems for $N > 1$ was estimated and used as input data for all cases of parallel powertrain in this thesis.

4.2.7 Case with varying parallel powertrain subsystem power rating

Thus far it has been assumed that the power rating of the subsystems in the parallel system is given by $P_{\text{subsystem}} = P/N$. At the design stage, there is freedom to choose the power rating of individual generators and power converters so that $P_{\text{subsystem}} = \alpha P$ where $(1/N) \leq \alpha \leq 1$. Although the installed powertrain and available capacity, $N\alpha P$, may be greater than the wind turbine rating, the system output power is limited by the wind turbine rating, P . This applies for all states, e.g. for N parallel subsystems, the installed powertrain and available capacity in State 1 is $N\alpha P$ but the output is limited to $P_1 = P$; when one subsystem fails the installed powertrain and available capacity is $(N-1)\alpha P$ but the output is limited so that $P_2 \leq P$. This can be expressed by using another variable, β , as shown

$$\begin{aligned}
A_{\text{eq},N} = & \beta_1 \binom{N}{N} \frac{(b_N \mu)^N}{(b_N \mu + a_N \lambda)^N} + \beta_2 \binom{N}{N-1} \frac{(b_N \mu)^{N-1} (a_N \lambda)}{(b_N \mu + a_N \lambda)^N} \\
& + \dots + \beta_{N-1} \binom{N}{1} \frac{(b_N \mu) (a_N \lambda)^{N-1}}{(b_N \mu + a_N \lambda)^N} \\
& + \beta_N \binom{N}{0} \frac{(a_N \lambda)^N}{(b_N \mu + a_N \lambda)^N}.
\end{aligned} \tag{4.26}$$

Where $\beta_1 = \begin{cases} 1, & \text{if } N\alpha > 1 \\ N\alpha, & \text{if } N\alpha \leq 1 \end{cases}$, $\beta_2 = \begin{cases} 1, & \text{if } (N-1)\alpha > 1 \\ (N-1)\alpha, & \text{if } (N-1)\alpha \leq 1 \end{cases}$, \dots , $\beta_{N-1} = \begin{cases} 1, & \text{if } \alpha > 1 \\ 2\alpha, & \text{if } \alpha \leq 1 \end{cases}$ and $\beta_N = \begin{cases} 1, & \text{if } \alpha > 1 \\ 2\alpha, & \text{if } \alpha \leq 1 \end{cases}$

For a given N , this leads to availability being a function of α . Plotting availability against α shows that there are different gradients in the intervals between $\alpha = 1/N, 1/(N-1), \dots, 1$. This change in gradient can be modelled using Macaulay brackets, i.e

$$\langle \alpha - x \rangle = \begin{cases} 0, & \alpha < x \\ \alpha - x, & \alpha \geq x \end{cases} \text{ in (4.27)}$$

$$\begin{aligned}
A_{\text{eq}} = & \frac{b_N \mu}{(b_N \mu + a_N \lambda)} + \langle \alpha - \frac{1}{N} \rangle (\gamma_1 + \gamma_2 + \dots + \gamma_{N-1}) \\
& - \langle \alpha - \frac{1}{N-1} \rangle \gamma_1 - \langle \alpha - \frac{1}{N-2} \rangle \gamma_2 - \dots \\
& - \langle \alpha - \frac{1}{2} \rangle \gamma_{N-1} .
\end{aligned} \tag{4.27}$$

Where $\gamma_1 = (N-1) \binom{N}{N-1} \frac{\mu^{N-1} \lambda}{(\mu + \lambda)^N}$, $\gamma_2 = (N-2) \binom{N}{N-2} \frac{\mu^{N-2} \lambda^2}{(\mu + \lambda)^N}$, $\gamma_{N-1} = N \frac{\mu \lambda^{N-1}}{(\mu + \lambda)^N}$.

Table 4.1: Input data for the availability model of different parallel powertrain configurations: (a) Generator and power converter in parallel (b) Parallel generator only (c) Parallel power converter only

Configuration of parallel powertrain	Generator and Power Converter	Generator Only	Power Only	Converter
λ	1.07	0.7905		0.252
μ	69.4	54.6		278
m_λ	0.357	0.2635		0.0933
m_{MTR}	0.0048	0.006		0.0012
Availability of powertrain unit when $N = 1$	0.985	0.986		0.999
Availability of the Rest of Turbine (including non-parallel powertrain units)	0.933	0.932		0.911

4.3 Results

The results of the methods outlined in this chapter are shown in Figs. 4.4-4.9. This was done with generic powertrain data to find the powertrain equivalent availability for three different configurations of parallelism using a combination of the availability equations above and the input data shown in Table 4.1

4.3.1 Results for a generic powertrain

Figure 4.4 gives the result of the availability for a 3MW generic wind turbine powertrain (generator and power converter) with a failure rate of 1.07 failures per turbine per year and a repair rate of 69.4 repairs per turbine per year ($m_\lambda = 0.357$ powertrain subsystem failures per year per MW and $m_{MTR} = 0.0048$ years per

powertrain subsystem repair per MW). It shows the equivalent availability for $N = 2, 3, 4, 5$ and 6 against α . The result shows that a higher value of N gives a wider range of possible values of α . The largest increase in A_{eq} is given when α changes from $1/N$ to $1/(N-1)$; the highest availability is achieved when $\alpha = 1$. The lowest availability is observed when $\alpha = 1/N$ for each N . If $\alpha = 1/N$, A_{eq} is independent of N .

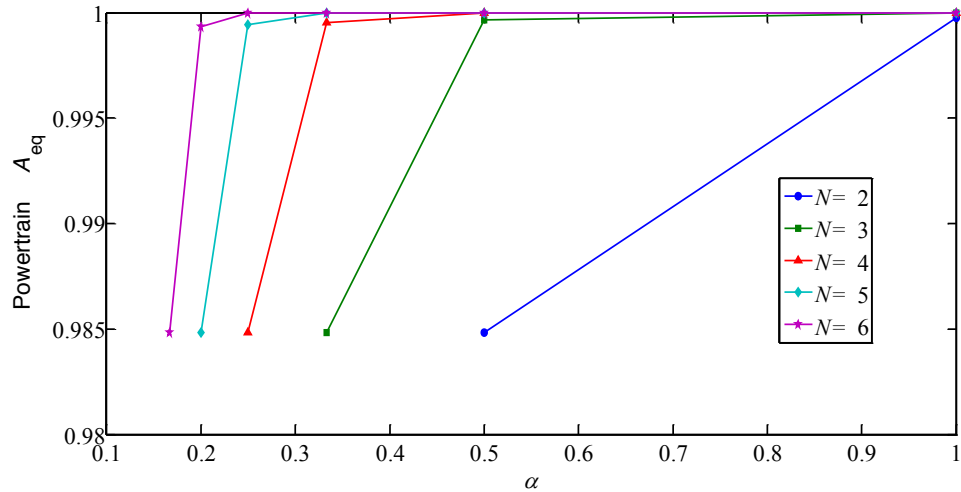


Figure 4.4: Effect of α and N on the equivalent availability of a 3MW parallel wind turbine powertrain (generator and power converter) based on generic powertrain failure ($m_\lambda = 0.357$) and repair data ($m_{MTTR} = 0.0048$)

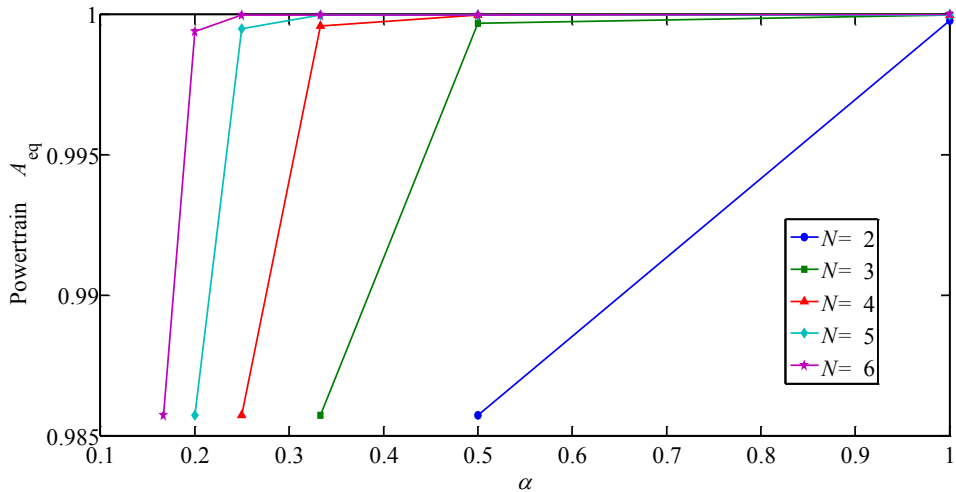


Figure 4.5: Effect of α and N on the equivalent availability of a 3MW parallel wind turbine powertrain (generator only) based on generic powertrain failure ($m_\lambda = 0.2635$) and repair data ($m_{MTTR} = 0.006$)

Figure 4.5 gives the result of the availability for a 3MW generic wind turbine powertrain (generator only) with a failure rate of 0.7905 failures per turbine per year and a repair rate of 55 repairs per turbine per year ($m_\lambda = 0.2635$ powertrain subsystem

failures per year per MW and $m_{MTTR} = 0.006$ years per powertrain subsystem repair per MW). Again, it shows the equivalent availability for $N = 2, 3, 4, 5$ and 6 against α and that a higher value of N gives a wider range of possible values of α . The largest increase in A_{eq} is given when α changes from $1/N$ to $1/(N-1)$; the highest availability is achieved when $\alpha = 1$. The lowest availability is observed when $\alpha = 1/N$ for each N . If $\alpha = 1/N$, A_{eq} is independent of N .

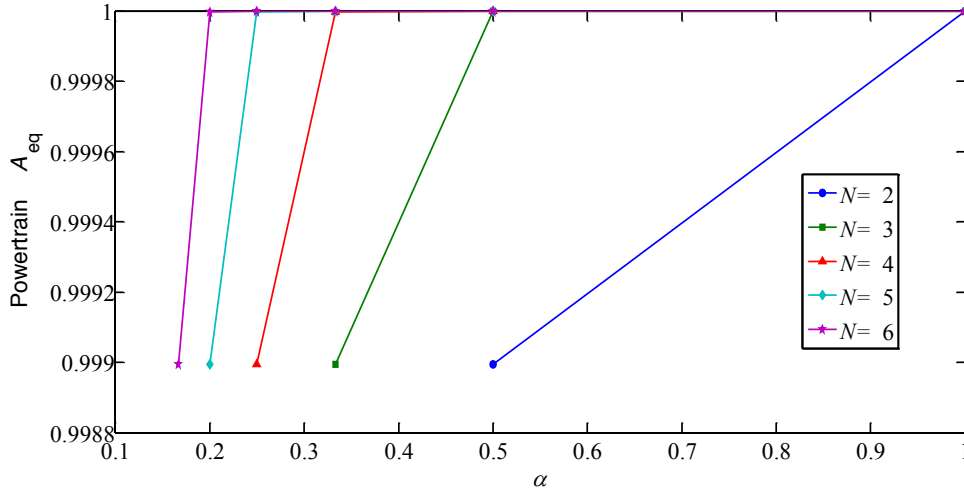


Figure 4.6: Effect of α and N on the equivalent availability of a 3MW parallel wind turbine powertrain based on generic powertrain (converter only) failure ($m_\lambda = 0.0933$) and repair data ($m_{MTTR} = 0.0012$)

Figure 4.6 gives result of the availability for a 3MW generic wind turbine powertrain (converter only) with a failure rate of 0.2799 failures per turbine per year and a repair rate of 278 repairs per turbine per year ($m_\lambda = 0.0933$ powertrain subsystem failures per year per MW and $m_{MTTR} = 0.0012$ years per powertrain subsystem repair per MW). Similar results as in the case above in terms of higher value of N offering a wider range of α and highest availability occurring at $\alpha = 1$. The largest increase in A_{eq} is given when α changes from $1/N$ to $1/(N-1)$; The lowest availability is observed when $\alpha = 1/N$ for each N . If $\alpha = 1/N$, A_{eq} is independent of N . However, in this particular case, the change in A_{eq} is small, not very significant moving from $\alpha=1/(N-1)$ to 1.

Comparing the three cases of parallelism, the lowest availability when $\alpha = 1/N$ for each N is observed from parallelism in generator and converter combined while highest availability comes from the case of converter only at $\alpha = 1$.

While Figures 4.4-4.6, shows the case of equivalent availability for the parallel powertrain units only, the results in Figures 4.7-4.9 indicate the case where the availability of the rest of turbine including all the non-parallel units in the wind turbine is also considered. In that case, the lowest availability when $\alpha = 1/N$ for each N is observed from the wind turbine having parallelism in converter only while highest availability comes from the case of generator and converter combined at $\alpha = 1$.

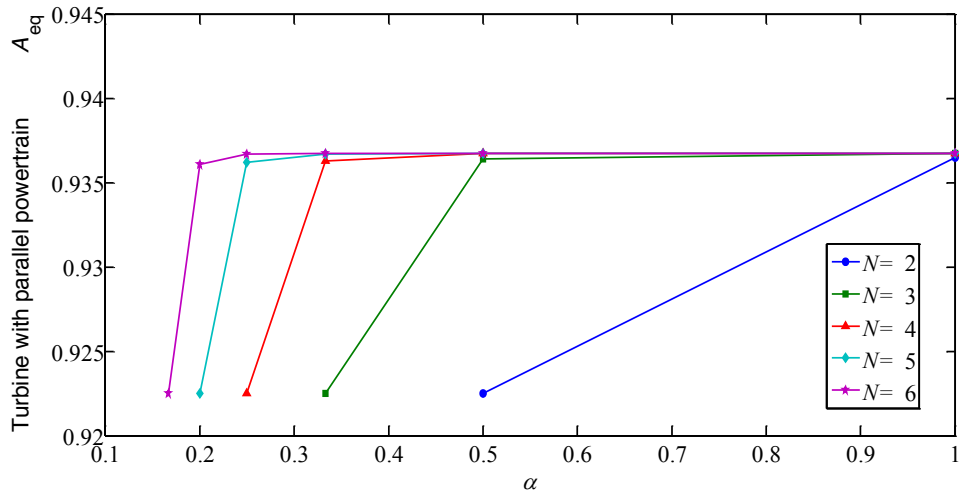


Figure 4.7: Effect of α and N on the equivalent availability of a 3MW parallel wind turbine powertrain (generator and power converter) based on generic powertrain failure ($m_\lambda = 0.357$), repair data ($m_{MTTR} = 0.0048$) and including rest of turbine availability $A_{RoT(inc.gb)}$

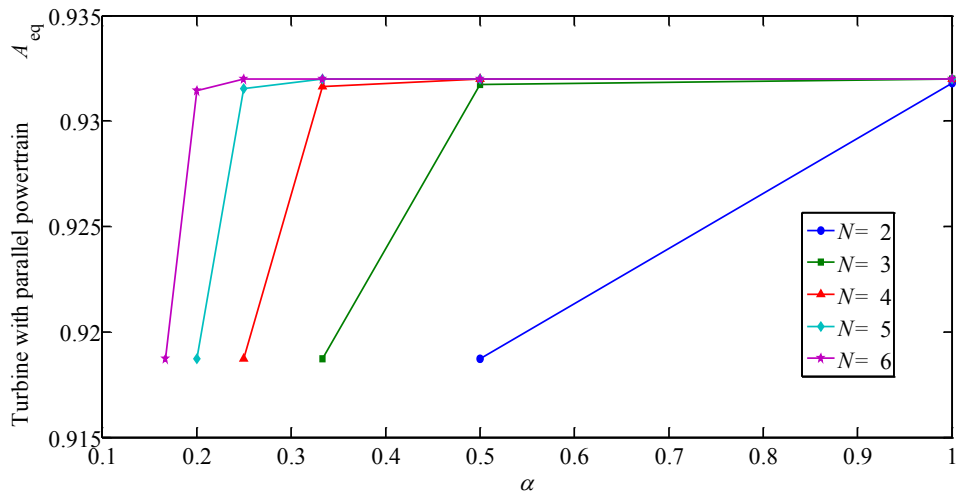


Figure 4.8: Effect of α and N on the equivalent availability of a 3MW parallel wind turbine powertrain (generator only) based on generic powertrain ($m_\lambda = 0.2635$) and repair data ($m_{MTTR} = 0.006$) and including rest of turbine availability $A_{RoT(inc.gb,pc)}$

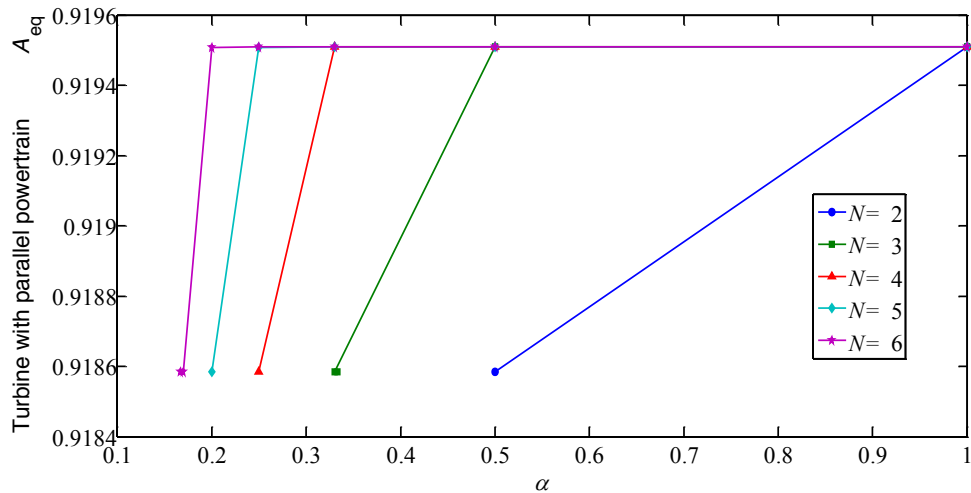


Figure 4.9: Effect of α and N on the equivalent availability of a 3MW parallel wind turbine powertrain (power converter only) based on generic powertrain failure ($m_\lambda = 0.0933$) and repair data ($m_{MTR} = 0.0012$) and including rest of turbine availability $A_{RoT(\text{inc.gb,gen})}$.

4.4 Discussion

The following sections discuss the implications of the models developed in Section 4.2 and their application.

4.4.1 Implications of the equivalent availability model

4.4.1.1 Parallel powertrains do not necessarily lead to higher equivalent availability

The first step in this chapter considered a simple Markov model with one generator and one power converter being used to determine the baseline equivalent availability. It had been assumed that the addition of extra parallel powertrains (i.e. $N > 1$, where each subsystem is rated at P/N) would lead to an increase in equivalent availability. In actual fact the equivalent availability was found to be independent of N . Even when the simple model was updated to include more realistic repair paths, the equivalent availability was still independent of N .

4.4.1.2 Effect of change in failure rate and repair rate on simple availability model

Equivalent availability can, however, be increased by (a) reducing subsystem failure rates, (b) increasing subsystem repair rates and (c) increasing the power rating of each subsystem above P/N implying an additional capital cost.

It has been suggested that a parallel powertrain might reduce repair time of each subsystem, therefore increasing repair rate and hence availability. There is some evidence that failure rate and repair rate vary with power rating; essentially a smaller subsystem fails less often and is quicker to repair. This was built into the simple model by incorporating a repair rate with power rating characteristic and a failure rate with power rating characteristic for the subsystems. The minimum power rating of a subsystem is P/N , so as N increases the failure rate and repair rate both improve. This implies that if the size of the subsystem is scaled down, one will see an improved availability compared to larger subsystems.

These secondary effects of using N parallel subsystems could be quite significant. For example, by varying only the failure and repair rates – based on industrial data – the equivalent availability improved by approximately 1.1% points when moving from $N = 1$ (baseline) to $N = 2$. Further increases can be observed as the number of parallel subsystems increase, but the marginal effect becomes smaller at larger N . It should be noted that these improvements will depend on the changes in the repair rate and failure rate with power rating characteristics.

In offshore wind turbines, having smaller components could ease some aspects of operation and maintenance strategies for the powertrain subsystems. A response to a major failure of an offshore wind turbine electrical generator often requires the hiring of a heavy lift vessel which can lead to long mean times to repair. The operator may have to wait for the vessel to be available for hire and such vessels have limited accessibility to the site which is determined by weather conditions. The same failure type in one of N parallel powertrain subsystems might be addressed using smaller, more ubiquitous vessels with less weather sensitivity. If that is the case then the failure will be repaired more swiftly. It is also possible that as the power rating of the

powertrain subsystem reduces (i.e. P/N gets smaller as N increases) then on-board hoisting and lifting equipment within the nacelle can be used, further increasing the repair rate.

4.4.1.3 Waiting to repair strategy

It is often suggested that when parallel powertrain subsystems are used and there is a failure in one of the subsystems then one can afford to wait longer (than in the baseline $N = 1$ case) to repair it without incurring the same downtime penalty. Assuming constant failure rates and that each subsystem is rated at P/N then waiting longer implies a lower repair rate and hence a reduced availability. If there is potential to wait longer (e.g. to reduce hiring costs of vessels) it is only because of the failure and repair with power rating characteristics or that the power rating of each subsystem is greater than P/N .

A further point is worth mentioning. Throughout this model, for a given N , the repair rate between states was assumed constant. For example, in Figure 4.3(c) $\mu_{2 \rightarrow 1} = \mu_{3 \rightarrow 1}$. In reality, one may be able to increase availability by adopting a variable strategy where $\mu_{3 \rightarrow 1} > \mu_{2 \rightarrow 1}$.

4.4.2 Application of the equivalent availability models

4.4.2.1 Results for a generic powertrain

The initial model implicitly assumed that the power rating of each subsystem was P/N . More explicitly, this was defined as $\alpha = 1/N$. It was shown that this α can be used as design variable with $1/N \leq \alpha \leq 1$. A larger N allows a wider choice of α , and this can be beneficial in terms of balancing the upside of additional equivalent availability and the downside of additional capital costs. From the range of α , the results show changes in availability at points $\alpha = 1/2, 1/3, 1/4, 1/5 \dots$ until a maximum availability is achieved at $\alpha = 1$.

Figure 4.4 shows that for $N = 4$, moving from each subsystem being rated at $P/4$ (i.e. $\alpha = 1/N$) to being rated at $P/3$ (i.e. $\alpha = 1/(N-1)$) gives an additional equivalent availability of 2.1%. The subsystem aggregate power rating in this case would be $4P/3$, which implies – if one assumes that capital cost are proportional to the power rating – that the subsystem cost will be one third more expensive than the baseline powertrain cost.

4.4.2.2 Results for different parallel powertrain configurations

In terms of equivalent availability of parallel powertrain excluding non-parallel units, the case with power converter only in parallel comes first, followed by the powertrain with the generator only in parallel, and finally by combining a parallel generator and a parallel power converter as shown in Figures 4.4-4.6. As shown in table 4.1, the reason for this might be partly down to the failure rate and repair rate estimated for the generic powertrain where the combination of generator and converter has the highest failure rate and lowest repair rate of 1.074 and 69.4, which is significantly higher than for the generator and power converter separately.

However, when the availability of the overall turbine is taken into account, the wind turbine with power converter only in parallel had the lowest availability of 0.9195, while parallel generator only had 0.934. The parallel generator and power converter combined is seen to have the highest availability at different ranges of α e.g. 0.9367 at $\alpha=1$. In this case, the availability of the rest of the turbine including non-parallel units is considered in each case of parallelism. The reason for this result is because the rest of turbine have better availability $A_{RoT(inc.gb)}$ in the case of generator and converter combined than the case of generator and converter separate $A_{RoT(inc.gb,pc)}$ and $A_{RoT(inc.gb,gen)}$. Although the equivalent availability of converter only is high as shown in Figure 4.8, due to quick repair time leading to low downtime, yet the overall availability including non-parallel units is low. This, therefore, implies that having more different turbine subsystems in parallel is better off than having only one kind of component in parallel. It is also very realistic to account for the rest of turbine when

analysing any proposed new technology to justify the impact on the overall wind turbine system.

4.4.3 Assumptions and limitations of the equivalent availability models

4.4.3.1 Limitations from failure rate and repair rate data

One limitation is the use of disparate onshore and offshore generator and power converter failure rate and repair rate data from a number of published sources. As better data becomes available it should be used instead. Having said that, the models themselves are independent of the data quality.

4.5 Chapter summary and conclusion

In this Chapter parallel powertrains for wind turbines have been analysed and modelled to investigate the equivalent availability using a Markov state space model. A simple baseline system was modelled and the equivalent availability compared to N parallel subsystems. A more advanced model of availability was investigated considering the more realistic repair transition paths however it yielded the same results as the simple model. The simple model approach was extended to include failure and repair rate that varies with subsystem power rating. A factor α was introduced so that each subsystem can be rated at greater than P/N .

When the powertrain failure and repairs are assumed to be constant and they are rated at P/N then there are no changes in availability with changes to N . If these rates vary with power rating then as N increases, so does the availability. The highest availability is achieved when $\alpha = 1$.

Based on the limitations of this model in this chapter, future work should consider better failure rate and repair rates of the powertrain at different power ratings if available.

Although the optimal parallel powertrain design will vary with turbine type and its location, a choice of $N > 3$ appears to be beneficial. A good balance between additional availability and extra capital and O&M costs can generally be struck when $\alpha = 1/(N-1)$. When using a parallel powertrain, it is important that the technology used has lower failure rates and higher repair rates when N increases and the subsystem power rating is reduced.

In conclusion to the analysis carried in this section, the novelty of the research carried out in this thesis has further been shown and the research questions set out at the beginning of this chapter has been answered. It has been shown that improvement in availability is possible using parallel powertrain. The results show that an increase in the number of parallel systems N does not automatically lead to a higher availability for a wind turbine powertrain; however, when failure and repair rates scale with module power ratings then there is an improvement. The designer can further improve availability by over-rating each parallel module. It also shows that $N > 3$ is a good degree of parallelism and that the best strategy is to have both generator and power converter in parallel.

Chapter 5 Modelling of annual energy production at different failure states

5.1 Introduction

Conventional (shown in Figure 4.1a) wind turbine powertrain consists of any gearbox, generator and power converter that converts the mechanical energy from the wind turbine rotor to electrical energy conditioned for the grid. In this chapter, the focus is on the extra energy production from parallel (shown in Figure 4.1b-d) powertrain.

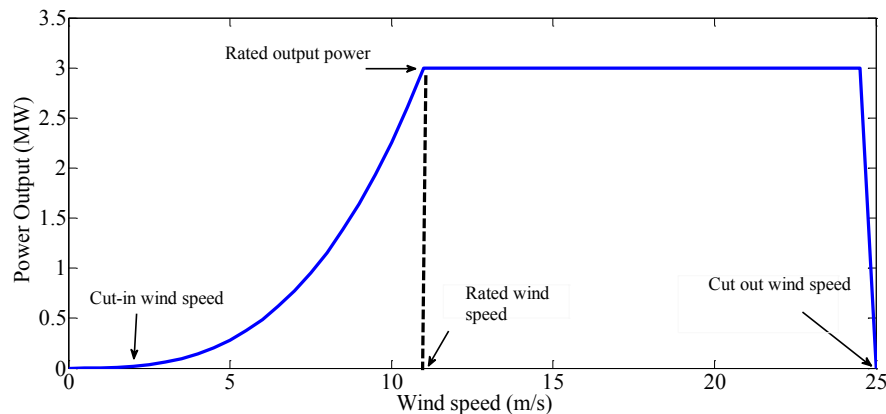


Figure 5.1: Wind turbine power curve for a wind turbine with a conventional (single gearbox, single generator and single power converter) powertrain

High energy capture – often expressed as the *AEP* – needs [108-111]: (a) a good wind resource, (b) a well-controlled wind turbine rotor with high maximum power coefficient, (c) a wind turbine power curve/rated power that matches the wind resource, (d) an efficient powertrain, (e) low wake and array losses in the wind farm and (f) a low number of hours of downtime. The wind resource of a site is often expressed as a Weibull or Rayleigh probability distribution [112][113]. The Weibull distribution is defined by 2 parameters; the Rayleigh is more approximate but is defined by a single scale parameter c . The scale parameters vary with the mean wind speed. The Rayleigh probability function, $p(v)$ describes the probability of a wind speed v

$$p(v) = \frac{2v}{c^2} \exp \left[-\left(\frac{v}{c}\right)^2 \right] \quad (5.1)$$

An idealized wind turbine power curve (“Power curve, 0 failures”) is shown in Figure 5.1.

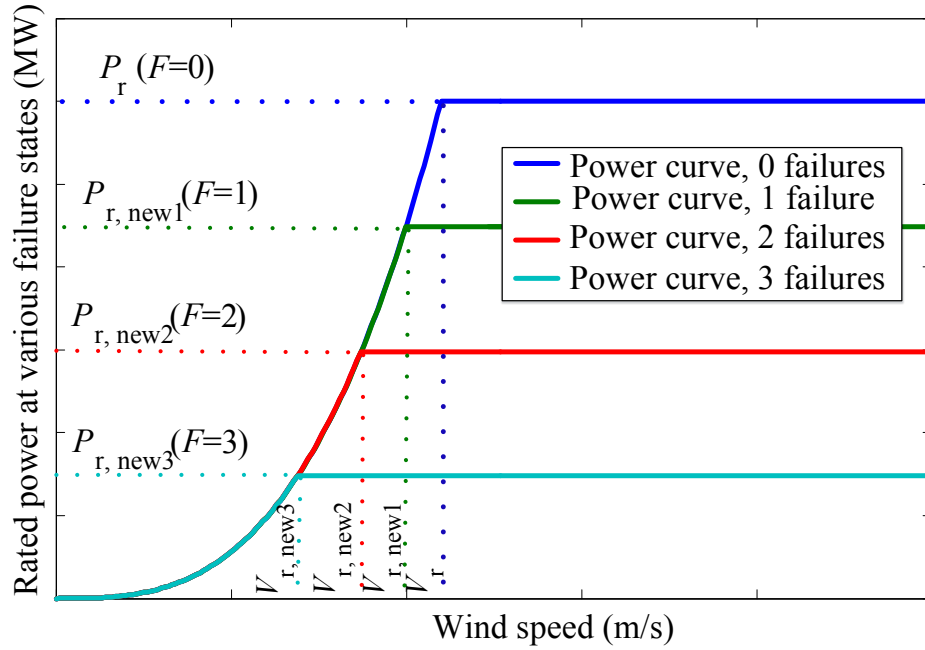


Figure 5.2: Power curves for a wind turbine with a conventional powertrain (*Power curve, 0 failures*) and a parallel powertrain ($N=4, \alpha=1$) in various failure states.

For a fixed power coefficient, the aerodynamic power of a wind turbine increases cubically with wind speed. This is correct for all $v_{ci} \leq v < v_r$, where v_{ci} is the cut-in wind speed and v_r is the rated wind speed:

$$P(v) = \frac{1}{2} \rho_{\text{air}} A v^3 c_p \quad (5.2)$$

where ρ_{air} is the density of air, A is the swept area of the rotor and c_p is the power coefficient. When the rotor and control system are well designed, c_p takes its maximum value, $c_{p\text{max}}$. Equation (5.2) can also be modified to include the powertrain efficiency $\eta(v)$ and any losses in the wind farm system. When the rated wind speed is reached the turbine produces rated power, i.e. $P(v_r) = P_r$. In an ideally regulated turbine, the power output stays constant for $v_r \leq v \leq v_{co}$ where v_{co} is the cut-out wind speed [114]. The energy production in a unit of time can then be expressed as:

$$EP = \int_{v_{ci}}^{v_{co}} P(v)p(v)dv \quad (5.3)$$

This result can then be multiplied by the amount of time in a year to find an ideal *AEP*. Equation (5.3) assumes that there are no periods of downtime, i.e. time when the turbine is not able to generate power. Downtime leads to the actual *AEP* being less than this ideal value.

The research in this chapter examines how powertrain design can be changed in order to increase *AEP* by using parallel powertrains to reduce the effective downtime of a powertrain fault. The novelty in this chapter lies in the development of a model to determine the extra energy production at various failure states of parallel powertrain using Raleigh probability distribution and the rated power of the wind turbine. This was vital to consider power not only at the rated power but to take into account the rest of the power curve. To address this, equations are developed that allow a baseline power curve to be modified so that a new rated power $P_{r,new}$ and rated wind speed $v_{r,new}$ can be used when there are failures in the parallel powertrain as shown in Figure 5.2. In such a case, the turbine controller would be able to adapt to the new failure state. To reduce the input mechanical power, the blades would pitch at progressively lower wind speeds, thereby reducing the cp_{max} when the speed goes above the new rated wind speed. This enables a new rated power and wind speed to be defined for the same turbine when operating in different failure state. This is important because it represents the times when the parallel powertrain system can still meet the required turbine power output at wind speed v , when $P(v) \leq P\alpha(N-F)$. It is noted that $P\alpha(N-F)$ represents the available power output at each failure state. Using this with the general approach allows the calculation of the energy production per unit time, *EP*. This then can be used with the probability of being in each state from the MSSM to find the *AEP*. Details of this systematic approach are explained in subsequent sections of this chapter and the findings from this work contributed to one of the publications (“*Energy yield and operations and maintenance costs of parallel wind turbine powertrains*”).

5.1.1 Conventional and parallel wind turbine powertrains

Past research has been carried out in the design and configuration of wind turbine powertrain aimed at investigating the best powertrain in terms of reliability, availability, energy yield, capital cost, O&M cost and cost of energy reduction. Polinder *et al.* carried out a useful comparison of geared and gearless powertrains based on turbine cost, energy yield and cost of energy [21]. Other papers compared the reliability of geared and gearless powertrain proposing improvement strategies to the system with gearbox [57], [115]. The majority of this past work employs a conventional single-input-single-output powertrain system with the wind turbine rotor connected to a single torque/speed conversion system (typically a gearbox), coupled to one generator electrically connected to a power converter. Such a system can be seen in Figure 4.1(a). The failure of one powertrain component leads to a shutdown of the whole turbine and hence zero power production.

Past work has proposed parallel powertrain subsystems for improved access, cost and availability [116]. A parallel powertrain system has at least one of its subsystems (gearbox, generator, power converter) made of parallel components. When there is a failure, some of the parallel subsystems can still produce power, albeit at a reduced powertrain power level. This implies that the parallel system has the capability of producing power and extra energy yield when a failure occurs in the system compared to the conventional powertrain where any failure in the powertrain components reduces the power and therefore energy production in the downtime period to zero. The introduction of parallelism in the wind turbine powertrain can be done in the gearbox, generator, converter or any combination thereof as shown in Figures 4.1(a-d).

Little past work on parallel powertrains has been encountered in the literature review for this research. It has been proposed that a system of parallel generators can help some configurations of power converters to achieve different ranges of voltage [89]. The use of high speed generators as a means of power splitting in the gearbox has also

been proposed [117]. Cottrell qualitatively compared a multiple-generator drivetrain configuration to a conventional drivetrain [23].

An *AEP* evaluation method for parallel powertrain considering the effect of failure states is proposed in this chapter. This method can be named as the multistate probability analysis method (*AEP*_{multi}). In Chapter 4, the availability of wind turbines with parallel powertrains was investigated. In that chapter, a MSSM was developed and a concept of ‘equivalent availability’ was proposed. It was shown that parallel powertrains give extra annual energy production if (a) the mean time to failure of a powertrain component increases with decreased subsystem power rating, (b) the mean time to repair decreases with decreased subsystem power rating and (c) when each subsystem power capacity of each parallel powertrain component is greater than the ratio of the wind turbine’s rated power, P , and the number of parallel units, N .

The rating of an individual component is termed $P\alpha$ where $1/N \leq \alpha \leq 1$. The total aggregate powertrain capability is $P\alpha N$ and if $\alpha > 1/N$ there is a degree of redundancy and additional capital cost. When there are failures in the powertrain subsystems, then the available powertrain capacity becomes $P\alpha(N-F)$, where F is the number of failures. The analyses in that chapter utilized MSSM to find the relative probability of each state and combined with the relevant remaining powertrain capability, it was possible to express the extra hours of partial power production as the availability equivalent to that of a conventional wind turbine powertrain (i.e. one without parallel powertrain). The research concluded that extra *AEP* was possible with parallel powertrains and that rating each of the N units at $\alpha = 1/(N-1)$ gave a good balance of extra *AEP* and modest extra capital cost.

One of the major drawbacks in the methodology of Chapter 4 is the rather simplistic method of calculating *AEP* using availability and capacity factor. The research in this chapter aims to address that shortcoming. To address this, equations are developed that allow a baseline power curve to be modified so that a new rated power $P_{r,new}$ and rated wind speed $v_{r,new}$ can be used when there are failures in the parallel powertrain. This is important because it represents the times when the parallel powertrain system can still meet the required turbine power output at wind speed v , when $P(v) \leq P\alpha(N-F)$. Combining this with the general approach in Section 5.2 allows the calculation of the

energy production per unit time, EP . This then can be used with the probability of being in each state from the MSSM in Chapter 4 to find the AEP .

In this chapter, the AEP of powertrain with parallel powertrain is analysed using Raleigh probability distribution and the rated power in order to quantify any extra benefit at below rated wind speed. The ideal AEP is analysed at rated power, rated wind speed and at no-failure state.

The following secondary research questions have been set out to be answered in this chapter.

- Can parallel powertrains generate ‘extra’ energy at failure states and consequently increase annual energy production? If so, by how much?

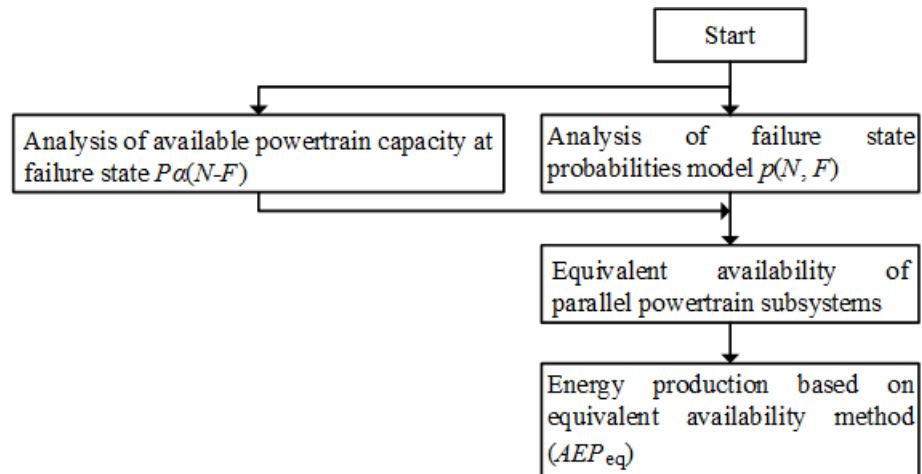
The aim is to quantify the extra energy production in failure states, since some power can be generated even after a fault has occurred.

- What happens to the torque, T of the system at failure states of parallel powertrain? Does efficiency suffer with parallel powertrain?

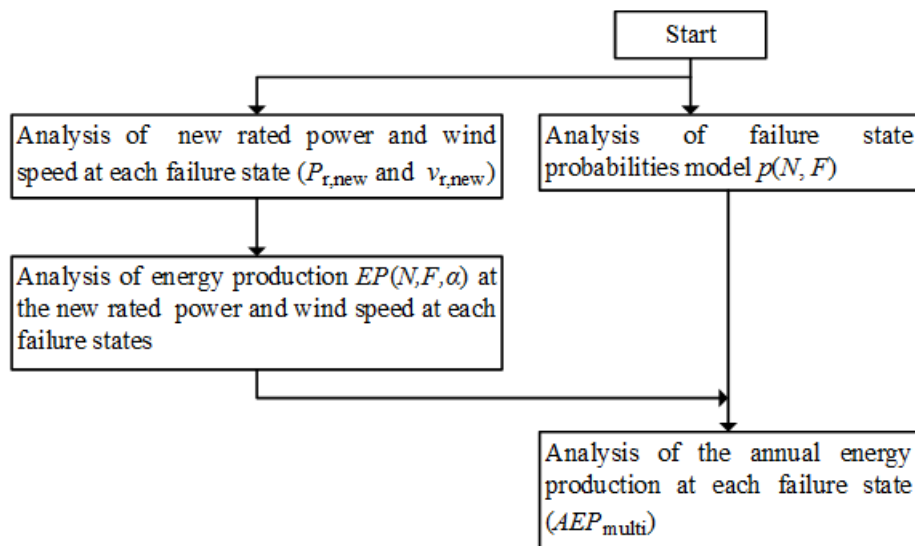
The following subsections, outline the approach adopted to answer these questions.

Sections 5.2 of this chapter describes the methodologies used to analyse the energy production for parallel powertrains as shown in subsections 5.2.1-5.2.4. Sensitivity analysis to show the impact of varying failure and repair rate is carried out in subsection 5.2.5. Section 5.3 presents the results of these models on energy production. Section 5.4 discusses these results and interpret them in the context of an offshore wind turbine of 3MW power rating. It is noted that the analysis in Section 5.2 neglects losses due to the failure states of the parallel powertrain. Therefore, Section 5.5 considers the losses due to the failure state of the parallel powertrain. Subsections 5.5.1 and 5.5.2 show the detail of the method used in analyzing the torque, losses and efficiency at failure state. In subsections 5.5.3 and 5.5.4, the results and the discussions are presented. Finally, Section 5.6 draws conclusions of the chapter and highlights some of the limitations of the methodology.

5.2 Methodology



(a)



(b)

Figure 5.3: (a) Flowchart showing the procedure to derive the annual energy production based on equivalent availability in Chapter 4 (b) Flowchart showing the procedures to derive the annual energy production based on the multi-state energy method in this chapter

Figure 5.3 show two methods for estimating the AEP for a parallel powertrain, with Figure 5.3(a) showing the method in Chapter 4 and Figure 5.3(b) showing the method in this chapter. Both methods use the same MSSM to calculate the probability of having F failures. This approach is introduced in Section 5.2.1. The two methods diverge when it comes to modelling the powertrain performance in those failure states. The new method (Figure 5.3b) synthesizes new power curves (with new rated power

and rated wind speed) for each failure F – shown in Section 5.2.2 – and combining this with a Rayleigh wind speed distribution finds energy production in a unit of time. This process is introduced in Section 5.2.3. Subsequently, this is combined with the probability of being in each state to find the annual energy production as shown in Section 5.2.4.

5.2.1 Failure state probabilities model

The probability of being in a state with a number of failures F can be modelled using MSSM as earlier described in Chapter 4 and the input data to the failure state probability model in this chapter was reproduced from chapter 4 for a generic powertrain. The number of states is effectively $N+1$ where the number of parallel subsystems is N . For any N parallel powertrain, the probability of each failure state as a function of N and F is,

$$p(N, F) = \frac{\binom{N}{N-F} \mu^{N-F} \lambda^F}{(\mu + \lambda)^N} \quad (5.4)$$

5.2.2 New power curves for F failures

If the powertrain is simply split into N parallel subsystems, then the power rating of the subsystems is given by $P_{\text{subsystem}} = P/N$. At the design stage, there is freedom to choose the power rating of individual generators and power converters, so that $P_{\text{subsystem}} = \alpha P$ where the ratio α is in the range $(1/N) \leq \alpha \leq 1$. The term $(N-F)\alpha P$ indicates the aggregate power rating of any installed powertrain subsystem when there are F failures. It may be greater than the wind turbine rating, but the usable capacity is assumed to be limited by the wind turbine rating, P_r . For instance, when one subsystem fails the installed powertrain and available capacity becomes $(N-1)\alpha P$ but the output is limited such that $(N-1)\alpha P \leq P_r$. To create these limits in the parallel system, a variable $\gamma(F, N, \alpha)$ is introduced to define a new rated power,

$$P_{r,\text{new}}(F, N, \alpha) = \gamma(F, N, \alpha) P_r \quad (5.5)$$

$$\text{where } \gamma(F, N, \alpha) = \begin{cases} 1, & \text{if } (N-F)\alpha > 1 \\ (N-F)\alpha, & \text{if } (N-F)\alpha \leq 1 \end{cases} \text{ and } F \leq N$$

At the rated turbine power, equation (5.2) can be rearranged to give the rated wind speed,

$$v_r = \sqrt[3]{\frac{P_r}{\frac{1}{2}\rho_{\text{air}}Ac_p}} \quad (5.6)$$

By extension this can be extended for a number of failures F , to give a new rated wind speed,

$$v_{r,\text{new}}(F, N, \alpha) = \sqrt[3]{\frac{\gamma(F, N, \alpha)P_r}{\frac{1}{2}\rho_{\text{air}}Ac_p}} \quad (5.7)$$

Up to this rated wind speed, the wind turbine output follows equation (5.2). Together, this means that each failure state effectively has its own power curve, as shown in Figure 5.2.

To derive the new rated power and new rated wind speed, a rated power, $P_r = 3\text{MW}$ and rated wind speed, $v_r = 11\text{m/s}$ was chosen. Equations 5.5 and 5.7 were then used to analyse the new rated power and new rated wind speed at each failure states, F for the parallel subsystem N and α . For example if $N=3$ and $\alpha=1/N$, then $P_{r,\text{new1}} = 2\text{MW}$, $P_{r,\text{new2}} = 1\text{MW}$ and $v_{r,\text{new1}} = 10\text{m/s}$, $v_{r,\text{new2}} = 8$ at $F=1$ and 2. The same process was then used for $\alpha=1/N-1$.

5.2.3 Energy production calculation with different power curves for different failure states

The energy production over the region of the power curve from the cut-in wind speed to the cut-out wind speed is analysed from the combination of equations (5.1) and (5.2) above by considering the integral of the bounded area as shown in equation (5.3). To simplify the integration, the power curve can be split into two, with the first part bounded by the cut-in and rated wind speeds and the second part bounded by the rated wind and the cut-out wind speeds,

$$EP = \frac{1}{2} \rho_{\text{air}} A c_p \left[\int_{v_{\text{ci}}}^{v_r} \frac{2v^4}{c^2} \exp \left[- \left(\frac{v}{c} \right)^2 \right] dv \right] + P_r \left[\int_{v_r}^{v_{\text{co}}} \frac{2v}{c^2} \exp \left[- \left(\frac{v}{c} \right)^2 \right] dv \right] \quad (5.8)$$

i.e. $EP = EP_{v_{\text{ci}} \rightarrow v_r} + EP_{v_r \rightarrow v_{\text{co}}}$. Integrating the first part of equation (5.8) gives:

$$EP_{v_{\text{ci}} \rightarrow v_r} = \frac{\rho_{\text{air}} A c_p}{2c^2} \left[\frac{3}{2} c^2 \left(\frac{1}{2} c^3 \sqrt{\pi} \operatorname{erf} \left(\frac{v}{c} \right) - c^2 v \exp \left[- \left(\frac{v}{c} \right)^2 \right] \right) \right]_{v_{\text{ci}}}^{v_r} - c^2 v^3 \exp \left[- \left(\frac{v}{c} \right)^2 \right] \quad (5.9)$$

Equation (5.9) includes the error function, $\operatorname{erf}(x)$. This is a function used in statistics defined as

$$\operatorname{erf}(x) = \frac{2}{\sqrt{\pi}} \int_0^x e^{-t^2} dt \quad (5.10)$$

A similar step to equation (5.9) is taken to evaluate the energy production per unit time in the region from the rated wind speed to the cut-out wind speed region ($EP_{v_r \rightarrow v_{\text{co}}}$),

$$EP_{v_r \rightarrow v_{\text{co}}} = P_r \left[\exp \left[- \left(\frac{v_r}{c} \right)^2 \right] - \exp \left[- \left(\frac{v_{\text{co}}}{c} \right)^2 \right] \right] \quad (5.11)$$

5.2.4 Annual energy production

The annual energy production was addressed using two methods (i) equivalent availability method (AEP_{eq}) and (ii) the multi-state energy method (AEP_{multi}).

The equivalent availability method follows that of the model in Chapter 4. This is shown in Figure 4.6, where the equivalent availability varies with α and different curves show different numbers of parallel subsystems, N . The input data (baseline failure rate, $\lambda = 1.074$ failures per turbine per year and baseline repair rate, $\mu = 69.4$ repairs per turbine per year) for the availability model was taken from Chapter 4 for a generic wind turbine powertrain, and varies with the power rating of each parallel powertrain, $P_{\text{subsystem}}$. Details of this analysis for $\lambda_{\text{subsystem}}$ and $\mu_{\text{subsystem}}$ is shown in Chapter 4 and represented by equations (4.26) and (4.28). Other wind turbine input data used in the AEP model in this chapter is shown in table 5.1 below.

The equivalent availability is calculated by $\sum P_r(N, F, \alpha)p(N, F)$ subject to the limits in Section 5.2.2. This leads to the equivalent availability from equation 4.31.

It was found in Chapter 4 that a good balance of additional energy yield with limited marginal costs could be found when $\alpha = 1/(N-1)$ for each case of N . The equivalent availability of the parallel wind turbine powertrain including rest of turbine showing one failure states which were used in this chapter was taken from Chapter 4.

It is noted that this is equivalent of availability of the powertrain only, hence to find the overall turbine availability, A_T is given by $A_{RoT}A_{eq}(N, \alpha)$, where the ‘rest of turbine’ availability, $A_{RoT} = 0.933$. It is noted that this will vary depending on where parallelism is applied. For instance, if only generator that is used as a parallel module, then the rest of the turbine will include gearbox and power converter, i.e. $A_{RoTinc.Gbpc}$ (rest of turbine including gearbox and power converter). This was then combined with the ideal energy production to obtain energy based on the equivalent availability method (AEP_{eq}),

$$AEP_{eq} = AEP_{ideal}A_{RoT}A_{eq}(N, \alpha) \quad (5.12)$$

The ideal annual energy production, AEP_{ideal} is the AEP of the wind turbine powertrain at no-failure state i.e. when all the powertrain subsystems are all working and is derived analytically as represented by equation (5.3) and multiplied by the number of hours in a year, i.e. 8760. The ideal annual energy production was analysed and modelled using equation (5.3) with a rated wind speed of 11m/s (used as the baseline rated wind speed).

To get the annual energy production with different power curves for different failure states, AEP_{multi} , the summation of the product of the energy production at each state and the probability of that state is evaluated as:

$$AEP_{multi} = \sum [EP(N, F, \alpha)p(N, F)]8760 \quad (5.13)$$

Table 5.1: Wind turbine parameters used in *AEP* model

Reliability data	
Powertrain failure rate λ (failures/turbine/year)	1.074
Powertrain repair rate μ (repairs/turbine/year)	69.4
m_λ	0.36
m_{MTTR}	0.0048
Availability Rest of Turbine A_{RoT}	0.933
Wind turbine characteristics	
Rated power P_r (MW)	3
Rated wind speed v_r (m/s)	11
Cut in wind speed v_{ci} (m/s)	4
Cut out wind speed v_{co} (m/s)	25
Power coefficient c_p	0.4
Wind turbine rotor radius (m)	54.5
Scale parameter c (m/s)	12

5.2.5 Effect of failure and repair rate on the annual energy production

A sensitivity analysis was carried out to analyse the impact of varying failure and repair rate on the annual energy production of the wind turbine. To do this, the failure rate was kept constant while the repair rate was varied (increased by 5%, 10%, 15% and 20% from baseline repair rate of 69.44). Secondly, the process was repeated by varying the failure rate (increased by 5%, 10%, 15% and 20% from baseline failure rate of 1.07) while keeping the repair rate constant.

5.3 Results and Sensitivity Analyses

The results of the methods outlined in Section 5.2 are shown in Figures 5.4-5.6.

5.3.1 Annual Energy Production

For the wind turbine and a location with wind speed distribution described in Table 5.1 and with no failures, the ideal energy production is 16.1 GWh. This was derived using analytical method (i.e. equations 5.1, 5.2, 5.9 and 5.11). When there is no

parallelism ($N=1$) in the powertrain, this AEP falls to 14.8 GWh (i.e. represents about 92% of the estimated ideal AEP) due to the system downtime.

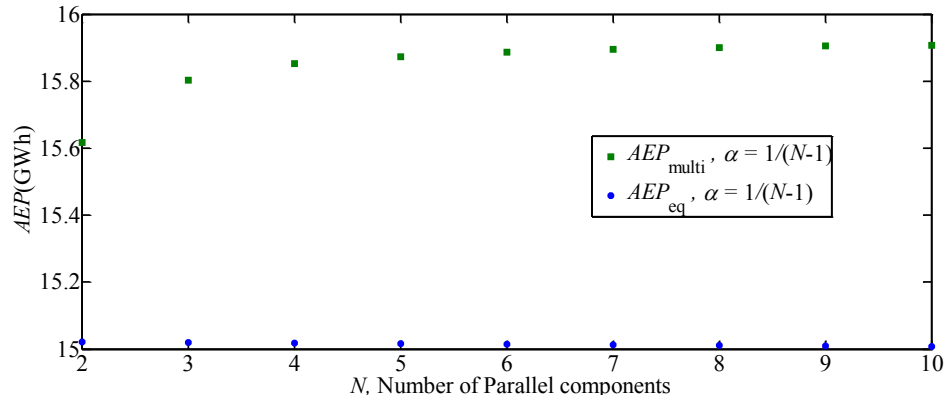


Figure 5.4: Results of AEP using probability state failure and equivalent availability at rated wind speed of 11m/s and at $\alpha=1/N-1$. ($AEP=14.8$ GWhr for no-parallelism i.e. $N=1$)

Figure 5.4 shows the AEP for the wind turbine when the parallel powertrains are used. Results for the equivalent availability method (AEP_{eq}) and multi-state method (AEP_{multi}) are shown. In both cases $\alpha = 1/(N-1)$ is assumed. It shows that the equivalent availability method tends to underestimate the energy production (due to parallelism) when below rated wind speeds are considered, i.e. AEP_{multi} . This method is able to quantify the additional energy production by up to 5% in the cases where there are one or more failures. Figure 5.4 also shows that there are increase in AEP_{multi} with higher N which is not seen in the results from AEP_{eq} .

An increase in AEP can be observed as the number of parallel subsystems increase, but the marginal effect becomes smaller at larger N . For this turbine, a parallel powertrain with $N = 10$ would give an additional AEP of 1.1GWh as compared to a non-parallel powertrain. From figure 5.4, the average energy from parallel powertrain is 15.85GWh which represents 98% energy available from the estimated ideal AEP .

5.3.2 Annual energy production for different parallel powertrain configurations

The AEP for the three configurations of parallelism is shown in Figure 5.5 for (a) generator and power converter both in parallel, (b) parallel generator only and (c) parallel converter only. The powertrain with generator and converters in parallel offers

the highest AEP and when the parallel powertrain includes the generator only, then there is still a significant increase, as seen by the data points which indicates closeness to the combined case. When only the power converter is in parallel the AEP is lowest.

The availability of the rest of the turbine including gearbox for the three configurations are 0.933, 0.932 and 0.91 which account for the close data points. The average percentage energy available from the estimated ideal energy are approximately 92% (for generator and converter), 92% (for generator only) and 91% (for converter only).

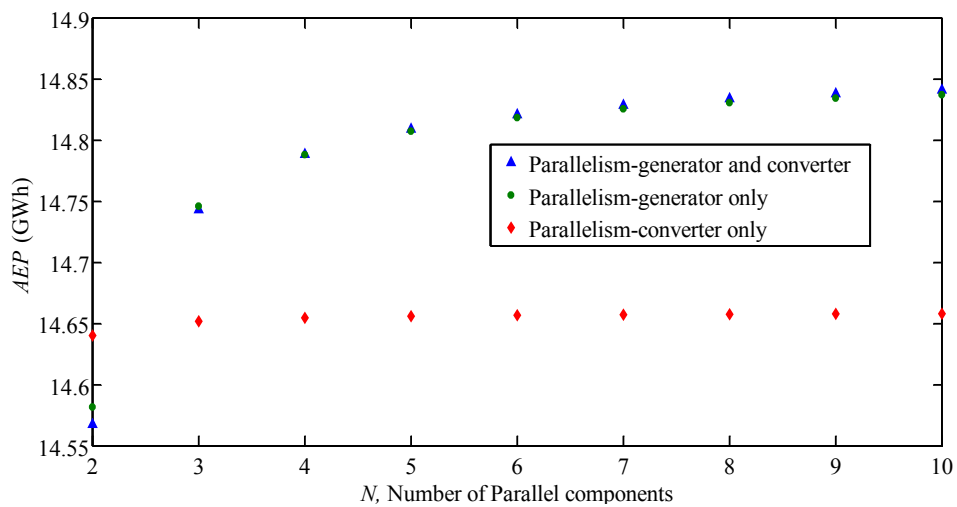


Figure 5.5: Comparison of AEP for parallel powertrain configurations: parallelism in generator and power converter, parallelism in generator only, parallelism in power converter only

5.3.3 Sensitivity analysis - Impact of constant failure rate and varying repair rates on AEP

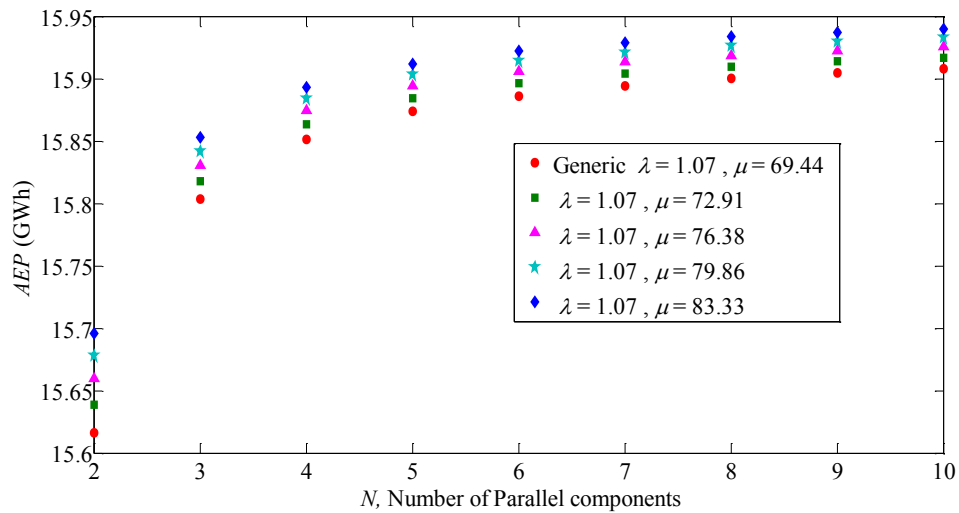


Figure 5.6: Sensitivity analysis to show the impact of repair rate on the AEP while the failure rate is kept constant for number of parallel subsystems for a 3MW wind turbine

Figure 5.6 shows the AEP result of different repair rate for different powertrain configuration while assuming a constant failure rate. As shown, the annual energy production increases with N with the maximum achieved at $N=10$. The results show that for every improvement in repair rate, there is an increase in the AEP . Increase in the repair rate would mean that faulty subsystem is repair quicker, resulting in restoring the turbine to its operational state and hence increasing the energy production. This work around the sensitivity of inputs is just to provide an indication of how results change when the inputs are varied. This was important to expose the results to the uncertainty around failure rates and repair rate.

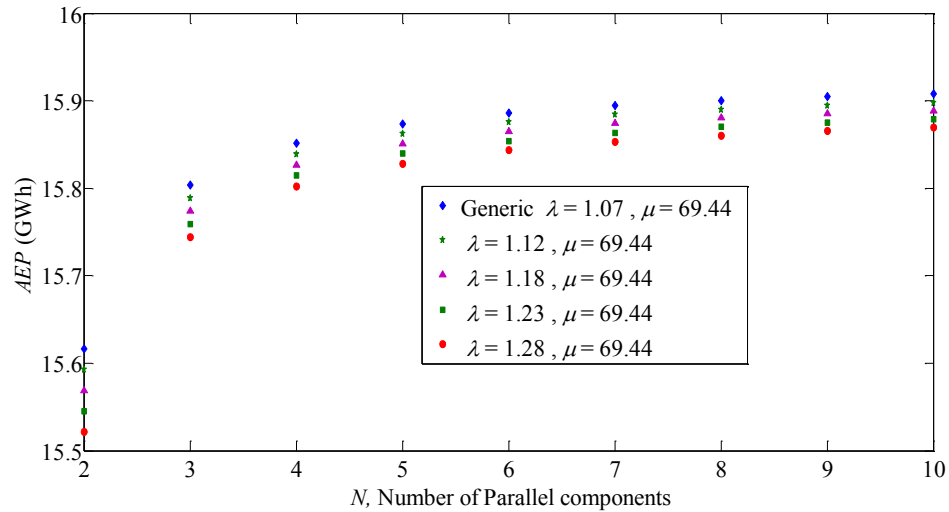


Figure 5.7: Sensitivity analysis to show the impact of failure rate on the *AEP* while the repair rate is kept constant for parallel subsystems for a 3MW wind turbine

Figure 5.7 shows the *AEP* results of different failure rates for different powertrain configuration while assuming a constant repair rate. As shown, the annual energy production increases with N with the maximum achieved at $N=10$. The results show that for every reduction in failure rate – even very marginal – the *AEP* increases. Again, the difference lessens as N gets larger.

5.3.4 Effect of different failure and repair rates using different powertrain topologies

Each failure state with higher probability contributes more to the *AEP* and consequently to the extra *AEP* that gives the additional net benefit. The failure rate, repair rate and the rest of turbine availability also influenced the *AEP*.

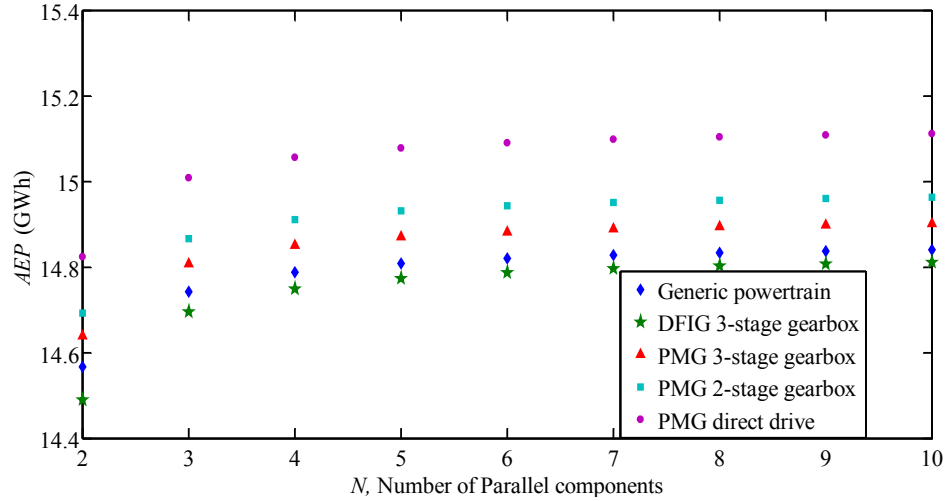


Figure 5.8: Sensitivity analysis: Comparison of AEP for different powertrain number of parallel subsystems (generator and power converter combined) for a 3MW wind turbine. Figure 5.8 shows the result of varying the failure and repair rate of the parallel powertrain while evaluating the AEP . As shown, the annual energy production increases with N with the maximum achieved at $N=10$. The initial failure and repair rate for the generic powertrain was compared to those from other types of powertrain showing variation in the reliability data for the different powertrain. The results show that for every variation, the AEP increases with N indicating the dependence of AEP on the reliability of powertrain expected from such turbine.

For the specific powertrain, the permanent magnet generator with direct drive () had the highest energy production due to its high reliability compared to others- no gearbox and hence higher availability. This brief sensitivity analysis demonstrates that even slight increases or decrease in the reliability of powertrain have an impact on the overall AEP for the site.

5.4 Discussions on AEP model

5.4.1 Influence of N on AEP

A comparison of the AEP from the two methods, AEP_{eq} and AEP_{multi} described in Section 5.2 showed that the highest AEP comes from AEP_{multi} . This is because the equivalent availability method fails to model the energy production correctly at below

rated wind speeds when the powertrain is in a failure state. The difference in the two models highlights the importance of including this feature in the analysis.

Increasing N allows more additional energy to be captured, partly because as N increases, the new rated power and the energy production from $F \geq 1$ is also higher. The highest AEP_{multi} comes from $N=10$ – the highest value of N studied in this research – but it is observed that the marginal increase falls moving from $N=2$ to $N=10$.

5.4.2 Annual energy production for different parallel powertrain configurations

In terms of AEP for the different parallel powertrain type, generator and power converter combined in parallel comes first, followed by the powertrain with generator and finally the case where only the power converter is in parallel. The non-parallel (baseline) case had the least AEP .

The failure rate, repair rate, rest of turbine availability including non-parallel units for each parallel powertrain type are contributing factors to the results of the AEP improvement.

5.4.3 Effect of failure and repair rate of different powertrain on AEP

In Figure 5.8, it could be seen that AEP from the PMGs were the highest at all N with the gearless/direct drive powertrain higher than the geared permanent generators due to their high reliability.

The doubly fed induction generator had the lowest AEP compared to the PMGs. This difference comes from the high reliability of the PMG system compared to the DFIG. This clearly demonstrates the significant role that the failure and repair rate plays in the energy production of wind turbine. It is evident that a powertrain technology with the potential of failure and repair rate improvement is important and scaling down powertrain as seen in the parallel subsystem may be useful.

Generally, the results of sensitivity analysis (Figures 5.6-5.8) indicate that when the two reliability parameters are taken into consideration, the failure rate appears to make more impact on the *AEP* than the repair rate. Improving the failure rate by 0.20 faults/subsystem/year can lead to increases of about of 0.05GWhr/year *AEP*, where it requires an improvement of around 17 repairs/subsystem/year to achieve the same results.

5.4.4 Neglecting additional powertrain losses in failure states

In the subsections 5.2-5.4 of this thesis, it was shown that the analysis on *AEP* neglected two forms of powertrain losses when the powertrain is in failure states $F \geq 1$. It was assumed that the efficiency was constant even when there was failure of one or more parallel modules. A drop in efficiency would be expected for the remaining functional powertrain modules as these are expected to generate power at higher torques than designed. Higher torque leads to higher load losses (e.g. higher I^2R losses for a generator). These additional losses mean that the AEP_{multi} in the previous section of this chapter is over-estimated. When a powertrain module fails, it may still incur so called no load losses – when rotating components continue to rotate – but these were neglected.

5.5 Losses and efficiency of parallel powertrain in failure states

This section seeks to analysed and account for the neglected losses in the previous sections and answers two of the research questions stated in the introduction section of the chapter:

What happens to the torque, T of the remaining healthy parallel powertrain subsystems during failure states? How does efficiency suffer with parallel powertrains in those circumstances?

The following subsections outline the approach adopted to answer these questions by examining copper losses which can be related back to current and hence torque.

5.5.1 Methodology

In this section, the research aims to consider the additional copper losses at the various failure states F . The following procedures and the simplified flowchart in Figure 5.10 outline the steps taken to evaluate the extra copper losses coming from the failure state of the powertrain and the resulting annual energy production of the wind turbine:

- (i) The extra torque is calculated based on the number of parallel powertrain modules, the number of failures and expressed in terms of the wind speed.
- (ii) That extra torque maps onto additional current and hence copper losses. The relationship between T and I of a machine was then used to establish changes in the current I hence I^2R . This additional loss is expressed in terms of wind speed.
- (iii) The difference between the original annual energy production (AEP_{multi}) and the new AEP_{new} with losses was then derived, using the AEP_{new} for each failure state and the probability of being in that state.

It must be noted that there are other losses in the generator and the changes in these are neglected (mostly non-torque related and the speed not really changing here). In addition, current/losses conduction in power electronics has been neglected but could be modelled in this way. Generally, copper losses are dominant [21].

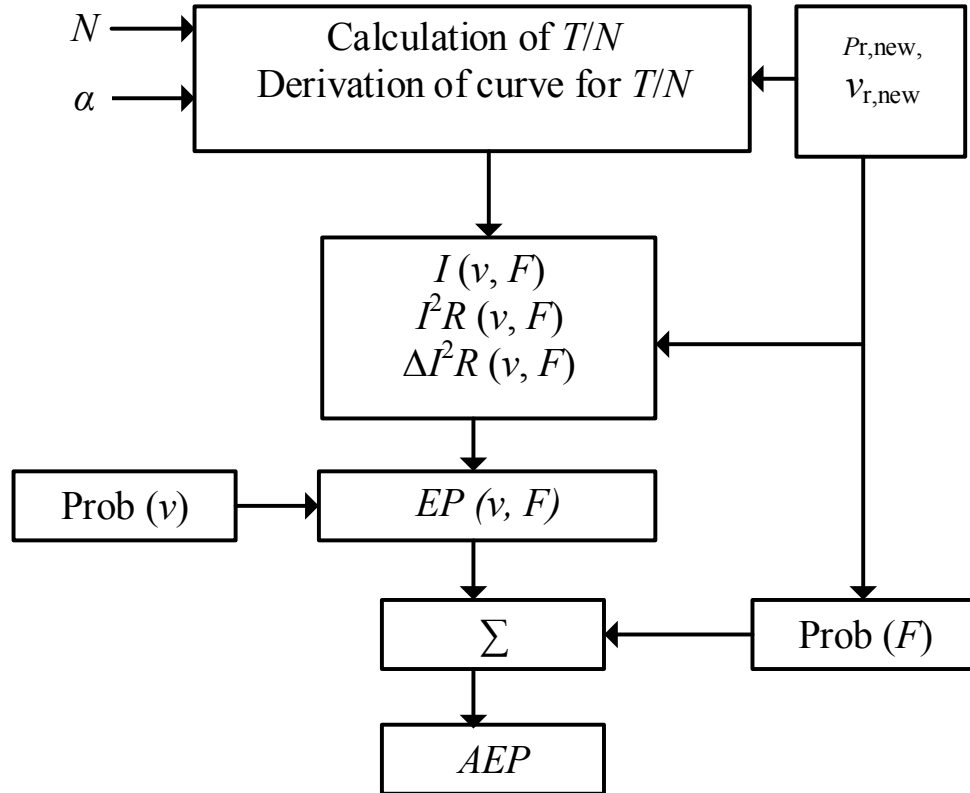


Figure 5.9: Flowchart showing the procedure to derive the resultant annual energy production of parallel powertrain at failure states using the probability of wind speed and the probability of each failure state

5.5.1.1 Torque per parallel module with no failure

This subsection seeks to find the changes in torque between the healthy torque of each parallel powertrain module and that in a failure state, doing so in a way for all wind speeds. The aim is to produce a model that works for N parallel modules, F failures and also includes the effect of over-rating the parallel powertrain α .

The aerodynamic power of a wind turbine for a fixed and maximum power coefficient was stated in equation 5.2.

Below the rated wind speed, the maximum power coefficient is achieved when the rotor speed of the turbine Ω is varied to achieve the optimal tip speed ratio, $\lambda_{\text{opt}} = \frac{\Omega r}{v_{\text{wind}}}$. This means the rotational speed can be found in terms of the wind speed

v_{wind} ,

$$\Omega = \frac{\lambda_{\text{opt}} v_{\text{wind}}}{r} \quad (5.15)$$

The healthy torque of the wind turbine T as a function of the wind speed, v_{wind} is then

$$T(v_{\text{wind}}) = \frac{P}{\Omega} = \frac{1}{2} \frac{\rho_{\text{air}} \pi r^3 v_{\text{wind}}^2 c_p}{\lambda_{\text{opt}}} \quad (5.16)$$

Introducing parallelism, the healthy torque of the wind turbine T as a function of the wind speed, v_{wind} per parallel module N up to rated wind speed is,

$$\frac{T(v_{\text{wind}})}{N} = \frac{1}{2} \frac{\rho_{\text{air}} \pi r^3 v_{\text{wind}}^2 c_p}{N \lambda_{\text{opt}}} \quad (5.17)$$

Above rated wind speed the power and the rotor speed is generally fixed by action of the blades pitching. Above the rated wind speed, the blades pitch and the turbine torque is

$$T_r(v_{\text{wind}}) = \frac{P_r}{\Omega_r} = \frac{r P_r}{\lambda_{\text{opt}} v_r} \quad (5.18)$$

where $v_{\text{wind}} \geq v_r$.

The healthy torque of the wind turbine T per parallel module N at above rated then becomes a fixed quantity,

$$\frac{T_r(v_{\text{wind}})}{N} = \frac{r P_r}{N \lambda_{\text{opt}} v_r} = \frac{1}{2} \frac{\rho_{\text{air}} \pi r^3 v_r^2 c_p}{N \lambda_{\text{opt}}} \quad (5.19)$$

where $v_{\text{wind}} \geq v_r$

5.5.1.2 Torque deficit in a fault scenario

The torque deficit during a fault scenario can also be evaluated. Each time there is failure of a parallel module, there is a loss of powertrain torque in the system. This will mean that extra torque is required to keep the system running with the remaining subsystem. When there is a fault, then $F \geq 1$. The number of remaining working modules is $N-F$ and the torque deficit is

$$T_{\text{def}} = F \cdot \left(\frac{T(v_{\text{wind}})}{N} \right) = F \cdot (\alpha T(v_{\text{wind}})) \quad (5.20)$$

In such a case the required torque is $T(v_{\text{wind}})$ but the delivered torque is

$$\begin{aligned} T_{\text{del}} &= T(v_{\text{wind}}) - T_{\text{def}} = T(v_{\text{wind}}) - F \left(\frac{T(v_{\text{wind}})}{N} \right) \\ &= T(v_{\text{wind}})(1 - \alpha F) \end{aligned} \quad (5.21)$$

At this failure state, the extra torque T_{ex} per module required to make up the deficit is equal to the ratio of torque deficit to the number of remaining modules, i.e. $(N-F)$,

$$T_{\text{ex}} = F \left(\frac{T(v_{\text{wind}})}{N(N-F)} \right) \quad (5.22)$$

This extra torque can then be added to the torque per module (given by 5.17 or 5.19, depending on what the wind speed is):

$$T_{\text{new}}(v_{\text{wind}}) = \frac{T(v_{\text{wind}})}{N} + F \left(\frac{T(v_{\text{wind}})}{N(N-F)} \right) = \frac{N}{N-F} \left(\frac{T(v_{\text{wind}})}{N} \right) \quad (5.23)$$

At below rated wind speed, the new torque per module is

$$T_{\text{new}}(v_{\text{wind}}) = \frac{N}{N-F} \left(\frac{1}{2} \frac{\rho_{\text{air}} \pi r^3 v_{\text{wind}}^2 c_p}{N \lambda_{\text{opt}}} \right) = \left(\frac{T(v_{\text{wind}})}{N-F} \right) \quad (5.24)$$

At above rated wind speed, the new torque per module is

$$T_{\text{new}}(v_{\text{wind}}) = \frac{N}{N-F} \cdot \left(\frac{1}{2} \frac{\rho_{\text{air}} \pi r^3 v_r^2 c_p}{N \lambda_{\text{opt}}} \right) = \left(\frac{1}{2} \frac{\rho_{\text{air}} \pi r^3 v_r^2 c_p}{(N-F) \lambda_{\text{opt}}} \right) \quad (5.25)$$

5.5.1.3 Ratio of new torque to old torque

Equations 5.24-5.25 and 5.17,19 represent the new and old torques and can be expressed as a ratio to give

$$\text{Torque ratio} = \frac{T_{\text{new}}(v_{\text{wind}})}{T_{\text{old}}(v_{\text{wind}})} = \frac{N}{N-F} \quad (5.26)$$

More failures of the parallel modules imply a higher torque ratio. This would mean that more torque is generated as failure occurs in the parallel modules.

5.5.1.4 Generator torque and current (old and new)

When electrical machines fail, there is a change in the torque compared to the healthy/original torque of the system. A change in torque at various wind speeds will cause changes in current and hence a new copper loss of the machine. The aim of this section is to quantify the change in copper loss during failure state for the parallel module. For any given generator with a fixed rotor field, the output current is

proportional to the torque. For a perfect generator, connected at unity power factor then,

$$P \approx 3IV = \eta T \omega \quad (5.27)$$

where I is the current, V is the terminal voltage, ω is the generator angular velocity in radians per second, η is the efficiency and T is the generator torque.

In general, the generator torque and its current, I are related by machine torque constant ' k ' so that,

$$T = kI \quad (5.28)$$

In terms of this parallel powertrains, one can assume that each generator module has the same current. Expressing the torque equation in terms of per modules, now with a different value of k gives,

$$\frac{T}{N} = kI \quad (5.29)$$

The extra torque is similarly related to extra current by the same ' k '

$$T_{\text{ex}} = kI_{\text{ex}} \quad (5.30)$$

The new current, I_{new} can then be expressed as

$$I_{\text{new}} = I_{\text{old}} + I_{\text{ex}} = \frac{1}{k} \left[\frac{T}{N} + F \left(\frac{T}{N(N-F)} \right) \right] = \frac{1}{k} \left(\frac{T}{N-F} \right) \quad (5.31)$$

Noting that the extra current can be expressed as

$$I_{\text{ex}} = I_{\text{old}} \frac{F}{N-F} \quad (5.32)$$

5.5.1.5 Copper losses

In the baseline case, it is assumed that the copper loss ($P_{\text{cu}} = 3NI^2R$) is 5% of the turbine rated power, P_r , such that

$$P_{\text{cu,r}} = 0.05P_r \quad (5.33)$$

At rated power, this can be stated as

$$I_r^2 R = \frac{0.05}{3N} P_r \quad (5.34)$$

Equation 5.17 shows that at below rated wind speed the torque is proportional to the square of wind speed and equation 5.29 shows that the current and torque are proportional, hence at rated and above conditions,

$$I_r^2 R = \frac{0.05}{3N} P_r = k_2 v_r^4 \quad (5.35)$$

where k_2 is a constant for a given machine. For below rated wind speed conditions this relationship

$$I(v_{\text{wind}})^2 R = k_2 v_{\text{wind}}^4 \quad (5.36)$$

Therefore, the copper losses can be restated in terms of the wind speed and the rated wind speed and power,

$$P_{\text{cu}} = 3NI(v_{\text{wind}})^2 R = 0.05P_r \left(\frac{v_{\text{wind}}}{v_r} \right)^4 \quad (5.37)$$

In the event of failure, there is a change in the current leading to a new copper loss,

$$P_{\text{cu,new}} = 3N(I_{\text{old}}(v_{\text{wind}}) + I_{\text{ex}}(v_{\text{wind}}))^2 R \quad (5.38)$$

Substituting equation 5.31 into 5.38 and expressing in terms of N , I , R , F , and v gives

$$\begin{aligned} P_{\text{cu,new}} &= 3N(I_{\text{old}}(v_{\text{wind}}) + I_{\text{ex}}(v_{\text{wind}}))^2 R \\ &= 3NI_{\text{old}}(v_{\text{wind}})^2 R \left[1 + 2 \frac{F}{N-F} + \left(\frac{F}{N-F} \right)^2 \right] \\ &= 0.05P_r \left(\frac{v_{\text{wind}}}{v_r} \right)^4 \left[1 + 2 \frac{F}{N-F} + \left(\frac{F}{N-F} \right)^2 \right] \end{aligned} \quad (5.39)$$

for $N \geq 2$ and $F < N$.

The change in copper losses, ΔP_{cu} is the difference between the new copper loss and the old copper loss,

$$\Delta P_{cu} = 3N(I_{old}(v_{wind}) + I_{ex}(v_{wind}))^2 R - 3NI_{old}(v_{wind})^2 R \quad (5.40)$$

This can be expressed in similar terms to equation 5.39, for $N \geq 2$ and $F < N$,

$$\begin{aligned} \Delta P_{cu} &= 3NI_{old}(v_{wind})^2 R \left[2 \frac{F}{N-F} + \left(\frac{F}{N-F} \right)^2 \right] = \\ &= 0.05P_r \left(\frac{v_{wind}}{v_r} \right)^4 \left[2 \frac{F}{N-F} + \left(\frac{F}{N-F} \right)^2 \right] \end{aligned} \quad (5.41)$$

5.5.1.6 Annual energy production at failure scenario

The baseline energy losses are considered as the losses of the powertrain at state for a non-parallel ($N=1$) case in one year,

$$EP_{loss,baseline} = \sum_{v=v_{ci}}^{v=v_{co}} P_{cu} \cdot p(v_{wind}) \cdot 8760 \quad (5.42)$$

Energy losses of the parallel module at failure state – if it were continuously in that state for a year – would be,

$$EP_{loss,N,F>0} = \sum_{v=v_{ci}}^{v=v_{co}} P_{cu,new}(F) \cdot p(v_{wind}) \cdot 8760 \quad (5.43)$$

Assuming that the results in equations 5.8 and 5.11 already include losses, the additional losses,

$$\Delta EP_{loss,N,F>0} = \sum_{v=v_{ci}}^{v=v_{co}} \Delta P_{cu}(F) \cdot p(v_{wind}) \cdot 8760 \quad (5.44)$$

Can then be subtracted from those results. A simplified version of efficiency – ignoring all other types of powertrain losses – can be stated,

$$\eta_{Cu} = \frac{P_{in} - \Delta P_{cu}(F, v_{wind})}{P_{in}} \quad (5.45)$$

5.6 Results based on losses

The results of the analysis based on the methods above are shown in Figures 5.10-5.17.

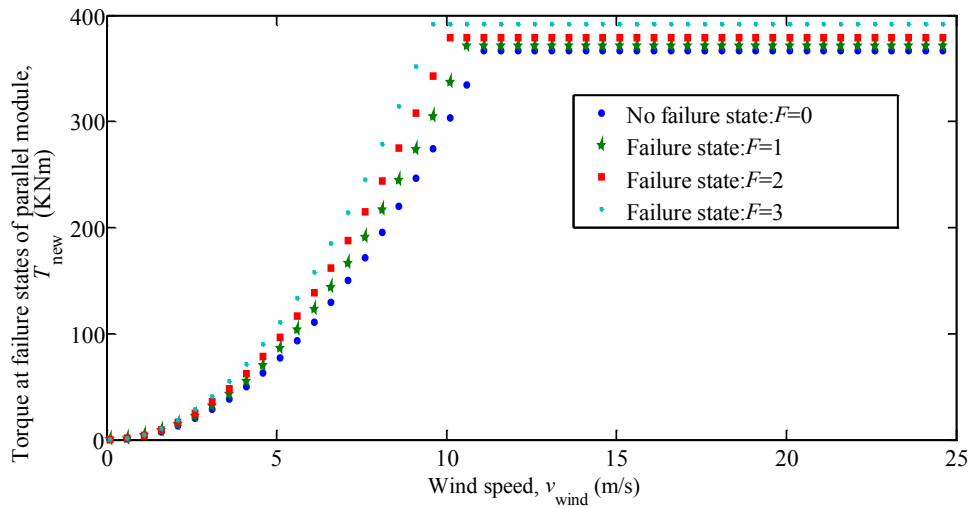


Figure 5.10: Torque of each healthy parallel powertrain modules against wind speed showing different new rated wind speeds and maximum torques. This case is for $N = 10$, $\alpha = 1/(N-1)$ and shows the first four failure states ($F=0-3$)

Figure 5.10 shows an example of how the torque per healthy module varies with both the number of failures F and the wind speed v . The healthy torque profile shows the torque rising quadratically with wind speed until the rated power and wind speed are met, after which the blades are pitched to regulate thrust, power and torque. As failures occur ($F \geq 0$), there is a new “rated” point of power, wind speed and torque per module. This rated wind speed drops as more failures occur and the rated torque per module increases, as the remaining modules have to work harder to address the torque deficit.

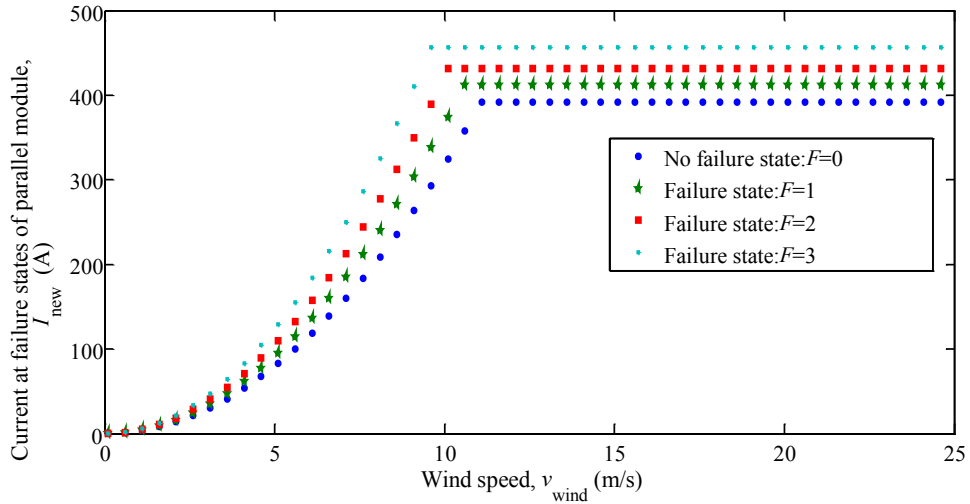


Figure 5.11: New current of wind turbine with parallel powertrain modules when $F=0-3$ at various failure states

Figure 5.11 shows the changes in the current as number of failures and wind speed increases. The new current resulting from the failure states of the parallel modules is observed to be increasing significantly as more failures occur in the parallel modules. When there are 3 failures the rated current increases by around 17%. Whether this is achievable in the electrical machine modules depends on the rating of the design.

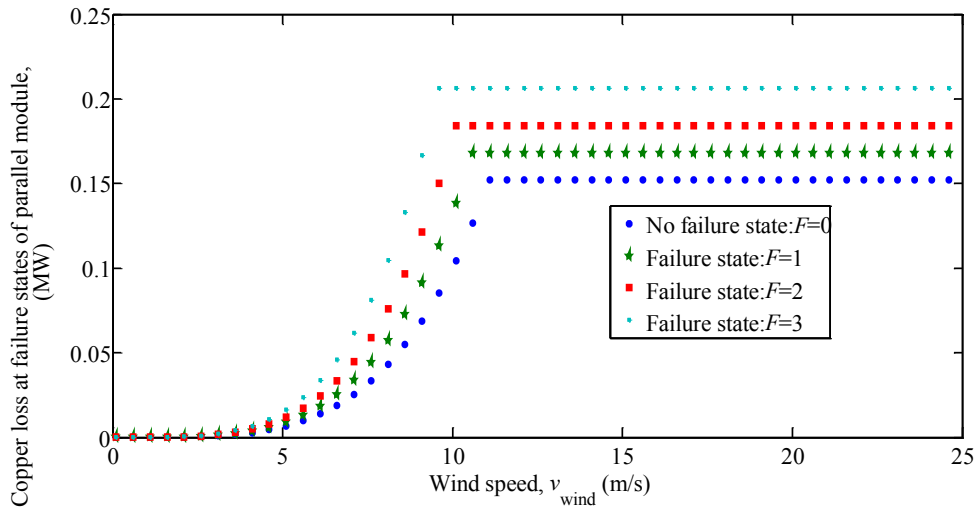


Figure 5.12: New copper of wind turbine with parallel powertrain modules when $F=0-3$ at various failure states

Copper losses increase significantly as F increases. This means that localised heat generation in the healthy modules will be a challenge in real machines. It suggests that a parallel powertrain should be able to reconfigure the cooling capability to the healthy modules to compensate for the increased local loss density.

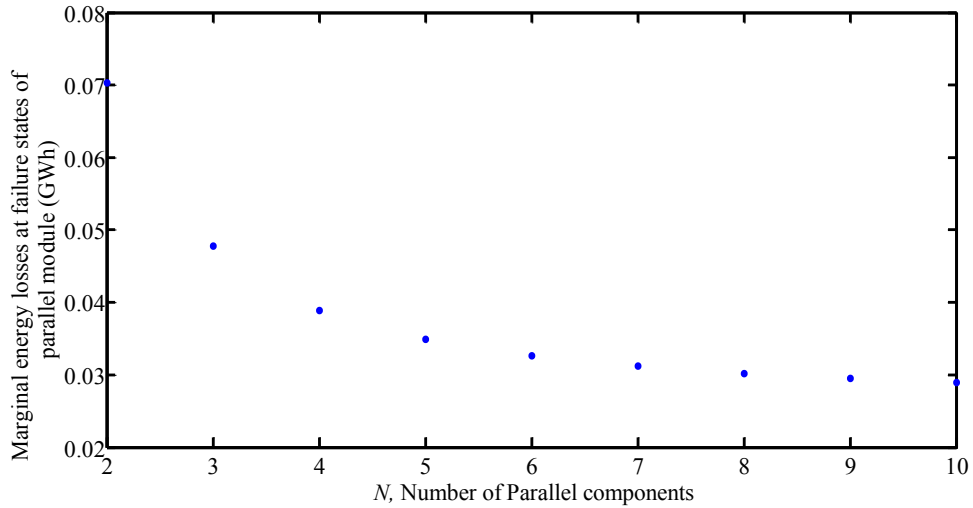


Figure 5.13: Marginal energy loss at failure states per parallel module

Figure 5.13 is the energy copper losses at the failure states of the parallel module. It shows the copper losses per N parallel module with the highest number occurring at $N=2$. These marginal changes in losses occur at each failure state in each parallel module. There is a gradually decreases in the losses as the number of parallel module N increases.

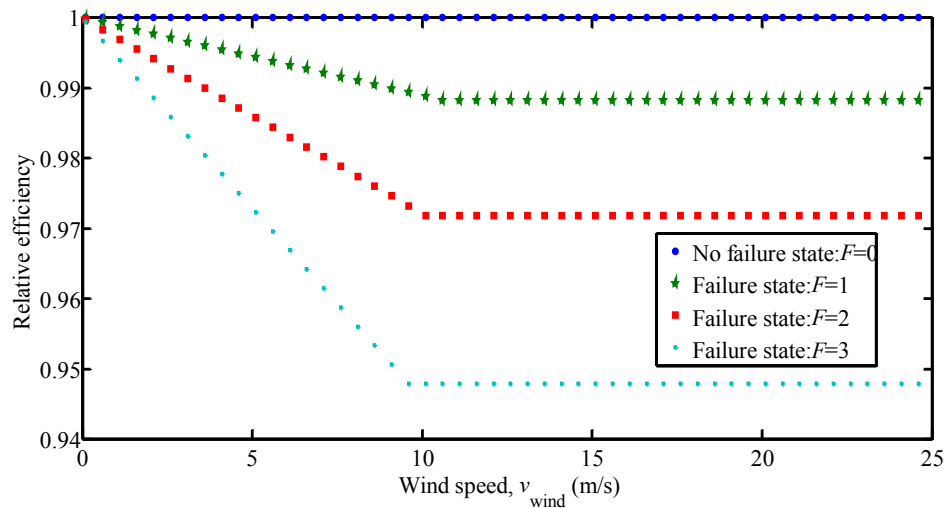


Figure 5.14: Relative efficiency at various failure states

The relative efficiency in terms of the rated power output and copper losses at the various failure states is shown in Figure 5.14. This is a little bit unusual compared to real powertrain efficiency curves as it ignores fixed losses and other variable losses

such as iron losses and switching losses. A decrease in efficiency continues as more parallel modules fail, such that lower efficiency is observed at higher F . The reduction in the efficiency comes from the higher copper losses as the number of failure states increases as shown in Figure 5.12.

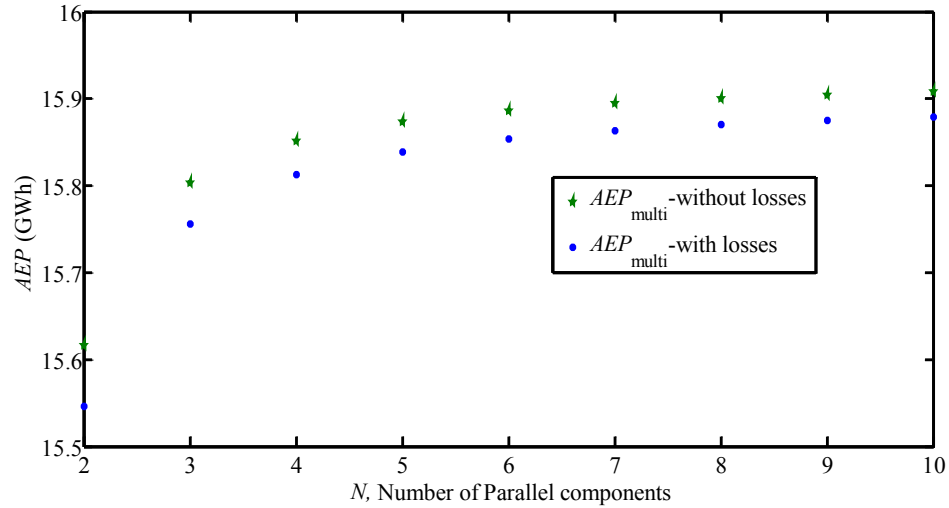


Figure 5.15: Results of AEP when losses at failure states are considered at rated wind speed of 11m/s and at $\alpha=1/N-1$. ($AEP=13.94$ GWh for no-parallelism i.e. $N=1$)

Figure 5.15 shows the AEP of the wind turbine with parallel powertrains comparing both cases of energy copper losses and without energy copper losses. The AEP with the neglected case is the AEP_{multi} , which was analysed in Section 5.2 i.e. when losses were assumed not to vary with failures. When the losses occurring at each failure state are taken into account, it is seen that the AEP drops. However, in both cases, AEP increase as the number of parallel modules increases.

5.7 Conclusions

In this chapter, parallel powertrains for wind turbines have been analysed and modelled to evaluate their effect on annual energy production.

In terms of *AEP*, this chapter proposed an approach that combines the wind speed distribution, multiple power curves (each corresponding to a failure state) and the probability of each failure state. This method is able to quantify the additional energy production in the cases where there are one or more failures. The earlier approach in Chapter 4 – based on an equivalent availability and capacity factor – underestimated *AEP* by up to 5%.

The *AEP* increased by 7% over a non-parallel powertrain when each parallel module is over-rated by a factor of $1/N-1$ and $N > 3$. Although the optimal parallel powertrain will vary depending on powertrain topology, failure and repair rates, turbine design and turbine location, a choice of $N \geq 4$ appears to be beneficial.

As the remaining healthy powertrain modules have increased torque, the current and therefore copper losses also increase with increasing failure states. This has been modelled.

In conclusion to the analysis carried in this section the research questions set out at the beginning of this chapter have been answered.

Firstly, it has been shown that parallel powertrain has the potential of generating extra energy in each failure states ($F=0$ and $F \geq 1$) of the N parallel module and consequently increasing the annual energy production by approximately 1.03GWh (difference between average *AEP* for $N > 1$ in Fig 5.5 and non-parallel $N=1$) which represents 7% increase compared to the non-parallel conventional powertrain.

Secondly, it has been shown that at failure states, functional parallel powertrain modules would generate power at higher torques, losses will occur and a drop in efficiency would be experienced.

Chapter 6 Operation and maintenance cost of offshore wind turbines with parallel powertrain

6.1 Introduction

The O&M costs of an offshore wind farm have been estimated to be roughly around 30% of the total levelised cost of energy of an offshore wind farm [64]. This cost is expected to rise as offshore wind turbines location gets further away into the sea shore due to travel time and accessibility issues leading to increase downtime. A number of strategies and innovations have been explored by wind turbine manufacturers, operators and researchers to see its impact on the O&M cost of wind turbines. It was reported in [118] that for offshore wind turbines, designs and innovation in the powertrain could have a positive impact on the operational cost. In [119][120] it was suggested that powertrain designs that have some level of redundancy will contribute to the reduction of the *AOM* cost.

While previous chapters showed that downtime might drop due to having parallel powertrains and that each fault may be quick to repair, the number of failures may increase. This chapter seeks to assess whether parallel powertrains lead to increased O&M cost (due to more failures) or decreased O&M costs (due to shorter repairs).

The work carried out in this chapter is novel for two reasons. First, O&M costs have never before been modelled for offshore wind turbines based on parallel powertrain subsystem. Another novelty in Chapter 6 comes from the analysis of the different maintenance and vessel for an offshore wind turbine with parallel powertrain subsystem. While [121] modelled O&M costs for a generic turbine no papers were encountered in which parallel powertrain was considered. In [122], the cost of energy for different drive train (non-parallel) types was modelled, but in doing so they assumed a fixed O&M cost per MWh.

This chapter concentrates on the analysis of the effect of *AOM* cost of having more subsystems in a parallel powertrain. This research employs an offshore wind farm accessibility model and investigates the *AOM* costs as the number of parallel

powertrain components varies. This incorporates two contrasting factors. The first factor is that failure rate, λ , of each powertrain component tends to increase with power rating; therefore, the component failure rate tends to reduce with larger numbers of parallel modules, N . At the same time, the total number of failures which can rise with increasing N per powertrain per year is $N\lambda$. Further complicating this is the influence of α and the sensitivity of repair rate to the power rating of each parallel powertrain module.

In this chapter, Section 6.2 describes the methodologies used to estimate the *AOM* cost for parallel powertrain subsystems. It is likely that operation of turbines with parallel powertrains may seek to use different repair vessels and repair strategies. This is investigated in more details. Section 6.3 presents the results for these analyses. Section 6.4 discusses these results and interprets them in the context of an offshore wind turbine of 3MW power rating. Finally, the chapter draws conclusions and highlights some of the limitations of the methodology.

This chapter will answer the research question “Do parallel powertrains add to the O&M cost due to the additional number of repair visits?”

Results will determine if the wind turbines with more parallel powertrain subsystems will lead to higher or lower O&M costs.

6.2 Methodology

This section will determine the O&M costs for the N parallel powertrain for an offshore wind turbine at hypothetical sites located at ~60km from shore. The choice of this distance was based on the fact that most offshore wind farms are located within this distance from the shore [52] and that turbines with parallel powertrain might be available for the generation of power at that distance from shore. In doing so a number of analyses on downtime, transport costs, repair times, repair costs and number of technicians required for repair will also be carried out.

6.2.1 The use of an offshore wind farm accessibility model to find O&M costs and their relationship to the number of parallel powertrain modules

The offshore wind farm accessibility model used for the O&M cost of the parallel powertrain for this analysis was developed at the University of Strathclyde by Dinwoodie. A detailed technical description of the model and its development can be seen in [121][123]. It is a time-based simulation of the lifespan operations of an offshore wind farm, with the failure characteristic implemented using a Monte Carlo Markov Chain approach. The maintenance and repair operations of the model are simulated based on available resources and site conditions. The model has the capability to determine accessibility and maintenance resource utilisation. The outputs of the model that are relevant for this thesis are the transport, staff and repair cost (cost of materials that is used or replaced in the turbine e.g. consumable materials such as carbon brushes, replacement parts such as full power converter units and full generators) required for the offshore wind turbines with parallel powertrains.

In this case, a hypothetical wind farm site with 50, 3MW turbines was simulated. Because this is a Monte Carlo method, a sufficiently large simulation sample is required. A total number of 50 simulations were performed for each N number of modules. The model considers input data such as site climate and sea state, turbine failure rate, in-turbine repair time, the vessel type required for repair, vessel operating parameters, vessel costs, fuel costs, mobilisation time, number of technicians required for repair, technician costs, as well as the material cost for repair. When a failure occurs, the model adds total transport costs, staff costs, and repair costs to determine the overall O&M costs. The input data (transport, staff and repair cost) for this model were obtained from [52][104][124], which provides operational and cost data for offshore populations of wind turbines in the MW scale. In the analyses, failure rates and associated parameters for non-powertrain components were held constant.

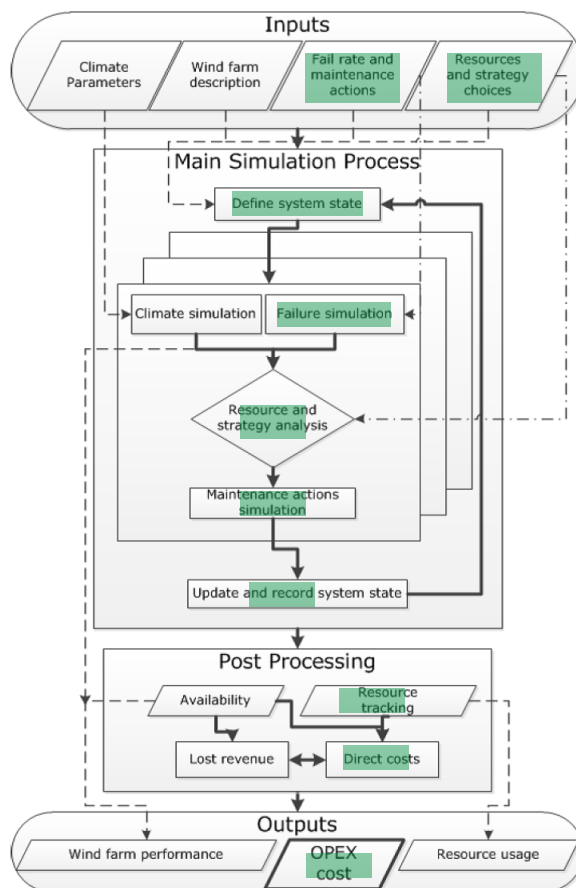


Figure 6.1: Model structural overview and interdependencies [123]

Since this thesis focuses on parallel powertrain, some of the model input (highlighted in green) parameters with green, shown at the top of Figure 6.1, had to be adjusted to represent N parallel powertrain system. For example, during the work for this thesis when a simulation was carried out for different N subsystems, adjustments were made to the “failure rate and maintenance actions” inputs and also to the “resource and strategy choices” inputs. In such a case, classification of the failure rate was done and type of vessel to be assigned to such failure type.

The failure and repair rates used for the parallel powertrain were based on the results from Chapter 4 which postulated how failure and repair rates of parallel powertrain wind turbine vary with the number of parallel powertrain subsystems, N . The baseline failure rate was 1.07 failures per turbine per year and an in-turbine repair rate of 69.4 repairs per turbine per year. In the previous chapter, a scaling of failure rates and repair rates was postulated, using values for m_λ and m_{MTTR} . These are used in this chapter too. This relationship implies that a single component fails less often and is quicker to

repair. As N increases, the power rating of each parallel powertrain component falls and generally, the module physical size is reduced. The consequence is that each failure is cheaper to repair and need less in terms of vessel and technician resources. One of the features of the *AOM* model is that it differentiates between different failure modes and uses the Reliawind failure classification where failures are defined as major replacement, major repair and minor repair [125][126]. Each of these categories was linked to a number of technicians and associated costs, a repair vessel type, its costs and weather operating parameters (from [127] and [128]) that are needed to make the repair happen. For the purpose of this analysis, HLVs were used for major replacements in the generators and gearboxes of the different powertrain configurations and CTVs were used for all minor and major repairs. The costing data for powertrain repair used in this paper were taken from [52][104][124] and they are a representation of turbine cost from an industrial partner that is a major wind turbine manufacturer.

6.2.2 Analysis of different operation and maintenance and vessel strategies for parallel wind turbine powertrain

The accessibility model was used to show the alternative repair and maintenance strategies to be implemented during failure states of parallel powertrain. The offshore wind farm accessibility model earlier described and used in Section 6.2.1 was used to estimate the *AOM* cost of some of the possible maintenance strategies of the parallel powertrain based on the offshore vessel strategies. The purpose of this analysis is to establish which vessel type will be cost effective since transport costs are the biggest contributor to the overall O&M costs. There are past works on the effect on O&M cost of using different HLV strategies for a generic wind turbine type [129][130]. In [52], O&M cost was carried out for non-parallel module, but here it is done for parallel subsystems.

In considering the maintenance and vessel strategies to use, four HLV strategies were modelled to estimate which one offers the lowest O&M cost when used for the repair

of parallel powertrain. As reported in [123], these are state-of-the-art operational strategies that are currently being considered by the offshore wind turbine industry. The inputs for the HLV strategies that were identified, adjusted and explored in this analysis include fix on failure until complete (FoFUC), purchase/lifetime charter (PLC), fixed monthly annual charter (FMAC), batch repair threshold and CTV or jack up vessel (JV) for major replacement, major repair or minor repair. The model was then run taking into consideration these new inputs. This provided simulated O&M cost outputs for different maintenance strategies for wind turbines with parallel powertrain subsystem. Other input parameters were kept consistent for all scenarios. The next subsection gives a brief description of the various maintenance and vessels strategies.

6.2.2.1 Fix on fail until complete strategy

This involves chartering vessel when a fault is predicted or observed. This is the baseline HLV strategy and very useful for small wind farms. The model allocates a vessel as soon as one is required for a major replacement. One of the challenges with this approach is the risk of prolonged mobilisation time and loss of power production. However, with the powertrain design proposed in this research, there is the possibility of having power generation albeit at a reduced level if the failure is associated with any of the parallel powertrain subsystems.

6.2.2.2 Purchase lifetime charter strategy

For this strategy, there is no delay once a failure occurs and repair is planned with available weather window because the operator owns the vessel instead of hiring it. Since there is no mobilisation time, it is possible that the vessel will be readily available for repairs.

6.2.2.3 Fixed Month annual charter strategy

Here, the vessel is chartered for a period of time during the year and any uncompleted repair or failure occurring outside this window is kept on hold until the next chartering period. For a conventional wind turbine with non-parallel subsystems, exposure to

significant downtime is expected. However, with redundant subsystems in place, impact of downtime coming from parallel subsystems is reduced.

The cost of hiring/chartering vessels depends on the different operating contracts. Previous analysis demonstrated that as the charter period increases in time, day rate costs are reduced [123]. Different strategies might be preferred with parallel powertrain as they may make cheaper contracts workable. For instance, having redundant subsystems in areas that are susceptible to failure might reduce the need for spot market contract since delays in immediate repairs present an alternative option. However, it is not certain if the cost savings from reduced spot market will outweigh the downtime.

6.2.2.4 Batch repair threshold strategy

In this case, chartering and allocation of vessels are kept on hold until a threshold number of failures have occurred. In the simulation, the model holds off on allocating the vessels until more failures have occurred that require a HLV. The threshold can be varied (1, 2 or 3) for this. This will mean that the contribution to the O&M cost will depend on the batch threshold input. In using the O&M model for the maintenance cost analysis in this chapter, it was decided that a maximum of three parallel powertrains has to be down in the turbine before a vessel is despatched for repair. The reason for this was to see whether the total number and hence the cost of trips could be reduced. A consequent downside is an increase in lost revenue due to greater downtime though lower mean repair rate.

The associated change in repair rate of the parallel module was considered to see how this affect availability using availability model developed in Chapter 4.

6.2.2.5 Use of CTV for major replacement

One design approach that has been adopted by wind turbine manufacturers is to install in-built cranes in the nacelles of turbines as a means to reduce the need for the hiring of HLVs which can have long waiting times with estimated day rates of the order of £100k [131][132][133]. With parallel powertrain, the use of HLV could be reduced even when a major replacement is required because of the small parallel nature of the

subsystem and the ease of using the inbuilt crane in the nacelle. In this analysis, O&M cost was simulated using smaller vessel types instead of HLV for the same operation and the cost was compared. It is noted that CTV was only used for major replacement of parallel powertrain while JV was still used for the rest of wind turbine components including gearbox.

6.2.3 Variation of O&M cost with N

As well as additional capital costs, the parallel powertrain could potentially add to the O&M costs. The unscheduled O&M costs can be thought of as being proportional to the number of repair visits, V , to the powertrain. This is given by

$$V = N\lambda_{\text{subsystem}} \quad (6.1)$$

For the case when the failure rate is assumed to be independent of the subsystem's power rating, then we can see from Fig 6.2 that the number of visits and therefore the cost of unscheduled O&M rise in line with the number of parallel subsystems. When the failure rate is given by equation 4.26 it can be seen that the failure rate of the subsystem and the number of visits will then be 1

$$V = m_{\lambda} P \alpha N \quad (6.2)$$

When $\alpha = 1/N$ then the number of visits and therefore unscheduled powertrain O&M costs are independent of the number of parallel subsystems.

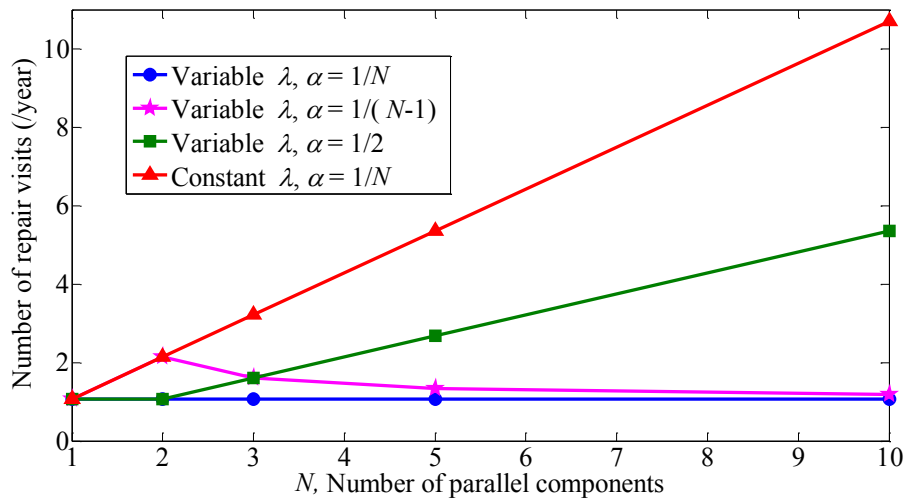


Figure 6.2: Expected number of visits for repairs with increasing number of parallel subsystems

6.3 Results

The results of the different maintenance and vessel strategies adopted for the repair of failed components in an offshore wind turbine having parallel powertrain is as shown below:

6.3.1 Results of Annual operation and maintenance costs and their relationship to the number of parallel powertrain modules

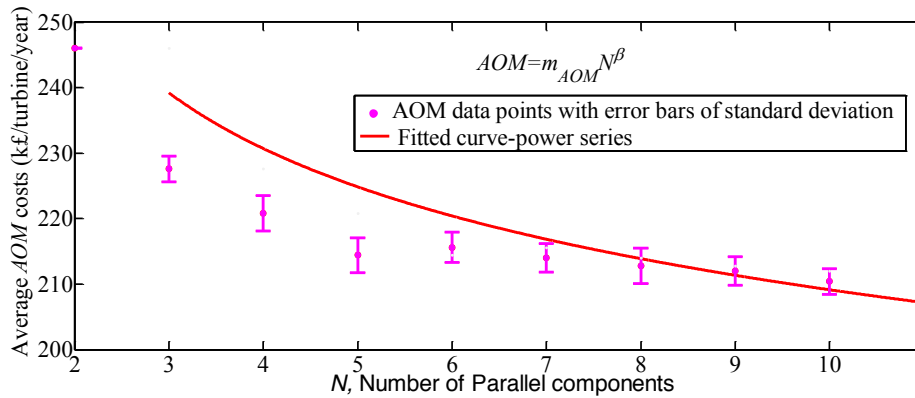


Figure 6.3: Comparison of operation and maintenance cost for wind turbine with different parallel subsystem. ($AOM=253.6\pm 0.8$ k£/turbine/year for no-parallelism i.e. $N=1$)

Figure 6.3 gives a plot of the AOM costs against N . As well as showing the average AOM cost, it also gives the standard deviation for the simulated results (as the error bars). For reference, the AOM for a non-parallel powertrain wind turbine was 253.6 ± 0.8 k£/turbine/year. This means that with $N=2$ there is a drop in AOM cost of around £8k/turbine/year as compared to $N=1$.

A curve has been fitted to the data to show the relationship between the number of parallel powertrain subsystems and the mean AOM , and is of the form,

$$AOM = m_{AOM} N^{\beta}, \quad (6.3)$$

where $m_{AOM}=\text{£}253.3\text{k/turbine/year}$ and $\beta=-0.087$ for $2 \leq N \leq 10$. In Figure 6.3, the total AOM is compared for the different parallel subsystem showing a drop in the total cost from $N=2$ to $N=10$. Although there are reductions in the AOM costs as the number of

parallel system increases, a similar cost for all powertrains with $N > 6$ suggests that there will be little or no drops in AOM as N increases.

The results in Figure 6.3 include all of the AOM cost. About 13% of the total AOM cost came from the powertrain while the rest of the system components accounted for the rest of the maintenance costs. A breakdown of the AOM cost shows the AOM costs per wind turbine per year for a site located at 60km from the shore is approximately £155k per turbine per year for transport cost, approximately £47k per turbine per year for staff cost. An average repair cost of £21k per turbine per year was observed. Although the transport and repair costs changed with N , the staff cost was almost the same, regardless of N . This is because the number of technicians was kept constant across all simulations, although the time and repair cost changed with N due to the differences in repair times of the parallel subsystems.

The total number of failures per powertrain per year is $N\lambda$ which would imply more repair visits and high AOM costs expected if λ was constant with N . However, it is assumed here that as N increases, the failure rate, λ , of each powertrain component reduces and the repair rate, μ , increases. Secondly, the sensitivity of repair rate to the power rating of each parallel powertrain module leads to an increase in repair rate implying quicker repair times. Then there is the influence of α , such that the rating of an individual component termed $P\alpha$ decreases with N .

6.3.2 Comparison of different operation and maintenance and vessel strategies for parallel wind turbine powertrain

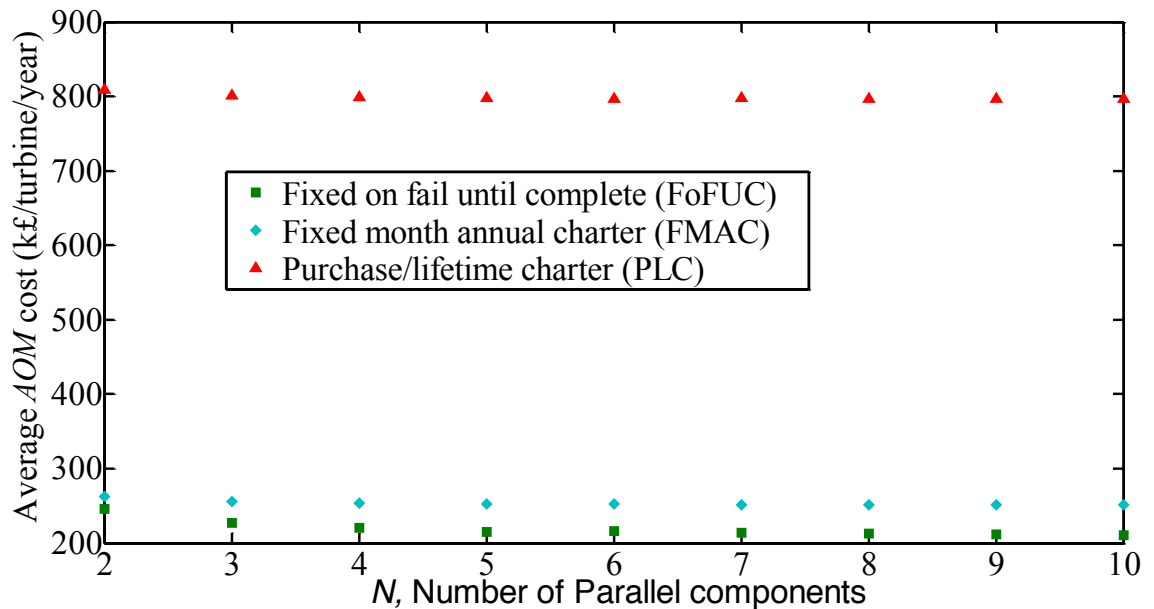


Figure 6.4: Comparison of operation and maintenance cost for wind turbine with different parallel subsystem using different maintenance and vessel strategy. JV used for all major replacement of wind turbine components.

Figure 6.4 shows the result of adopting different vessels strategies for the repair of a faulty parallel powertrain subsystem. The results reveal that there is a gradual decrease in the *AOM* cost as the number of parallel subsystems increases. Figure 6.4 shows there is a very high cost associated with the PLC charter strategy across the board for any *N* parallel subsystem. The purchase strategy gives a higher cost of maintenance. This is because the wind farm operator will have to purchase and own this vessel which will drive up the transport cost for each maintenance activity. The benefit of owning the vessel is that it will be permanently available with high increase in response to failure. The vessel strategy that offers the lowest *AOM* cost will be a preferred choice for the wind farm operator. The FoFUC strategy gave the lowest cost of maintenance with an average of £219k per turbine per year. This represents approximately 16%

reduction in *AOM* cost when compared to FMAC and over 250% reduction in *AOM* cost when compared to PLC. The drivers of the costs of FoFUC and FMAC strategy comes from the cost associated with repeatedly chartering vessels from the spot market.

6.3.3 Result of waiting strategy-different batch threshold

One of the elements of O&M costs is that which is associated with the allocation and hiring of a vessel. The frequency of despatching these vessels over a period of time could increase the maintenance cost. Waiting and allowing the number of failures to reach a certain threshold before sending the repair crew reduces the cost.

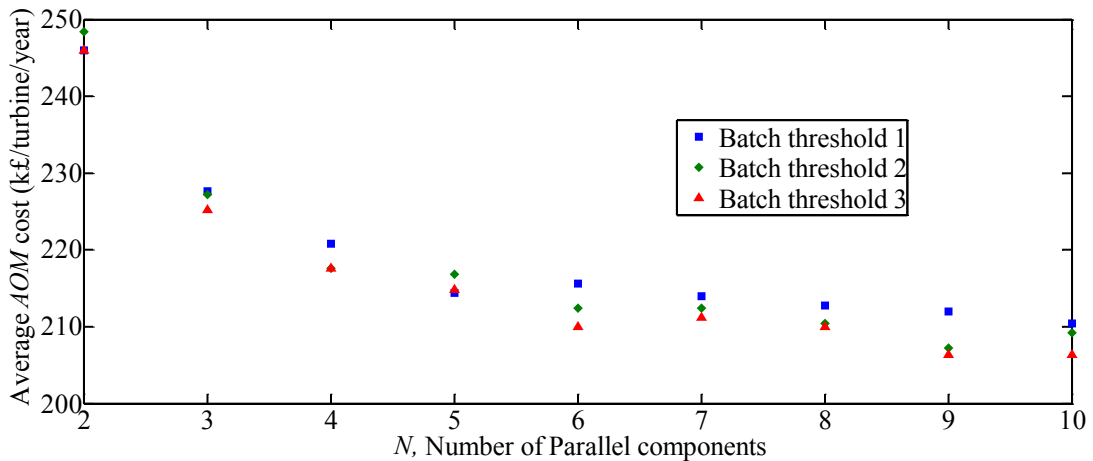


Figure 6.5: Comparison of operation and maintenance cost using different batch threshold for the waiting strategy and the same vessel strategy – FoFUC

Figure 6.5 shows the resultant *AOM* cost in the cases where response to repairs of subsystems are delayed until more failure happens before despatching the repair crew and vessel for maintenance. Again, there is a decrease in *AOM* cost as *N* increases for the three batch thresholds. As shown, waiting for more failures to occur before repairs has lower *AOM* cost. For instance, batch threshold 3, which implies waiting for up to three components to fail, contributed to the lowest cost compared to the cases with batch 1 and 2. Consequently, considering the order of magnitude of *AOM* cost as the threshold gets higher then, Batch 1 > Batch 2 > Batch 3. This means that an average of

over 0.5% and 1.3% reduction in the *AOM* cost will be gained for exploring waiting strategy approach of maintenance for batch 2 and 3.

It was observed that the availability of the wind turbine increases as the repair time of the parallel powertrain reduces due to small design- easy and quick to fix. Although the batch threshold strategy leads to reduction in *AOM* cost, in reality, there is the possibility of decrease in overall turbine availability expected from the batch threshold strategy due to the waiting option for the threshold to be reached before responding to repairs. Conversely, the improvement in availability as repair time changes suggests the benefit of small parallel powertrain.

The possibility of loss of revenue resulting from this approach will increase with increase in the batch threshold due to prolonged downtime. Using this strategy will, therefore, require a choice of balance between an acceptable batch threshold and the related lost production.

6.3.4 Using CTV for major replacement of parallel subsystem

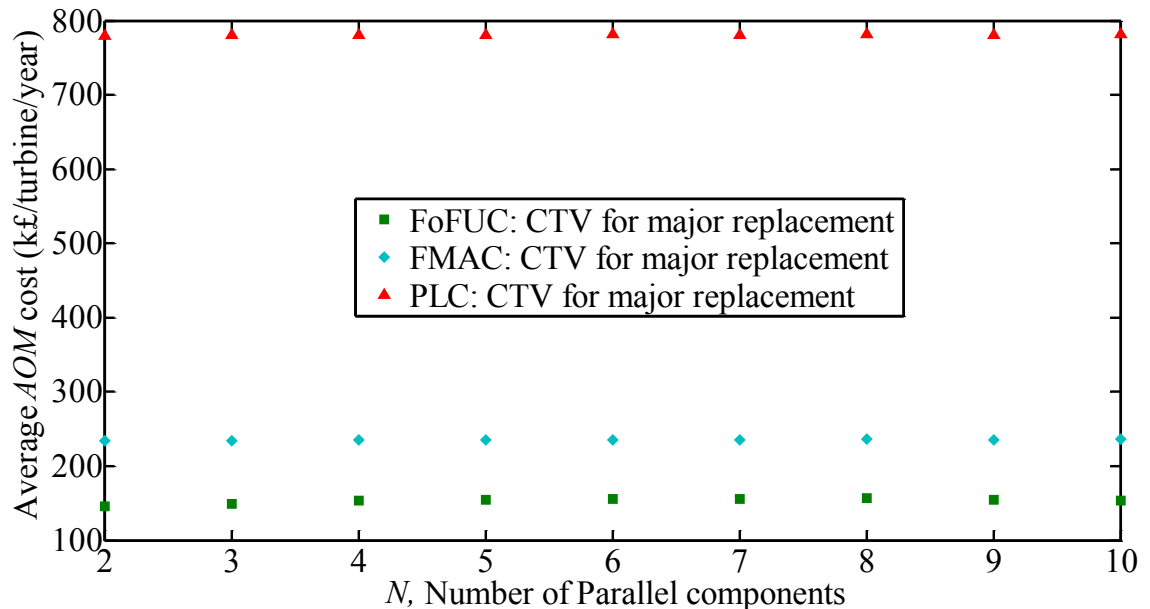


Figure 6.6: Comparison of operation and maintenance cost using CTV instead of JV for major replacement of parallel subsystems

Figure 6.6 shows a situation where the use of CTV is utilised for the repairs of powertrain subsystems failure involving major replacement. It is observed that there

is increase in *AOM* cost as the number of parallel subsystems increases i.e. $N > 1$ with the lowest cost at $N = 2$ for major replacement involving all three strategies.

Using CTV for major replacement of small parallel powertrain will mean significant cost savings considering the high cost of hiring heavy lift vessel such as jack vessel (JV) when the result in Fig 6.6 is compared to Fig 6.4. Obviously, there is a drop in the cost of maintenance when CTVs are used to fix failures that required complete major change out or replacement of parallel subsystems. Comparing the results of Figure 6.6 to Figure 6.4 indicate a substantial cost savings of over 30 and 7 percent for FoFUC and FMAC. Similarly, 2 percent reduction in maintenance cost is observed for PLC.

Although the overall *AOM* cost is lower for this maintenance option, in reality, operators may still want to dispatch JV for major replacement of parallel module to avert the risk of incomplete repairs due to a CTV not being capable for some major change out operations. Feasibility studies and test of the CTV approach may mitigate the risks of adopting this new approach.

6.3.5 Assumptions on data used in the O&M accessibility model

The capital cost, failure rate and repair rate data were assumed from a baseline powertrain and adapted due to lack of available data for a parallel powertrain. Naturally, empirical data from a parallel power train would have given a better result but this was not possible due to the lack of operating turbines that use parallel power trains.

The failure rate and repair rate were assumed to scale with the rating of the subsystem, $P_{\text{subsystem}}$. In reality, these may not scale linearly with the power ratings as N increases. However, the models themselves and the methodologies are effective for any available input data.

6.4 Summary and Conclusions

In this chapter, parallel powertrains for wind turbines have been analysed and modelled in terms of their effect on *AOM* costs in an offshore wind farm. A benchmarked offshore accessibility model was used to investigate the impact on O&M cost. It was assumed that the powertrain module failure and repair rates scale with module rating (i.e. small units fail less often and are quicker to repair). Results from the simulations showed that the *AOM* cost reduces as the number of parallel modules increases. The increase in total powertrain failure rate ($N\lambda$) is offset by a reduction in time to repair. When using a parallel powertrain, it is important that the technology used has lower failure rates, higher repair rates when N increases and the subsystem power rating is reduced.

There are high costs and potential delays associated with the use of specialist vessels such as JVs. Powertrain designs with parallel subsystems have the potential to reduce the dependence on these types of vessels.

The analysis in this chapter shows how dependent the *AOM* cost is on failure and repair rate. It further points to the potential of parallel powertrain to offer alternative repair strategy to operators especially when access is a challenge. The use of parallel powertrain design allows the delay of faulty subsystem since there is more than one parallel subsystem. This maintenance approach is in line with the existing and current methods of repairs in the offshore wind turbine industry where batch threshold repair strategy (delaying chartering and allocation of vessels until a threshold number of failures have occurred) is used.

Chapter 7 Cost of energy assessment of parallel powertrain

7.1 Introduction

In this research, the cost of energy method was adopted to assess the balance of benefit and cost of parallel powertrain design as compared to more conventional powertrain design.

Most of the conventional wind turbine powertrains tend to use single-input-single-output (SISO) topologies (i.e., one gearbox coupled to a generator with a power converter). Each of these different powertrains is associated with different cost as well as performance and reliability [52]. For parallel powertrain, there are different ways and configuration in which parallelism can be introduced as earlier described in previous chapters. In this chapter, powertrains with parallel subsystems are analysed in terms of the net benefit and *CoE* of parallel powertrains which depends both on the turbine and the type of powertrain technology. The cost of energy for different configuration of parallelism is also assessed.

Extra availability of parallel powertrain was modelled in Chapter 4. That additional availability is used to carry out the net benefit analysis in this chapter with other inputs (data of table 3.5) taken from Chapter 3. In Chapter 5, the extra energy produced at the failure states of the parallel powertrain were quantified and in Chapter 6, the maintenance cost for N parallel subsystem were estimated using the accessibility model described in Chapter 6. These results form part of the key elements required in the cost of energy analysis carried out in this chapter.

The following secondary research questions have been set out to be answered in this chapter.

- What strategy is best to introduce parallelism in terms of net benefit and *CoE* improvement?
 - Parallel generator and power converter combined
 - Parallel generator only
 - Parallel power converter only

- Does parallel powertrain have the potential for cost of energy reduction?
- What degree of parallelism, N is most effective in terms of net benefit and cost of energy reduction?

This is aimed at quantifying the benefit of powertrains with parallelism compared to those with SISO structure.

This was done based on three different ways of achieving parallel powertrain arrangement as stated in the research questions above. To answer the above research questions in this chapter, net benefit analysis is performed building on the extra availability derived from different configuration of parallel powertrain as shown in Chapter 4. The CoE is then estimated using the results of AEP , AOM as inputs to the model.

This chapter is structured and organised into sections. Section 7.2 gives detail of the method that is used for net benefit analysis. In Section 7.3 and 7.4, the results of the net benefit analysis are presented as well as the discussion and application. The method used for the CoE assessment and the results are shown in Section 7.5. The chapter ends with a conclusion and reference section.

7.2 Methodology: net benefit based on availability improvement

This section answers two of the research questions stated in the introduction section of the chapter: What strategy is best to introduce parallelism in terms of net benefit? What degree of parallelism, N is most effective in terms of net benefit?

To investigate the ‘net benefit’ expected from parallel powertrains based on their improved powertrain availability modelled derived from Chapter 4, a site was used with four different types of powertrain configurations. A simple (non-discounted) net benefit can be calculated,

$$\begin{aligned} \text{Net benefit} = & \Delta \text{revenue due to parallel powertrain} \\ & - \Delta \text{costs due to parallel powertrain} \end{aligned} \quad (7.1)$$

A 3MW turbine with a life of 25 years, a baseline capacity factor 0.35 (with a mean wind speed of 8.4m/s, and a ‘rest of turbine’ availability, $A_{ROT}=0.97$) was assumed. Some of the details for this turbine at an IEC Class IIA site [135] can be seen in the

‘Site 1’ entry in Table 7.1 below. The overall turbine availability, A_T is given by $A_{ROT}A_{eq}(N, \alpha)$ where $A_{eq}(N, \alpha)$ comes from the analysis in Chapter 4 and is based on a variable failure and repair rate. It is assumed that the turbine owner receives £120 per MWh of electrical power generated. The powertrain costs were taken from [104][124]. In reality, cost per unit power is not constant, nor is the mass and volume per unit power. Larger power units tend to be more effective in terms of per unit cost, mass, and volume, however, at larger power ratings, the variation with power or number of units is relatively modest. In this thesis, to simplify the analysis the baseline powertrain costs were scaled by $N\alpha$ where appropriate. For every N , α was varied until the maximum net benefit was found.

A sensitivity analysis was carried out for different powertrain types using the data in Table 7.2; this gives the turbine availability and coefficients for different powertrain types based on [57][104]. A further sensitivity analysis was performed on the same turbine using different failure and repair rate data from a number of sources [57][95][102] to see the impact of these inputs on the net benefit.

As well as the case that the generator and power converter is configured in parallel units, it is possible to introduce the parallelism into the generator only or the power converter only. The methods described above were adapted and used to analyse and compare the equivalent availability (A_{eq}) and net benefit of three cases: (a) generator and power converter both in parallel (b) parallel generator only and (c) parallel converter only. Table 7.3 show details of the data used in the analysis, essentially the generic powertrain failure and repair rate as used before but with the failure and repair rate separated. In the case when only the generator is in a parallel configuration, the rest of the turbine availability from (a) is reduced to include the downtime for the power converter with $N = 1$; the analysis is conducted with m_λ , m_{MTTR} and costs for the generator. Similarly, in the case when only the power converter is in a parallel configuration, the rest of the turbine availability from (a) is reduced to include the downtime for the generator with $N = 1$; the analysis is conducted with m_λ , m_{MTTR} and costs for the power converter.

A final sensitivity analysis was carried out by repeating the analysis for two other sites which have higher mean wind speeds (both IEC Class IA). Although the sites are different, the 3MW turbine power curve was considered to be the same for all 3 sites.

The increase in energy capture was modelled using a Rayleigh probability distribution. Higher mean wind speeds also lead to an increase in turbine and powertrain failure rates. The failure rate to mean wind speed relationship in [57] was used to change the failure rates and this can be seen in the availability in Table 7.1. The three sites are all 10km from shore and it was assumed that the altered wind speed distribution did not affect the turbine or powertrain repair rate.

Table 7.1: Wind turbine and site details for sensitivity analysis [135][95]

	Site 1	Site 2	Site 3
IEC Wind Class	IIA	IA	IA
Mean wind speed (m/s)	8.4	9.5	10
Rest of Turbine failure rate (failures/turbine/year)	8.21	9.91	10.7
Availability Rest of Turbine	0.97	0.964	0.961
Generator and power converter failure rate per MW (failures/MW/year)	0.36	0.43	0.47
$N=1$ generator and power converter failure rate (failures/turbine/year)	1.07	1.29	1.40
Availability $N=1$ generator and power converter	0.977	0.973	0.971

Table 7.2: Data for sensitivity analysis for different 3MW powertrain types [104]

Powertrain type	m_λ	m_{MTTR}
DFIG 3 stage gearbox	0.39	0.0052
PMG 3 stage gearbox	0.47	0.0035
PMG 2 stage gearbox	0.49	0.0035
PMG direct drive	0.51	0.0035

Table 7.3: Input data for net benefit of different parallel powertrain configurations: (a) Generator and a power converter in parallel (b) Parallel generator only (c) Parallel power converter only [57][95][100][102]

Configuration of parallel powertrain	Generator and Power Converter	Parallel Generator Only	Parallel Power Converter Only
m_{λ}	0.36	0.26	0.09
m_{MTR}	0.0048	0.0061	0.0012
Availability of powertrain unit when $N=1$	0.985	0.986	0.999
Availability of the Rest of Turbine (including non-parallel powertrain units)	0.933	0.932	0.911

7.2.1 Initial capital cost of a different configuration of parallelism

The *ICC* includes the capital cost of the powertrain, the rest of the turbine costs, the balance of plant costs and other capital costs. The balance of plant costs includes costs for port and staging, substructure, and foundation, electrical infrastructure, assembly and installation, commissioning, engineering and management costs. The turbine costs consist of a generator, power converter, gearbox and the rest of turbine (e.g. tower) cost. The other capital costs are made of construction insurance, decommissioning, finance costs and contingency. In this analysis, data for the overall *ICC* components were taken collected from [52][126] and was a representation of the initial capital cost per MW installed for single-input-single-output DFIG.

In this thesis, the cost per unit power has been assumed constant and so a single 3MW generator and power converter cost the same as 3 parallel 1MW generators and power converters. In reality, the cost per unit power tends to drop as powertrain units increase in power rating and as $N \rightarrow 1$ as fixed cost decrease in importance. If one were to plot

the cost of a powertrain unit, C , against its power rating, P , one can fit a function of the form [124][122]:

$$C = c + mP \quad (7.2)$$

where c is a fixed cost and m is the marginal cost. If c and m are known then the specific powertrain cost can be found

$$\frac{C}{P} = \frac{c}{P} + m \quad (7.3)$$

Equation (7.3) can be used to model the change in the cost of the powertrain units as the number of parallel units, N , and hence their power rating, P , varies.

Therefore, the ICC for the three different types of parallelism investigated in this thesis was assumed to be the same irrespective of the number of parallel units, N

The fixed charge rate, FCR allows the capital costs through the lifetime of the wind farm to be expressed as an annual cost. The fixed charge rate determines how much revenue is required to pay the return on debt, return on equity, taxes, depreciation, and borrowing insurance. In this analysis, a fixed charge of 0.117 or 11.7% was used in the CoE calculation [136].

Some of the wind turbine parameters/data used in the four major inputs to the CoE model are shown in Table 7.4

Table 7.4: Input cost data for cost of energy assessment [52][124]

Cost Inputs	
Fixed charge rate FCR	0.117
Initial capital cost due to Balance of plant ICC_{BOP} (£/MW)	254703
Initial capital cost due to other costs ICC_{others} (£/MW)	116475
Initial capital cost due to rest of turbine ICC_{ROT} (£/MW)	335000
Initial capital cost due to baseline powertrain $ICC_{powertrain}$ (£/MW)	19500

7.3 Results and sensitivity analyses of net benefit

The results of the methods for evaluating the net benefit as outlined in Section 7.2 are shown in Figures 7.1-7.4. This is first done with generic powertrain data to find the powertrain equivalent availability as described in Chapter 4 and then the improved availability is used to estimate the net benefit for this population of turbines and others in this chapter. Results for different generator and power converter types and parallel powertrain configurations are presented in Chapter 4. The sensitivity of the net benefit

to factors such as assumed failure rate data, assumed repair rate data and the nature of the wind turbine site is then shown.

The balance of additional availability and the additional capital cost was evaluated for a particular wind turbine using a net benefit measure. In order to express the two measures in the same units, it was necessary to compute the revenue that is derived by the additional availability.

The results vary depending on the assumed turbine, its capacity factor, the availability of the rest of turbine, the turbine life and the site wind conditions as well as the revenue produced for unit energy produced. For the assumed values, it can be seen that this net benefit generally increases as N increases. This is because at higher N , there is a greater possible range of α , and the same increase in availability can be produced by smaller additions to the aggregate power rating of the powertrain. The choice of α varies with N and the type of turbine. Generally, $\alpha_{\text{optimal}} > 1/N$. In some cases, the net benefit can be zero or even negative, meaning that the parallel powertrain is disadvantageous and the additional costs outweigh the benefits.

7.3.1 Results for different powertrain topologies

Each point on Figure 4.4 has both an equivalent availability and a powertrain cost. The net benefit of each point was calculated using equation (7.1); the result for the maximum value for each N is shown in Figure 7.1. There are five curves, one for each powertrain configuration in Table 7.2 and also a curve for a generic powertrain with the data described in Chapter 4 ($m_\lambda = 0.357$, $m_{MTR} = 0.0048$).

Figure 7.1 shows that using larger N generally gives a higher net benefit, with the effect levelling out at different N for different powertrain types. For the specific powertrain types, the powertrain with the highest net benefit is the DFIG – this has the lowest availability in the baseline case ($N = 1$) [104]. In order to positively benefit from parallelism, N has to be higher for the powertrains with already high baseline availability (e.g. the direct drive PMG). For these powertrain topologies (which tend to have higher capital cost), $N > 2$ before there is a significant benefit.

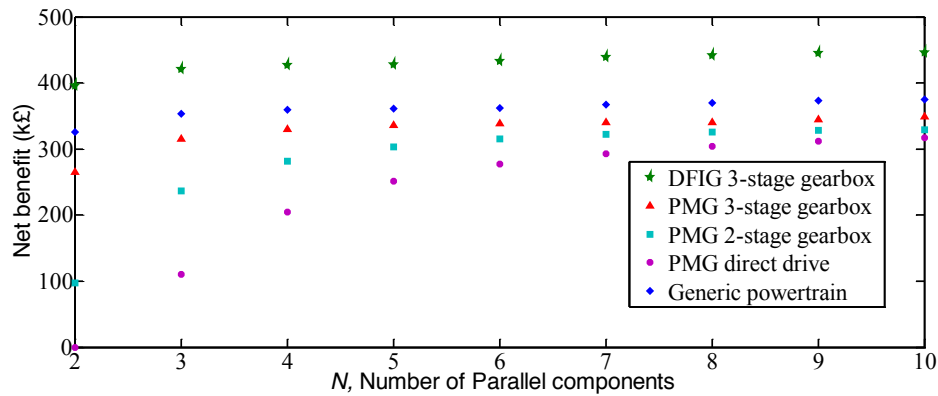


Figure 7.1: Maximum net benefit comparison of different powertrain types and number of parallel components for a 3MW wind turbine

From the input data used in the result of Figure 7.1, in terms of failure rate, the Direct drive powertrain has the highest failure rate followed by the PMG with three and two stage gearbox. The DFIG and the generic powertrain have the least failure rates which could be seen as one of the dominant factors in the best net benefit.

Looking at the repair rate point of view, the two, three and direct drive PMG have the highest repair rate whereas the DFIG and the generic powertrain have the least repair rate. However, this factor appears not to have much impact on the net benefit since the results shows the generic powertrain and DFIG both have the highest net benefit.

The capital costs of the powertrain train technologies used in this analysis show highest capital cost from and then the other PMGs with the induction generator and generic powertrain costing the least. This capital cost is seen here to have a vital effect/impact on the net benefit of the above powertrain technologies with the generic powertrain having the highest benefit.

In general, when considering the factors that play dominant impact on the net benefit of the powertrain, then failure rate, repair rate and the initial capital cost became more pronounced.

7.3.2 Results for different parallel powertrain configurations

The net benefit of three configurations are shown in Figures 7.2 for (a) generator and power converter both in parallel, (b) parallel generator only and (c) parallel converter only. The powertrain with generators and converters both in parallel offers the highest net benefit of over £375k. When the parallel powertrain includes only the generator, then there is still significant net benefit; when only the power converter is in parallel the net benefit is very modest.

This might be partly down to the failure rate, repair rate and cost data assumed for the generic powertrain where the generator has significantly higher baseline downtime than for the power converter; yet the generator is a little bit over twice the power converter cost.

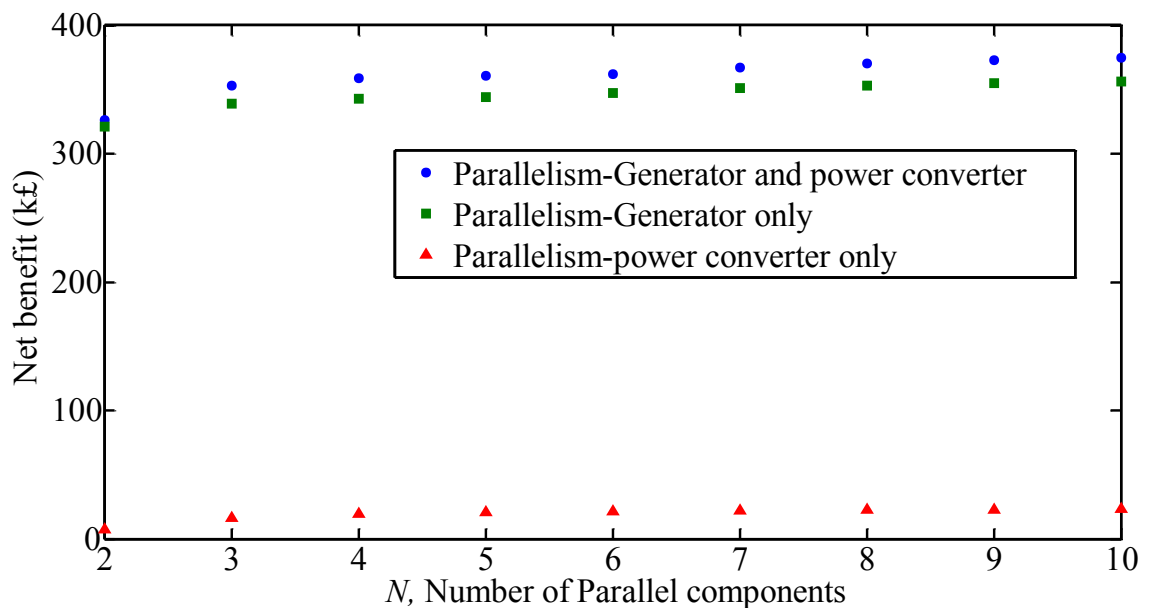


Figure 7.2: Net benefit comparison of parallel powertrain configurations: parallelism in generator and power converter, parallelism in generator only and parallelism in power converter only

7.3.3 Sensitivity to different failure and repair rates from different turbine types and sizes

By way of a sensitivity analysis, Figure 7.3 shows the maximum net benefit with different failure and repair rates from Table 3.5. The maximum net benefit of having a parallel powertrain is biggest for turbines with high powertrain failure rate, low repair rate and lower capital cost; generally, those that are larger turbines. For components with low failure rate and high repair rate, there is very low maximum net benefit and in some cases $N > 1$ can lead to a net cost. In some cases, the parallel powertrain is clearly beneficial yet in other cases the benefit is marginal or 0. The pairing of the failure rate and repair rate data point in Figure 7.3 were based on the same size/rating of the turbine. It represents a population of different types of wind turbine generators from [57][95][102]. For instance, $(\lambda = 0.669, \mu = 66)$ is for PMG while $(\lambda = 0.055, \mu = 219)$ is for SCIG.

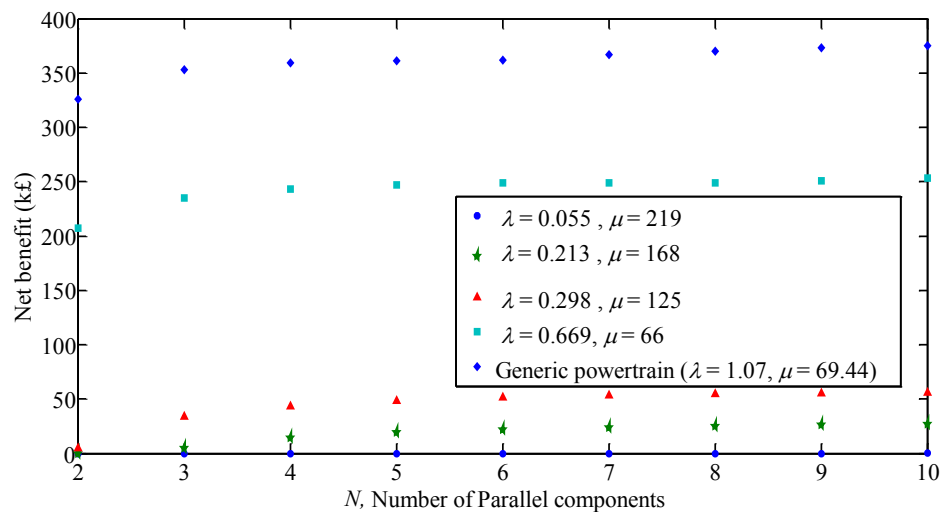


Figure 7.3: Comparison of maximum net benefit based on different powertrain failure and repair rates drawn from different wind turbine populations

7.3.4 Sensitivity to different sites and wind speed distribution

Figure 7.4 shows the sensitivity of the maximum net benefit using the generic powertrain failure and repair data ($m_\lambda = 0.357$, $m_{MTTR} = 0.0048$) to different sites and their wind resource data in Table 7.1. The results of the sensitivity analysis for different sites show that parallel powertrains are more beneficial as the wind resource improves and the opportunity cost associated with downtime increases.

Higher mean wind speeds lead to a higher maximum net benefit, as marginal uptime produces more revenue and because the rest of the turbine has a higher failure rate.

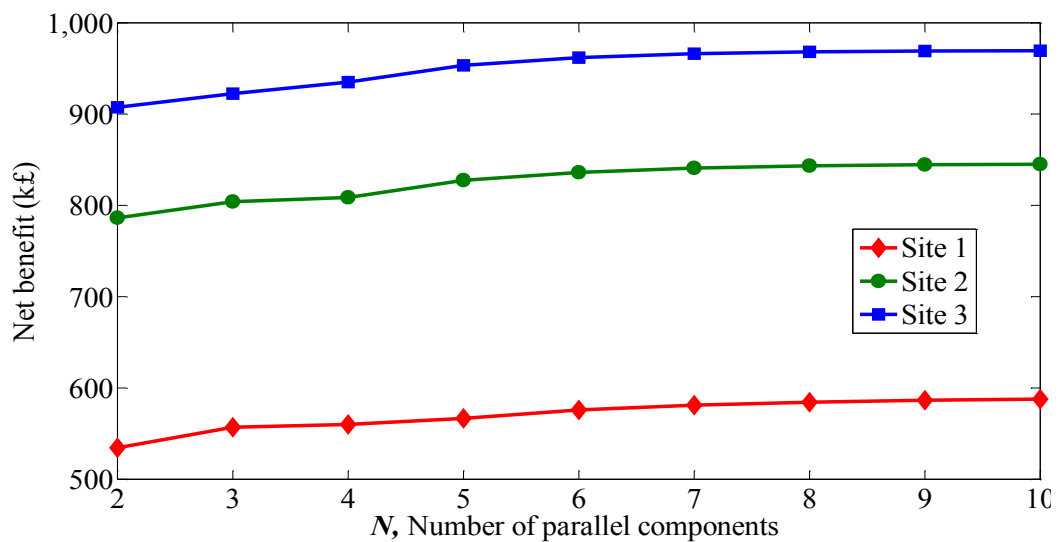


Figure 7.4: Sensitivity analysis of maximum net benefit to sites using generic powertrain failure and repair rates

7.4 Cost of Energy assessment of parallel powertrain

7.4.1 Cost of Energy definition

Cost of energy is the unit cost to produce energy from the wind turbine. According to [134], cost of energy is a metric used to evaluate and compare the cost of generating electricity from different sources and projects. Although there are different methods of calculating the *CoE* yet the four major inputs to the *CoE* evaluation are the same in all cases [1][136-138] and described in equation 7.2 below. It all amounts to the sum of all discounted lifetime costs divided by the amount of energy produced during the overall lifetime of the wind turbine/wind farm to give a cost per kWh or MWh.

This section answers two of the research questions stated in the introduction section of the chapter: What strategy is best to introduce parallelism in terms of cost of energy? What degree of parallelism, N is most effective in terms of cost of energy? The following subsection, outlines the approach adopted to answer these questions.

In carrying out the cost assessment, certain parameters such as wind farm costs, BoP costs, turbine costs and other capital costs must be considered. Assessment of the net benefit and cost energy of such parallel systems would inform the decision of wind turbine manufacturers, developers and operators to progress in the prototype design, implementation of such technology and in choosing the right turbine types for certain sites.

Generally, the cost of energy per MWh is defined as [136]:

$$CoE = \frac{(ICC \times FCR) + AOM}{AEP} \quad (7.4)$$

7.4.2 Cost of energy analysis for parallel powertrain

In addition to the *ICC*, the other elements of the *CoE* such as *AEP* and *AOM* have been derived from the analyses in Chapter 5 and 6 and the results obtained became an input to the cost of energy model used in this chapter to evaluate the *CoE*. This was done for the three different cases of parallelism as earlier mentioned.

7.4.3 Results for cost of energy for different methods

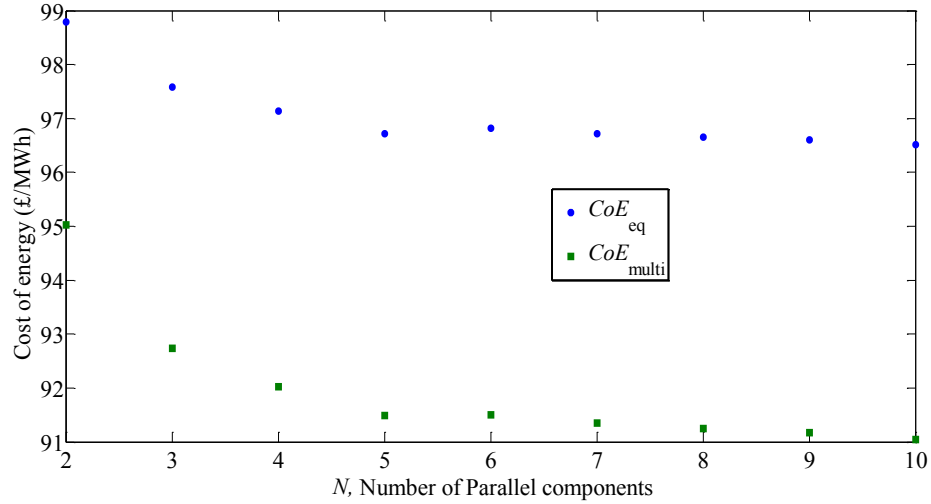


Figure 7.5: Comparison of cost of energy for wind turbine with different parallel subsystem. ($CoE=101.6$ £/MWh for no-parallelism i.e. $N=1$)

Figure 7.5 shows the cost of energy results from the two methods of deriving AEP in the energy production model used in this thesis with details in Chapter 5. Because of the additional energy production at below rated wind speeds – when $F > 0$ – the lowest cost of energy comes from AEP_{multi} .

Comparing the no-parallel ($N=1$) and parallel ($N>1$) indicates a reduction in the CoE as N varies for the parallel powertrain subsystem while the unparallel system shows $CoE=101.6$ £/MWh. From the cost of energy modelling results, it can be seen that the cost of energy is lower for a parallel powertrain than for an equivalent non-parallel powertrain (the best parallel powertrain has a 7% lower cost of energy).

The AEP and AOM were the dominant factors for this reduction in the energy cost while ICC is a smaller factor.

It is possible that different α at different N may affect the cost, as well as λ , μ which in turn will affect the AOM , AEP and then the CoE . However, it was performed at $\alpha = 1/N-1$ which gives a good balance of extra AEP and modest extra capital cost. This additional cost reduces as $N \rightarrow \infty$ and $N\alpha = N/(N-1) \rightarrow 1$. Once the $N=10$, the powertrain capital cost is 11% higher than when $N=1$. Although this additional cost seems

significant, it is relatively minor when one compares it to the total capital cost and the additional annual energy production.

The difference in the cost of energy for the two methods is about 5% for all N parallel system.

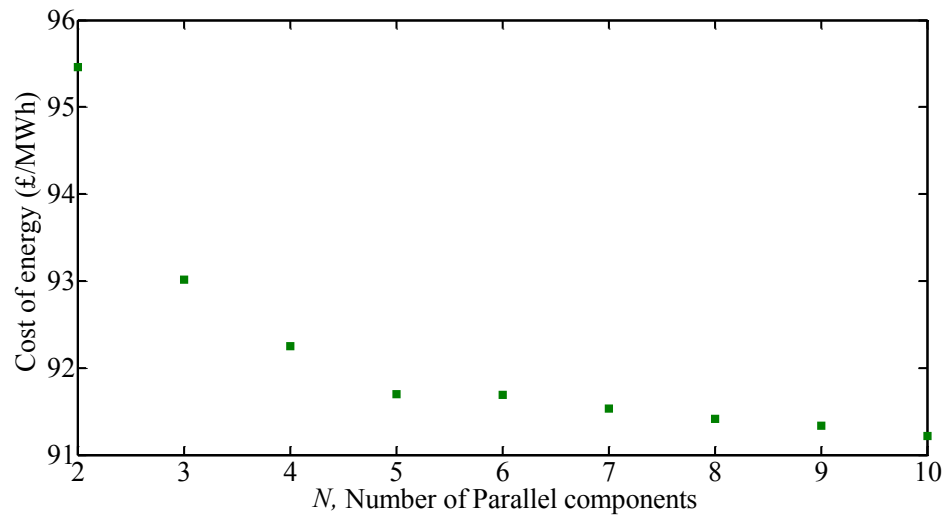


Figure 7.6: New cost of energy considering losses at failure states

Figure 7.6 shows the impact of the losses on the cost of energy for parallel powertrain at various failure states ($F \geq 0$). It is observed that the CoE increased by approximately 0.2% compared to the results in Figure 7.5 which is due to the energy losses reduction of the AEP .

7.4.4 Cost of Energy comparison for different parallel powertrain configuration

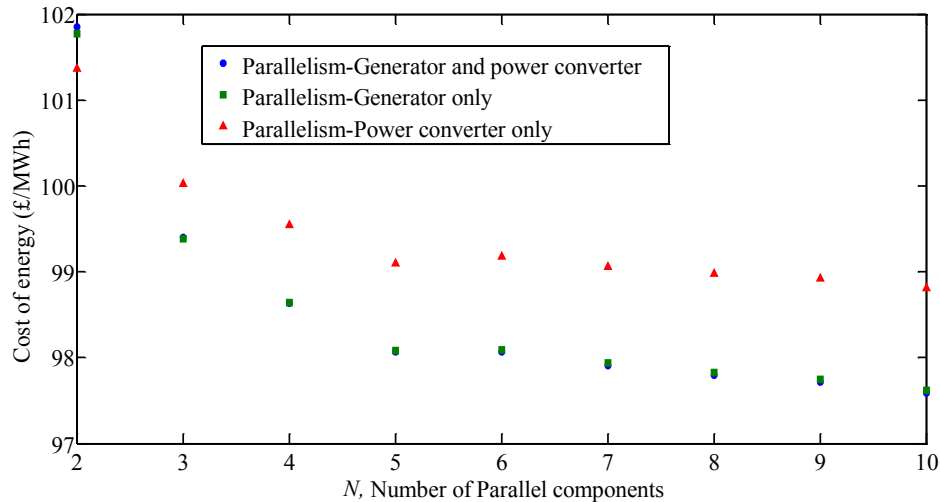


Figure 7.7: Comparison of cost of energy for different parallel subsystem

Figure 7.7, shows the *CoE* results for the three different configurations of parallelism. As shown, the *CoE* is observed to reduce as the number of parallel modules, N increases and the best reduction coming from $N=10$. Comparing the different parallel powertrain, the lowest cost of energy comes from the combined case of generator and converter while the power converter only offered the highest *CoE*. This comes from the results of the different parallel cases for *AEP* and *AOM* cost in chapter 5 and 6. Effectively, all three cases of parallelism showed cost of energy reduction potential compared to the non-parallel case.

7.5 Summary and conclusion

Firstly, it has been shown that parallel powertrain is beneficial when introduced to the wind turbine powertrain. In terms of net benefit, the best strategy is to introduce parallelism by combining a parallel generator and a parallel power converter. Although the optimal parallel powertrain design will vary with turbine type and its location, a choice of $N > 3$ appears to be beneficial. A good balance between additional availability and extra capital and O&M costs can generally be struck when $\alpha = 1/(N-1)$. When using a parallel powertrain it is important that the technology used has lower

failure rates and higher repair rates when N increases and the subsystem power rating is reduced.

Secondly, it has been shown that there is reduction in CoE if the parallel powertrain concept is introduced in the generator and power converter combined. Incorporating the changes in AEP and AOM cost due to changes in the number of parallel components shows that the cost of energy reduces by around 4% when N increases from 2 to 10. Although the optimal parallel powertrain will vary depending on powertrain topology, failure and repair rates, turbine design and turbine location, a choice of $N \geq 4$ appears to be a good consideration in terms of cost of energy.

Chapter 8 Conclusion and Future Work

8.1 Research questions and overview of conclusion

In view of the problem statement that high CoE is expected for the offshore wind power generation, elongated downtime due to access difficulties and low availability, this thesis seeks to answer the following research question:

“Can parallel powertrains reduce the cost of energy of offshore wind turbines?”

The answer to this main and primary research question is that:

“parallel powertrain can reduce cost of energy of offshore wind turbines” This comes from the introduction of parallel powertrain in the generator and power converter combined. Incorporating the changes in AEP and AOM cost due to changes in the number of parallel components shows that the cost of energy reduces by around 4% when N increases from 2 to 10.

The answer to this main and primary research question precipitated a few other secondary research questions, which were first answered throughout each chapter of this thesis. In this chapter, a summary of the major concluding points from each of the previous chapters in this thesis is highlighted. Comprehensive conclusions, discussions or answers to the secondary research questions are well articulated and can be found at the end of each chapter of this thesis. It is pertinent to say that the conclusions presented in this chapter are based on justifiable assumptions with some degree of uncertainty around them. Details of these assumptions and uncertainty levels can be found in the chapters themselves. In drawing a curtain on this thesis, the practical application of the findings in this thesis to the offshore wind industry will be expressed. Finally, it terminates with a brief outline of future work.

8.2 Summary of conclusions

8.2.1 Key points from Chapter 3

Chapter 3 answers the research question “*How do failure and repair rates of powertrain equipment vary with size and power?*” In Chapter 3, the failure and repair rates of wind turbine powertrain are analysed. It is revealed that data from other industry shows that failure rate and repair rates of electrical machines vary with their size. This is because of increased torque rating and number of component parts which could influence the failure rate. Similar assessments are seen from the wind turbine industry showing powertrain components’ failure and repair rates varying with their size. There is also evidence that failure rates in power converters vary with power rating, especially when the number of identical converter modules is increased.

The discoveries also show that a population of larger turbines from offshore site has the highest failure rate. When comparing the powertrain components, it shows that there is a modest correlation between generator failure rate and power rating. However, for power converter, the failure rate versus power rating has a very strong correlation. Although the size of turbines is a key determinant of failure rate, other factors such as different technologies, operating experience and wind speed. could lead to changing failure rates.

8.2.2 Key points from Chapter 4

Chapter 4 of this thesis gave answers to two research questions:

“Is any improvement in availability possible using parallel powertrain?”

“What degree of parallelism is most beneficial in terms of availability?”

In Chapter 4, parallel powertrains subsystems were analysed using Markov state space models in order to quantify any improvements in availability. A baseline powertrain’s availability and that of different parallel powertrains were evaluated using wind turbine powertrain failure and repair rate data.

The results show that an increase in the number of parallel systems, N , does not automatically lead to a higher availability for a wind turbine powertrain. It was seen

that improvement in availability was possible when failure and repair rates scale with module power ratings. It was also observed that at the design stage, the designer can further improve availability by over-rating each parallel module which led to the introduction of α , such that $P_{\text{subsystem}} = \alpha P$ where $(1/N) \leq \alpha \leq 1$.

When the powertrain failure and repairs are assumed to be constant and they are rated at P/N then there are no changes in availability with changes to N . If these rates vary with power rating then as N increases, the availability will increase too. The highest availability is achieved when $\alpha = 1$ but this is expensive. A good balance between additional availability and extra cost can generally be struck when $\alpha = 1/(N-1)$.

In terms of the number of parallel subsystems N , it was shown that the optimal parallel powertrain design will vary with turbine type and its location, a choice of $N > 3$ appears to be beneficial. The wind turbine with parallel generator and power converter combined is seen to have the highest availability.

8.2.3 Key points from Chapter 5

Four important research questions were answered in Chapter 5, which states:

“Can parallel powertrains generate ‘extra’ energy at failure states and consequently increase annual energy production? If so, by how much?”

“What happens to the torque, T of the system at failure states of parallel powertrain? Does efficiency suffer with parallel powertrain?”

In Chapter 5, parallel powertrains for wind turbines were analysed and modelled in terms of their effect on annual energy production. Two methods (equivalent availability method, AEP_{eq} and the multi-state energy method, AEP_{multi}) for estimating the AEP of a parallel powertrain were adopted. The methods adopted used the same MSSM model to calculate the probability of having F failures. The first method was based on the equivalent availability method of Chapter 4 while the second approach combined the Rayleigh wind speed distribution, multiple power curves (each corresponding to a failure state) and the probability of each failure state.

The result shows that the AEP_{multi} method is able to quantify the additional energy production in the cases where there are one or more failures, the remaining working powertrain capacity is greater than the instantaneous turbine power, i.e. at below-rated

wind speed. The earlier approach in Chapter 4 – based on an equivalent availability and capacity factor – underestimated *AEP* by up to 5%. It is shown that *AEP* increases with the number of parallel modules, N , when each module is overrated by a factor of $1/N-1$. The *AEP* increases by 7% over a non-parallel powertrain when each parallel module is over-rated by a factor of $1/N-1$ and $N > 3$. The wind turbine with parallel generator and power converter combined is seen to have the highest energy production at failure states.

It has also been shown that at failure states, functional parallel powertrain modules would generate power at higher torques, losses will occur and a drop in efficiency would be experienced.

8.2.4 Key points from Chapter 6

One important research question was answered in Chapter 6, which states:

“Do parallel powertrain affect the O&M cost due to the number of repair visits?”

Chapter 6 estimates the O&M costs of parallel powertrain based on wind farm accessibility model to find *AOM* costs and their relationship to the number of parallel powertrain modules. The offshore wind farm accessibility model used for the *AOM* cost of the parallel powertrain for this analysis was developed at the University of Strathclyde.

It was seen that the introduction of parallel powertrains increases the *AOM* costs (i.e. comparing $N = 1$ to $N = 2$). The average number of failures per powertrain per year is $N\alpha\lambda$ which would imply more repair visits and higher *AOM* costs expected if λ and α were constant with N . In this thesis, it was assumed that $\alpha = 1/(N-1)$ and also that λ and μ vary with N . Taken together, these mean that as $N \rightarrow \infty$, $N\alpha \rightarrow 1$, and that the total number of failures drops with a greater degree of parallelism. This accounts for the subsequent fall in *AOM* cost as N increases.

In terms of HLV strategies, the result shows that the batch repair strategy offered the lowest O&M cost for an offshore wind turbine with a parallel powertrain. Since power can still be produced when certain components fail, the consequence of waiting until other components fail is not as high as in traditional powertrains with no redundancy.

8.2.5 Key points from Chapter 7

Three important research questions were answered in Chapter 7, which states:

“What strategy is best to introduce parallelism in terms of net benefit and CoE improvement?”

“Does parallel powertrain have the potential for cost of energy reduction?”

“What degree of parallelism is most beneficial in terms of net benefit and cost?”

In Chapter 7, the net benefit and *CoE* of parallel powertrain is considered. Chapter 7 estimates the *CoE* of parallel powertrain using results from Chapters 5 and 6, as input data to the *CoE* model. Details of other cost components used in analysing the *CoE* were outlined in Chapter 7.

Firstly, it has been shown that parallel powertrain is beneficial when introduced to the wind turbine powertrain. In terms of net benefit, the best strategy is to introduce parallelism by combining a parallel generator and a parallel power converter. Although the optimal parallel powertrain design will vary with turbine type and its location, a choice of $N > 3$ appears to be beneficial.

Secondly, it has been shown that there is reduction in *CoE* if the parallel powertrain concept is introduced in the generator and power converter combined. Incorporating the changes in *AEP*, *AOM* cost and capital costs due to changes in the number of parallel components shows that the cost of energy reduces by around 4% when N increases from 2 to 10. Although the optimal parallel powertrain will vary depending on powertrain topology, failure and repair rates, turbine design and turbine location, a choice of $N \geq 4$ appears to be a good consideration in terms of cost of energy. Therefore, according to the cost, wind turbine and reliability assumptions in this thesis, increasing the number of parallel powertrain subsystems from $N = 1$ to $N = 4$ can yield significant improvements in cost of energy.

From the cost of energy modelling results, it can be seen that the cost of energy is lower for a parallel powertrain than for an equivalent non-parallel powertrain (the best parallel powertrain has a 7% lower cost of energy). The improvement in cost of energy comes from the additional annual energy production, which overrides any additional *ICC* and *AOM*.

8.3 Assumptions, limitations, and uncertainties

One important factor to be considered about the results and conclusions made in this work is the quality of the input data used in the models and the quality of the models themselves. For instance, there is limitation in the use of disparate onshore and offshore generator and power converter failure rate and repair rate data from a number of published sources. The results and conclusions may be influenced as better data becomes available and is used instead. The capital cost, failure rate, and repair rate data were assumed from a baseline generic powertrain. Other turbine and powertrain systems will have different characteristics. The parallel module costs, failure rate, and repair rate were assumed to scale with the rating of the subsystem, $P_{\text{subsystem}}$. In reality, these may not scale linearly with the power ratings as N increases. However, the models themselves and the methodologies are effective for any available input data and independent of the data quality.

It is a common place with modelling, to have some level of uncertainty surrounding the results but consideration to the further work presented in the following sections could help reduce that uncertainty.

In this research, the cost per unit power was assumed constant and so a single 3MW generator and power converter cost the same as 3 parallel 1MW generators and power converters. In reality, the cost per unit power tends to drop as powertrain units increase in power rating and as $N \rightarrow 1$ as fixed costs decrease in importance. This could give rise to further uncertainties around the results.

8.4 Sensitivity Analyses

The sensitivity analyses carried out on some of the chapters of this thesis such as the failure rate and repair time etc. for the net benefit gives some level of clarity to what is expected in the event of variation in the input parameters and data used in the various models of this work.

8.5 Contribution to knowledge

In view of the high cost of energy for the offshore wind, many *CoE* targets have been set by wind turbine manufacturers and government agencies for 2020. The outcome of this research has shown that one of the steps toward achieving such goal is the design of parallel powertrain technology and this is in line with the report by BVG shown in Table 1.1 and reference [1]. The result in this thesis therefore, shows that the new innovative powertrain technology could lead to *CoE* reduction of around 4% for an offshore wind turbine. However, this will depend on the readiness of manufacturers and other stakeholders to deploy this new technology after feasibility studies and further risk analysis.

The author believes that the outcome of this research is a major step towards the impact of new powertrain technology such as parallel powertrain on the cost of energy reduction and making offshore wind energy truly cost competitive with traditional fossil fuel sources.

8.5.1 Chapter 3 contribution

It is expected that the survey of reliability data work in Chapter 3 for failure and repair rate data of powertrain equipment and their variation with size and ratings will help inform the wind turbine manufacturers about the complexity of large equipment. This is evident in the fact that more failure rates are expected when the number of components is increased for large power rating. Obviously, this could create room for redesigning of some components in terms of size and ratings to reduce the complexity associated with the resultant failures.

8.5.2 Chapter 4 contribution

Chapter 4 establishes the fact that the addition of extra parallel powertrains (i.e. $N > 1$, where each subsystem is rated at P/N) would not necessarily lead to an increase in equivalent availability. For any improvement in availability to be plausible, then there must be: (a) reduction in subsystem failure rates, (b) increase in subsystem repair rates

and (c) increase in the power rating of each subsystem above P/N implying an additional capital cost

This is very important at the design stage when seeking to factor in availability so that effort and resources are not expended only in increasing the number of parallel modules without paying attention to the impact of variation on failure rate and repair rate.

8.5.3 Chapter 5 contribution

Chapter 5 highlights the fact that it is possible to have additional energy production at below rated wind speeds when the parallel powertrain is in a failure state and that this increases with the number of parallel modules, N . This is extremely important to offshore wind turbine operators who are faced with loss of energy production arising from delayed response to repair of failed components due to sea and weather condition.

8.5.4 Chapter 6 contribution

Chapter 6 highlights the influence of failure and repair rate for the *AOM* costs of parallel powertrain showing that variation of λ and μ with N leads to decrease in *AOM* cost as N increases. It also presents possible maintenance strategies that could lead to maintenance cost reduction. The results from these strategies are pointers to the operators of offshore wind farm in making decision for cost effective maintenance and operations of the wind farm.

8.5.5 Chapter 7 contribution

Chapter 7 highlights the cost of energy decrease that can be seen for a parallel powertrain than for an equivalent non-parallel powertrain (the best parallel powertrain has a 7% lower cost of energy).

This is quite beneficial to wind turbine manufacturers that are interested in the cost of energy potential of new powertrain technology for any justifiable decision before investment.

8.6 Future work

A number of areas have been mentioned throughout this thesis in which improvements could be made with further work. The following subsections will outline what further work could be carried out to improve and build on this thesis.

8.6.1 Reducing Uncertainty

As with all modelling, the quality of the inputs determines the quality of the outputs. Throughout this thesis, models were populated with available data from different sources. However, no field cost or operational data was obtained for the parallel powertrain wind turbine configurations. If data of this type was obtained it would remove an element of uncertainty from this work and in turn improve the quality of this thesis. Failure rates were also estimated for some class of MW power ratings of the generators and converters used as input data to the models. To remove uncertainty in this area, a field reliability analysis could be carried out to determine failure rates for smaller generators and converters of different power ratings.

8.6.2 Use of more sophisticated approach to predict failure rate of small parallel modules

The method used in this thesis to predict reliability of parallel module was based on failure rate data from different sources and for different powertrain configuration. A more "bottom-up" engineering and reliability block diagram approach could be used on preliminary designs of parallel powertrains. With sufficient reliability data at a component level, and an understanding of which components are common and which will need to increase in number with number of parallel powertrains it would be possible to build up a detailed reliability picture of different parallel powertrains.

8.6.3 Use of more sophisticated operation and maintenance tool for parallel powertrain

The quality of the O&M estimations in Chapter 6 could also be improved if field cost data for the different power ratings of parallel modules, N used as input to the costing sheet of the O&M model could be obtained.

In addition, the quality of the O&M cost results from Chapter 6 could be better, if a wind farm accessibility tool specifically built for parallel powertrain wind turbine could be assessed and developed to estimate O&M costs.

8.6.4 Switching operation at failure states of parallel module

The switching process from one failure state to the other of the parallel powertrain modules was not considered and is an area of interest for future work. It could possibly improve the powertrain efficiency as it could address part of variable losses in switching.

8.6.5 Extension of parallel powertrain systems to gearbox design

The research in this thesis only focussed on the introduction of parallelism in generator and power converter without modelling the gearbox. Future research could involve designing the gearbox for the purpose of providing redundancy and investigating the benefit of parallelism in the gearbox.

8.7 References

- [1] The Crown Estate. Offshore Wind Cost Reduction Pathways Study. Technical report, May 2012.
- [2] B. Valpy, G. Hundleby, K. Freeman, A. Roberts, and A. Logan, “Future renewable energy costs: offshore wind”, Technical report-BVG associates, updated 2017.
- [3] A. McDonald, J. Carroll, “Design of generators for offshore wind turbines. Book: Offshore Wind Farms: Technologies, Design and Operation”, Woodhead Publishing 2016.
- [4] American Superconductor (AMSC), USA, [Online] Available: https://www.amsc.com/wp-content/uploads/wt10000_DS_A4_0212.pdf. last accessed 13/05/2019
- [5] W. Yang, P.J. Tavner, C.J. Crabtree, Y. Feng, Y. Qui, “Wind turbine condition monitoring: Technical and commercial challenges”, Wind Energy 2014, vol. 17, no. 5, pp. 673–693, May 2014.
- [6] History of wind turbines, [Online] Available: <https://www.renewableenergyworld.com/ugc/articles/2014/11/history-of-wind-turbines>. last accessed 13/05/2019.
- [7] B. Godfrey, "Renewable Energy: Power for a Sustainable Future", vol. Third edition, Oxford, United Kingdom, Oxford University Press, pp. 297–362, 2012.
- [8] Renewables account for 70% of 2017 power addition, [Online] Available: <https://www.windpowermonthly.com/article/1466423/renewables-account-70-2017-power-additions> last accessed 13/05/2019.
- [9] Wind in our sails, [Online] Available http://www.ewea.org/fileadmin/files/library/publications/reports/Offshore_Report.pdf last accessed 13/05/2019.
- [10] Wind Europe history, [Online] Available <https://www.windeurope.org/about-wind/history/> last accessed 13/05/06/2019.
- [11] UK National Grid Logs New Wind Energy Record, [Online] Available <https://www.offshorewind.biz/2018/03/19/uk-national-grid-logs-new-wind-energy-record/> last accessed 13/05/2019.
- [12] UK Energy Statistics, Q1 2018, [Online] Available https://assets.publishing.service.gov.uk/government/uploads/system/uploads/attachment_data/file/720182/Press_Notice_June_18.pdf last accessed 13/05/2019.
- [13] J. Coultate, “Wind Turbine Drivetrain Technology and Cost Drivers”, Report from Romax Technology, 2011.
- [14] I.P. Girsang, J.S. Dhupia, L.Y. Pao, E. Muljadi, and M. Singh, “Gearbox and Drivetrain Models to Study Dynamic Effects of Modern Wind Turbines,” vol. 50, no. 6, pp. 3777–3786, Nov/Dec. 2014.

- [15] G. Bywaters, V. John, J. Lynch, P. Mattila, G. Norton, and J. Stowell, “Northern Power Systems WindPACT drive train alternative design study report,” NREL, Golden, Colorado, Report no. NREL/SR-500-35524, 2004.
- [16] “Epicyclic gearing”, Article from Wikipedia, 2015, last accessed 19/06/2018.
- [17] A. Bonanomi, “Powerful analysis of wind turbine gearboxes,” Power Transmission World, Report, July 2014.
- [18] C.D. Schultz, “The Effect of Gearbox Architecture on Wind Turbine Enclosure Size”, AGMA Technical paper, Alexandria, Virginia, pp. 4–18, September 2009.
- [19] J.H.O. Seanbra, D.E. P. Gonçalves, C.M.C.G. Fernandes, and R.C. Martins, “Torque loss in a gearbox lubricated with wind turbine gear oils”, Lubrication Science, Wiley online library, volume 25, pp. 297–311, February 2013.
- [20] E. Hau, “Wind Turbines fundamentals, technologies, application and economics”, Third Edition, New York London, Publisher: Springer, pp. 350–365, 2013.
- [21] H. Polinder, F.F.A. Van Der Pijl, G.J. De Vilder and P.J. Tavner, “Comparison of Direct-Drive and Geared Generator Concepts for Wind Turbines”, IEEE Transaction. Energy Conversion, vol. 21, no. 3, pp. 725–733, Sep. 2006.
- [22] K. Hart, A. McDonald, H. Polinder, E. Corr, and J. Carroll, “Improved Cost of Energy Comparison of Permanent Magnet Generators For Large Offshore Wind Turbines”, Conference on EWEA, Barcelona, Spain, 2014.
- [23] J. R. Cotrell, “A preliminary evaluation of a multiple-generator drivetrain configuration for wind turbines”, Conference, ASME 2002 Wind Energy Symposium, Reno, Nevada, pp. 345–352, January 14-17.
- [24] B.-R. Höhn, K. Michaelis and M. Hinterstoißer, “Optimization of Gearbox Efficiency”, GOMABN, vol. 48, no. 4, pp. 462–480, 2009.
- [25] C. Changenet and P. Vexel, “Housing Influence on Churning Losses in Geared Transmissions”, ASME Proceedings, 10th ASME international power transmission and gearing conference, Nevada, USA, vol. 7, pp. 681-688, September 4-7, 2007.
- [26] A. Ragheb, M. Ragheb, “Wind turbine gearbox technologies,” Ist International Nuclear and renewable energy conference (INREC10), Amman, Jordan, pp. 1–8, March 21-24, 2010.
- [27] P. Tavner, “Offshore wind turbines reliability, availability and maintenance”, First Edition, London, UK, Publisher: IET, 2012.
- [28] W. Musial, S. Butterfield, and B. McNiff, “Improving Wind Turbine Gearbox Reliability”, European Wind Energy Conference, Milan, Italy, pp. 1–13, May 7-10, 2007.
- [29] International Organization for Standardization, Wind Turbines – Part 4: Standard for Design and Specification of Gearboxes, ISO/IEC 81400-4:2005, ISO Geneva, Switzerland, February 2005.

- [30] “Wuthering Heights: The Dangers of Wind Power” press news, Spiegel International, August 2007.
- [31] S. Faulstich, B. Hahn and P.J. Tavner, “Wind turbine downtime and its importance for offshore deployment”, Research article on Wind energy, Wiley online library, vol. 14, pp. 327–337, July 2010.
- [32] D. Yao and R.G. Harley, “Present and future trends in wind turbine generator designs”, Power Electronics Machines Wind Application, PEMWA 2009, Lincoln, NE, USA, no. 11, pp. 1–6, 2009.
- [33] A.S. McDonald, “Structural analysis of low speed, high torque electrical generators for direct drive renewable energy converters”, PhD thesis, University of Edinburgh, 2008.
- [34] R. Datta and V.T. Ranganathan, “Variable-speed wind power generation using doubly fed wound rotor induction machine-a comparison with alternative schemes”, IEEE Transaction Energy Conversion, vol. 17, no. 3, pp. 414–421, 2002.
- [35] P.D. Chung, “Comparison of Steady-State Characteristics between DFIG and SCIG in Wind Turbine”, International Journal on Advanced Science and Technology, vol. 51, pp. 135–146, 2013.
- [36] A.D. Hansen, F. Iov, F. Blaabjerg and L.H. Hansen, “Review of Contemporary Wind Turbine Concepts and their Market Penetration”, Wind Engineering volume 28, No. 3, pp. 247–263, 2004.
- [37] B. Babypriya, R. Anita, “Modelling, simulation and analysis of doubly fed induction generator for wind turbines”, Journal of Electrical Engineering, vol. 60, no. 2, pp. 79–85, 2009.
- [38] www.en.wikipedia.org/wiki/Permanent_magnet_synchronous_generator, last accessed 19/06/2018. Wikipedia, “Permanent magnet synchronous generator” Wikipedia, pp. 1–2, 2018.
- [39] M. Mueller, H. Polinder, "Electrical Drives for Direct Drive Renewable Energy Systems," First Edition, Cambridge, UK, Woodhead Publishing Limited, pp. 80–105, 2013.
- [40] F. Blaabjerg, M. Liserre, and K. Ma, “Power electronics converters for wind turbine systems”, Industrial Applications, IEEE transaction vol. 48, no. 2, pp. 708–719, 2012.
- [41] A. Matveev, S. Ovrebo, R. Nilssen, and A. Nysveen, “State of the art in generator technology for offshore wind energy conversion systems”, 2011 IEEE International Electric Machines Drives Conference, Niagara Falls, ON, pp. 1131–1136, 2011.
- [42] Z. Chen, J. M. Guerrero, F. Blaabjerg, and S. Member, “A Review of the State of the Art of Power Electronics for Wind Turbines”, IEEE Transaction on Power Electronics, vol. 24, no. 8, pp. 1859–1875, 2009.

- [43] M. Liserre, R. Cárdenas, M. Molinas, and J. Rodríguez, “Overview of multi-MW wind turbines and wind parks”, *IEEE Transaction Industrial Electronics*, vol. 58, no. 4, pp. 1081–1095, 2011.
- [44] R. Pena, J.C. Clare and G.M. Asher, “A doubly fed induction generator using back-to-back PWM converters supplying an isolated load from a variable speed wind turbine”, *IEE Proceedings, Electric Power Applications, IET*, vol. 143, no. 5, pp. 380–387, 1996.
- [45] K. Ma, F. Blaabjerg, and D. Xu, “Power devices loading in multilevel converters for 10 MW wind turbines”, *Industrial Electronics ISIE 2011, 2011 IEEE International Symposium*, Gdansk, pp. 340–346, 2011.
- [46] J.M. Carrasco, L.G. Franquelo, J.T. Bialasiewicz, E. Galván, R.C.P. Guisado, M. Ángeles, M. Prats, J.I. León and N. Moreno-alfonso, “Power-Electronic Systems for the Grid Integration of Renewable Energy Sources: A Survey”, *IEEE Transaction Industrial Electronics*, vol. 53, no. 4, pp. 1002–1016, 2006.
- [47] J. Rodriguez, S. Bernet, P.K. Steimer and I.E. Lizama, “A survey on neutral-point-clamped inverters”, *IEEE Transaction Industrial Electronics*, vol. 57, no. 7, pp. 2219–2230, 2010.
- [48] R. Teichmann and S. Bernet, “A comparison of three-level converters versus two-level converters for low-voltage drives, traction, and utility applications”, *IEEE Transaction Industrial Electronics*, vol. 41, no. 3, pp. 855–865, 2005.
- [49] G.J.W. van Bussel and M.B. Zaaijer, “Reliability, Availability and Maintenance aspects of large-scale offshore wind farms, a concepts study” in *Proceedings of MAREC*, 2001.
- [50] H. Li and Z. Chen, “Design optimization and evaluation of different wind generator systems”, in *Proceedings of the 11th International Conference on Electrical Machines and Systems, ICEMS*, pp. 2396–2401, Wuhan, China, 2008.
- [51] A.D. Hansen, F. Iov, F. Blaabjerg and L.H. Hansen, “Review of Contemporary Wind Turbine Concepts and their Market Penetration”, *Journal on Wind Engineering*, vol. 28, no. 3, pp. 247–263, 2004.
- [52] J. Carroll, “Cost of energy modelling and reduction opportunities for offshore wind turbines”, PhD Thesis, Electronic and Electrical Engineering, University of Strathclyde, Glasgow, UK, 2016.
- [53] R.B. Ronald, N. Allan, *Reliability Evaluation of Engineering Systems*, Second Edition, New York and London: Plenum Press, p. 12-15, 64-67, 221-302, 448, 1983.
- [54] P.J. Tavner, J. Xiang and F. Spinato, “Reliability analysis for wind turbines”, *Wind Energy*, Wiley online library, vol. 10, no. 1, pp. 1–18, July 2006.
- [55] J. Ribrant and L. M. Bertling, “Survey of Failures in Wind Power Systems With Focus on Swedish Wind Power Plants During 1997–2005”, *IEEE Transaction on Energy Conversion*, vol. 22, no. 1, pp. 167–173, Mar. 2007.

- [56] M. Wilkinson, B. Hendriks, F. Spinato and T. Van Delft, "Measuring wind turbine reliability, results of the reliawind project", European Wind Energy Association Conference, pp. 1 – 8, 2011.
- [57] J. Carroll, A. McDonald, D. McMillan, "Reliability comparison of wind turbines with DFIG and PMG drivetrains", IEEE Transactions on Energy Conversion, vol. 30, no. 2, pages 663-670, June 2015.
- [58] P. Tavner, S. Faulstich, B. Hahn and G.J.W. Bussell, "Reliability & Availability of Wind Turbine Electrical & Electronic Components Availability", European power electronics and drives Journal, pp. 1–25, January 2011.
- [59] P. Tavner, F. Spinato, G.J.W van Bussell and E. Koutoulakos, "Reliability of Different Wind Turbine Concepts with Relevance to Offshore Application", April, 2008.
- [60] F. Spinato, P.J. Tavner, G.J.W van Bussel and E. Koutoulakos, "Reliability of wind turbine subassemblies", IET Renewable Power Generation, vol. 3, no. 4, p. 387, 2008.
- [61] B. Hahn, M. Durstewitz and K. Rohrig, "Reliability of Wind Turbines, Experiences of 15 years with 1,500 WTs", Wind Energy, pp. 1-4, 2007.
- [62] H. Polinder, J.A. Ferreira, B.B. Jensen, A.B. Abrahamsen, K. Atallah and R.A. McMahon, "Trends in Wind Turbine Generator Systems", IEEE Journal, Emerging and Selected Topics on Power Electronics, vol. 1, no. 3, pp. 174–185, 2013.
- [63] W. Yang, P.J. Tavner, C.J. Crabtree and M. Wilkinson, Cost Effective Condition Monitoring for Wind Turbines, IEEE Trans. Industrial Electronics, Vol. 57, no. 1, pp. 263-271, 2010.
- [64] C.J. Crabtree, D. Zappala, S.I. Hogg, "Wind energy: UK experiences and offshore operational challenges" Journal of power and energy, vol. 229(7), 727-746, 2015.
- [65] S.J. Watson, J.P. Xiang, W. Yang, P.J. Tavner, and C.J. Crabtree, "Condition monitoring of the power output of wind turbine generators using wavelets", Energy conversion, IEEE transaction, vol. 25, no. 3, pp. 715–721, 2010.
- [66] W. Yang, P.J. Tavner, "Condition monitoring and fault diagnosis of a wind turbine synchronous generator drive train", Renewable Power Generation, IET, vol. 1, pp. 10–16, April 2009.
- [67] J.J. Wolmarans, J.A. Ferreira, H. Polinder, I. Josifovic and D. Clarenbach, "Design for fault tolerance and predictive failures", CIPS 2010, Nuremberg, Germany, pp. 1-6, March 16–18, 2010.
- [68] H. Polinder, H. Lendenmann, R. Chin, and W.M. Arshad, "Fault tolerant generator systems for wind turbines," 2009 IEEE International Electrical Machine Drives Conference, Miami, FL, USA, 3-6 May 2009.
- [69] W.L. Heimerdinger and C.B. Weinstock, "A Conceptual Framework for System Fault Tolerance", Technical report, CMU/SEI-92-TR-033, October 1992.

- [70] J. Wolmarans, H. Polinder, J. A. Ferreira and D. Clarenbach, "Design of a Fault Tolerant Permanent Magnet Machine for Airplanes," 2008 international conference on electrical machines and systems, Wuhan, China, pp. 2882–2887, 17-20 October 2008.
- [71] B.C. Mecrow, A.G. Jack, D.J. Atkinson and J.A. Haylock, "Fault tolerant drives for safety critical applications," IEE Colloquium on New Topologies for Permanent Magnet Machines (Digest No: 1997/090), no. 90, London, UK, 18-18 June 1997.
- [72] U. Shipurkar, J. Dong, H. Polinder, and B. Ferreira, "Availability of Wind Turbine Converters with Extreme modularity", IEEE Transactions on Sustainable Energy vol. 9, no. 4, Oct. 2018.
- [73] T.M. Jahns, "Improved Reliability in Solid-State AC Drives by Means of Multiple Independent Phase Drive Units", IEEE Transaction Industry Application, vol. IA-16, no. 3, 1980.
- [74] F. Mekri, S. Benelghali, M. Benbouzid and J.F. Charpentier, "A fault-tolerant multiphase permanent magnet generator for marine current turbine applications," 2011 IEEE International Symposium Industrial Electronics, Gdansk, pp. 2079–2084, 2011.
- [75] N.A. Ayehunie, "MultiPhase Permanent Magnet Synchronous Generators for Offshore Wind Energy System," MSc dissertation, Norwegian University of Science and Technology, 2011.
- [76] H. Polinder, H. Lendenmann, R. Chin and W.M. Arshad, "Fault Tolerant Generator Systems for Increasing Availability of Wind Turbines", EWEA 2009, France, 16-17 March 2009.
- [77] G.K. Singh, "A six-phase synchronous generator for stand-alone renewable energy generation: Experimental analysis", Journal on Energy, vol. 36, no. 3, pp. 1768–1775, 2011.
- [78] M.A. Mueller, "Design and Performance of a 20kW, 100rpm, Switched Reluctance Generator for a Direct Drive Wind Energy Converter", IEEE International conference on Electric Machines and drives conference, no. 1, pp. 56–63, May 15 2005.
- [79] S. Nandi, H. A. Toliyat and X. Li, "Condition monitoring and fault diagnosis of electrical motors - A review", IEEE Transactions on Energy Conversion, vol. 20, no. 4, pp. 719–729, 2005.
- [80] U. Shipurkar, F. Wani, J. Dong, G. Alpogiannis, H. Polinder, P. Bauer and J.A. Ferreira "Comparison of wind turbine generators considering structural aspects", IECON 2017-43rd Annual Conference of the IEEE Industrial Electronics Society, Beijing, China, 29 Oct.-1 Nov. 2017.
- [81] U. Shipurkar, H. Polinder and J.A. Ferreira "Modularity in wind turbine generator systems-Opportunities and challenges", 18th European Conference on Power Electronics and Applications (EPE'16 ECCE Europe), Karlsruhe, Germany, 5-9 Sept. 2016.

- [82] B.A. Welchko, T.A. Lipo, T.M. Jahns and S.E. Schulz, "Fault tolerant three-phase AC motor drive topologies: A comparison of features, cost, and limitations", *IEEE Trans. Power Electronics*, vol. 19, no. 4, pp. 1108–1116, 2004.
- [83] A.D. Hansen and L.H. Hansen, "Wind turbine concept market penetration over 10 years (1995-2004)," *Wind Energy*, Wiley online library, vol. 10, no. November 2006, pp. 81–97, 2007.
- [84] G.J.W. van Bussel and A.R. Henderson, "State of the Art and Technology Trends for Offshore Wind Energy: Operation and Maintenance Issues", *Proceedings on offshore wind energy special topic conference*, Brussels, Belgium, 10-12 December 2001.
- [85] W. Cao, Y. Xie, and Z. Tan, "Wind Turbine Generator Technologies." Intech, open access publication 2012.
- [86] Wind power Engineering, "Four Onboard Generators Mean Almost Never Having to Shut Down", Technical report, pp. 1–5, October 2009.
- [87] F. Geoffrey, J.G.P. Dehlsen, "Distributed powertrain for high torque, low electric power generator", Patent, US6304002 B1 ,2001.
- [88] A. Mikhail, "Distributed generation drivetrain for high torque wind turbine applications", Public interest energy research program (PIER), Final project report 2011.
- [89] K.P. Astad and M. Molinas, "Double input AC/AC nine-switch converter for multiple-generator drivetrain configuration in wind turbines", *Industrial Electronics (ISIE)*, IEEE International Symposium, Bari, 2010.
- [90] N. Goudarzi and W.D. Zhu, "Offshore and Onshore Wind Energy Conversion: The Potential of a Novel Multiple-Generator Drivetrain", *Key Engineering Materials*, vol. 569–570, pp. 644–651, Jul. 2013.
- [91] P. Albrecht, J. Appiarius, E. Cornell, D. Houghtaling, R. McCoy, E. Owen, and D. Sharma, "Assessment of the reliability of motors in utility applications-updated," *IEEE Trans. Energy Convers.*, vol. EC-1, no. 1, pp. 39–46, (current version) Jan. 2009.
- [92] O.V. Thorsen and M. Dalva, "Survey of faults on induction motors in offshore oil industry, petrochemical industry, gas terminals, and oil refineries", *IEEE Trans. Ind. Appl.*, Vancouver, BC, vol. 31, no. 5, pp. 1186–1196, Oct. 1995.
- [93] P.J. Tavner, "Predicting the design life of high integrity rotating electrical machines", *IEE 9th International EMD Conference*, Canterbury, pp 286–290, 1999.
- [94] P. O'Donnell, "IEEE reliability working group, report of large motor reliability survey of industrial and commercial installations. Part I", *IEEE Trans. on Ind. Appl.*, vol. 1A-21, no. 4, pp. 853–872, July 1985.
- [95] J. Carroll, A. McDonald, and D. McMillan, "Failure rate, repair time and unscheduled O&M cost analysis of offshore wind turbines", *Journal on Wind Energy*, vol. 17, pp. 657–669, Aug. 2015.

- [96] K. Fischer, T. Stalin, H. Ramberg, T. Thiringer, J. Wenske, and R. Karlsson, "Investigation of converter failure in wind turbines", Elforsk, Tech. Rep. 212966, 2012.
- [97] P.J. Tavner, J. Xiang and F. Spinato, "Reliability analysis for wind turbines", *Wind Energy*, vol. 10, pp. 1–18, 2007.
- [98] K. Xie, Z. Jiang, and W. Li, "Effect of Wind Speed on Wind Turbine Power Converter Reliability" *IEEE Transactions on energy conversion*, vol. 27, no. 1, March 2012.
- [99] H. Arabian-Hoseynabadi, H. Oraee, P.J. Tavner "Failure Modes and Effects Analysis (FMEA) for wind turbines", *International journal on Electrical Power and Energy Systems* vol. 32, no. 7, pp. 817–824, September 2010.
- [100] F. Spinato, P.J. Tavner, G.J.W. van Bussel and E. Koutoulakos, "Reliability of wind turbine subassemblies," *IET Renew. Power Generation*, vol. 3, no. 4, pp. 387-401, Dec. 2009.
- [101] J. Ribrant and L. Bertling "Survey of failures in wind power systems with focus on Swedish wind power plants during 1997-2005" *IEEE Trans. Energy Convers.*, vol. 22, no. 1, pp. 167–173, Mar. 2007.
- [102] F. Spinato, "The reliability of wind turbines," PhD Thesis, School of Engineering, University of Durham, UK, 2008.
- [103] M. Lange, M. Wilkinson, T. van Delft, "Wind turbine reliability analysis"
- [104] J. Carroll, A. McDonald, I. Dinwoodie, D. McMillan, M. Revie and I. Lazakis "A comparison of the availability and operation & maintenance costs of offshore wind turbines with different drive train configurations", *Wiley Journal on Wind Energy*, vol. 20, no. 2, pp. 361-378, 26 July 2016.
- [105] IEC 60812:2006. "Analysis techniques for system reliability – procedure for failure mode and effects analysis (FMEA)", International Electrotechnical Commission
- [106] U. Shipurkar, H. Polinder, and J.A. Ferreira, "A review of methods to increase the availability of wind turbine generator systems", *CPSS transaction on power electronics and applications*, vol. 1, no 1, pp. 66-82, December 2016.
- [107] V. Najmi, J. Wang, R. Burgos, and D. Boroyevich, "Reliability modeling of capacitor bank for multilevel converter based on Markov state-space model," *IEEE Applied Power Electronics Conference (APEC)*, Charlotte, NC, pp. 2703–2709, Mar. 2015.
- [108] D. Astanei, C. Nemes, F. Munteanu, A. Ciobanu, "Annual Energy Production Estimation based on Wind Speed Distribution," *International Conference and Exposition on Electrical and Power Engineering (EPE)*, Iasi, Romania, 20-22 Oct. 2016.
- [109] S.H. Jangamshetti, V.G. Rau, "Normalized Power Curves as a Tool for Identification of Optimum Wind Turbine Generator Parameters" *IEEE Transactions on Energy Conversion*, vol. 16, No. 3, pp. 283-288, September 2001.

- [110] M. Deldar and A. Izadian, "Reconfiguration of a Wind Turbine with Hydrostatic Drivetrain to Improve Annual Energy Production", Energy conversion congress and exposition (ECCE), 2015 IEEE, Montreal, Canada, 20-24 September 2015.
- [111] D. Villanueva and A. Feijóo, "Normal-Based Model for True Power Curves of Wind Turbines", IEEE Transactions on Sustainable Energy, vol. 7, no. 3, July 2016.
- [112] D.S. Zinger and E. Muljadi, "Annualized Wind Energy Improvement Using Variable Speeds", IEEE Trans. on Industry Appl., vol. 33, no. 6, pp. 1444-1447, November/December 1997.
- [113] S. Jung, H. Jung, S. Hahn, H. Jung and C. Lee, "Optimal design of direct driven PM wind generator for maximum annual energy production", IEEE Transactions on Magnetics, vol. 4, no. 6, pp. 1062-1065, June 2008.
- [114] M. Lydia, A.I. Selvakumar, S.S. Kumar, and G.E.P. Kumar "Advanced Algorithms for Wind Turbine Power Curve Modeling", IEEE Transactions on Sustainable Energy, vol. 4, no. 3, July 2013.
- [115] H. Arabian, P.J. Tavner, H. Oraee, "Comparison of reliability of geared and direct drive wind turbine concepts," Wiley Wind Energy Journal, vol. 13, no. 1, pp. 62-63, January 2010.
- [116] A. McDonald and G. Jimmy, "Parallel wind turbine powertrains and their design for high availability," IEEE Transactions on Sustainable Energy, vol. 8, no. 2, pp. 880-890, April 2017.
- [117] C. Andrei, S. Serowy, F. Barenhorst, B. Riemer, R. Schelenz, and K. Hameyer, "Alternative wind turbine drive train with power split and high-speed generators," European Wind Energy Conference, Paris, France, Nov. 2015.
- [118] BVG associates "Offshore wind cost reduction pathways: Technology work stream" Technical report, May 2012.
- [119] E. Echavarria, G. van Bussel, T. Tomiyama, "Finding Functional Redundancies in Offshore Wind Turbine Design", Wind Energy, vol. 15, no.4, pp. 609-626, May 2012.
- [120] J. Holierhoek, et al. "Procedures for testing and measuring wind turbine components; results for yaw and pitch system and drive train", Wind Energy, vol. 16, no. 6, pp. 827-843, 2013.
- [121] I. Dinwoodie, D. McMillan and F. Quail, "Analysis of offshore wind turbine operation & maintenance using a novel time domain meteo-ocean modeling approach", Copenhagen, ASME Turbo Expo 2012.
- [122] K. Hart, A. McDonald, H. Polinder, E. Corr and J. Carroll, "Improved cost energy comparison of permanent magnet generators for large offshore wind turbines", Barcelona, EWEA 2014.
- [123] I. Dinwoodie, "Modelling the operation and maintenance of offshore wind farms" PhD Thesis, University of Strathclyde, UK, 2014.

- [124] J. Carroll, A. McDonald, D. McMillan, T. Stehly, C. Mone and B. Maples “Cost of energy for offshore wind turbines with different drive train types.” EWEA 2015 conference, Paris, France, Nov. 2015.
- [125] M. Wilkinson, K. Harman, F. Spinato, B. Hendriks and T. Van Delft, “Measuring Wind Turbine Reliability - Results of the Reliawind Project”, in Proc. Eur. Wind Energy Conf. Brussels 2011.
- [126] GH, ReliaWind “Reliability focused research on optimizing Wind Energy systems design, operation and maintenance: tools, proof of concepts, guidelines & methodologies for a new generation”, Reliawind, Report, 2007
- [127] Y. Dalgic, I. Lazakis, I. Dinwoodie, D. McMillan and M. Revie, “Advanced logistics planning for offshore wind farm operation and maintenance activities”, Ocean Engineering, vol. 101, pp. 211–226, June 2015.
- [128] Y. Dalgic, I. Lazakis and O. Turan, “Vessel charter rate estimation for offshore wind O&M activities”, 15th International Congress of the International Maritime Association of the Mediterranean IMAM 2013, A Coruna, Spain, October 2013.
- [129] I. Dinwoodie and D. McMillan, “Heavy Lift Vessel Strategy for Offshore Wind”, European Wind Energy Conference and Exhibition (EWEA 2013). pp. 1612-1620, Vienna, 2013.
- [130] Y. Dalgic, I. Lazakis, O. Turan and S. Judah, “Investigation of Optimum Jack-Up Vessel Chartering Strategy for Offshore Wind Farm O&M Activities”, Ocean Engineering, vol. 95, pp. 106-115, 1 February 2015.
- [131] J. Igba, K. Alemzadeh, K. Henningsen and C. Durugbo, “Effect of Preventative Maintenance Intervals on Reliability and Maintenance Costs of Wind Turbine Gearboxes”, Wind Energy, vol. 18, no.11, pp. 2013-2024, November 2015.
- [132] Vestas Promotional Material. V112-3MW Offshore. [Online] Available www.vestas.com/Files/Filer/EN/Brochures/Productbrochure_V112_Offshore_UK.pdf
- [133] I. Dinwoodie, O.E.V. Endrerud, M. Hofmann, R. Martin and I.B. Sperstad, “Reference Cases for Verification of Operation and Maintenance Simulation Models for Offshore Wind Farms”, Wind Engineering, vol. 39, no. 1, pp 1–14, 2015.
- [134] L. Wang, T. Yeh, W. Lee, Z. Chen, “Benefit Evaluation of Wind Turbine Generators in Wind Farms Using Capacity- Factor Analysis and Economic-Cost Methods” IEEE Transactions on Power Systems, vol. 24, no. 2, May 2009.
- [135] International Electrotechnical Commission, “IEC 61400-1: Wind turbines Part 1: Design requirements.” International Electrotechnical Commission, 2005.
- [136] C. Moné, A. Smith, B. Maples, M. Hand, “2013 Cost of Wind Energy Review”, National Renewable Energy Laboratory, Technical Report, NREL/TP-5000-63267, February 2015.

- [137] C. Moné, T. Stehly, B. Maples and E. Settle, “2014 Cost of Wind Energy Review”, National Renewable Energy Laboratory, Technical Report, NREL/TP-6A20-64281, October 2015.
- [138] Willow C, Valpy B, “Approaches to cost reduction in offshore wind”, BVG Associates, A report for the committee on climate change, June 2015.